PhD degree in Systems Medicine

(curriculum in Molecular Oncology & Human Genetics)

European School of Molecular Medicine (SEMM),

University of Milan and University of Naples "Federico II"

Settore disciplinare: Med/04

Dissecting the role of lysine-specific demethylase1 (LSD1): identification of

markers/effectors of sensitivity to LSD1 inhibitors in cancer

Seyed Amir Hosseini

European Institute of Oncolgy (IEO), Milan

Supervisor: Prof. Saverio Minucci

European Institute of Oncolgy (IEO) and University of Milan, Milan

Added supervisor: Dr. Diego Pasini

European Institute of Oncolgy (IEO), Milan

Prof. Luciano Di Croce

Centre de regulaciò genomica (CRG), Barcellona

Anno accademico 2016-2017

This dissertation is dedicated to my lovely family, especially to my mom and my wife who supported me each step of the way. Thank you for your unconditional love.

Table of contents

Figures & Tables index

List of abbreviations

5mC 5-methylcytosine

aa Amino acids

ac (ex. H3K9ac) acetylated residues

ADPR PARP-1catalyze the polymerization of ADP-ribose

Akt V-Akt murine thymoma viral oncogene homolog

ALL acute lymphoblastic leukemia

AML acute myeloid leukemia

APL acute promyelocytic leukemia

AR Androgen receptor

ATO Arsenic Trioxide

ATP Adenosine Triphosphate

ATP Adenosine triphosphate

ATRA/RA All-Trans Retinoic Acid

B-RAF v-raf murine sarcoma viral oncogenes homolog B1

BCoR Bcl6- interacting Co-Repressor

bp Base pairs

BSA Bovine serum albumin

CD chromodomains

CDK Cyclin-dependent kinase

CDKN1A Cyclin-Dependent Kinase Inhibitor 1A

CFU   Colony Forming Unit

ChIP Chromatin Immuno Precipitation

ChIP-seq chromatin immunoprecipitation-sequencing

CKI CDK inhibitor protein

CoREST Corepressor of Repressor Element 1 Silencing Transcription

CoREST RE1-silencing transcription factor corepressor 1

DDR DNA damage response

DMEM Dulbecco's modified Eagle medium

DMSO Dimethyl Sulfoxide

DNA deoxyribonucleic acid

DNMT DNA Methyltransferase

E2F E2 Factor

ECL Enhanced chemoluminescence

EDTA Ethylene Diamine Tetra Acetic acid

EMT Epithelial-to-mesenchymal

ER estrogen receptor

ERK Extracellular Regulated Signaling Kinase

ESC Embryonic Stem Cell

EST Expressed Sequence Tag

FAB French-American-British

FACS Fluorescence Activated Cell Sorting

FBS Fetal bovine serum

FDA Food and Drug Administration

GAPDH Glyceraldehyde 3-Phosphate dehydrogenase

GFP Green- Fluorescent- Protein

H (ex.H3) histone H3

H2A histone 2A

H2B histone 2B

H3 histone 3

H3K4 Lys4 of histone H3

H4 histone4

HATs Histone acetyltransferases

HDACs histone deacetylases

HDM histone demethylase

HMG High Mobility Group

HMTs histone methyltransferases

HP1 heterochromatin protein 1

HSC hematopoietic stem cell

JMJD histone/lysine demethylase

K lysine

kb Kilobase

KD Knock-Down

KDa Kilodalton

KDM lysine demethylase

KMTs lysine methyltransferases

KO Knockout

LIC Leukemia Initiating Cell

LSD1 lysine-specific demethylase 1

MAO A/B Monoamine Oxidase A/B

MAPK Mitogen-activated protein kinase

MC LSD1 inhibitor

MDS myelodysplastic syndroms

me (ex.H3K4me3) methylated residues

miRNA microRNA

MLL mixed lineage leukemia

mRNA Messenger RNA

N-CoR Nuclear receptor Co-Repressor

N-RAS Neuroblastoma RAS viral oncogenes homolog

NAD Nicotinamide Adenine Dinucleotide

NCoR-SMRT Nuclear Receptor Corepressor- Silencing Mediator of Retinoid and Thyroid

ncRNAs Non-coding RNAs

NSCLC non-small-cell lung cancer

NT Non- treated cells

NuRD Nucleosome remodeling and deacetylation

NuRD Nucleosome Remodeling Deacetylase

O-GlcNAc β-N-acetylglucosamine

P phosphorylation

PAD4 peptidylarginine deiminase 4

PADI Peptidylarginine deiminases

PARP-1 Poly(ADP-Ribose) Polymerase-1

PBS Phosphate-Buffered Saline

PCR Polymerase chain reaction

PELP1 Proline glutamic acid and leucine-rich protein 1

PHD plant homeodomain

PI Propodium-Iodide

PML Promyelocytic Leukemia protein

PML-RARα Promyelocytic Leukemia- Retinoic acid receptorα

Pol II RNA Polymerase II

PRDMs PR domain-containing proteins

PRMTs arginine methyltransferases

PTEN Phosphatase and tensin homologue deleted on chromosome 10

PTM Post-translational modification

PTMs post-translational modifications

qRT-PCR Quantitative reverse transcriptase-polymerase chain reaction

R arginine

RA HIGH Pharmacological concentration of RA (1μM)

RA LOW Physiological concentration of RA (0.01μM)

RARα Retinoic Acid Receptor

RCOR1 RE1-silencing transcription factor corepressor 1

RNA Ribonucleic acid

RNAi RNA interference

RPM Revolutions per minute

RT Room temperature

S serine

SAHA SuberoylAnilidehydroxamic acid

SAM S-adenosyl-L-methionine

SAM S-adenosyl-L-methionine

SCLC small-cell lung cancer

SD Standard- deviation

SDS Sodium dodecylsulfate

SDS-PAGE   Sodium dodecyl sulfate- polyacrylamide gel electrophoresis

SET Su (var), Enhancer of Zeste, and Trithorax

siRNA small interference RNA

SMRT Silencing Mediator of Retinoic acid and Thyroid hormone receptors

SMYD3 SET- and MYND-domain containing protein 3

SV40 simian virus 40

SWIRM Swi3p/Rsc8p/Moira

T threonine

T-ALL T cell acute lymphoblastic leukemia

TAE Tris-Acetate-EDTA

TBS Tris-Buffered Saline

TF   Transcription Factor

TFBS Transcription factor binding site

TSA Trichostatin A

TSS Transcription Start Site

Ub ubiquitination

USP/UBP ubiquitinspecific protease

UV Ultraviolet

WT Wild-type

Y tyrosine

Abstract

Post-translational modification of histone tails plays a critical role in chromatin regulation, gene activity and nuclear architecture. The addition or removal of post-translational modifications from histone tails is fairly dynamic and is achieved by a number of different histone modifying enzymes. Given the fundamental roles of histone modifications in gene regulation and expression, it is not surprising that aberrant patterns of histone marks are found in cancer. Such modifications include histone lysine methylation, which can either promote or repress gene activity depending on the extent of methylation and its context. Histone lysine methylation is maintained by dynamic opposition of methyltransferase and demethylase enzymes, both of which are implicated in normal embryonic development and tumorigenesis.

LSD1 is a flavin-containing amine oxidase that, by reducing the cofactor FAD, demethylates H3K4me1/2 and H3K9me1/2 at target loci in a context-dependent manner. LSD1 can act as either a transcriptional co-repressor, as a part of several chromatin complexes such as CoREST and NuRD, or as a co-activator in association with androgen and estrogen receptor.

In cancer cells, it has been shown that LSD1 is required for the development and maintenance of acute myeloid leukemia (AML) and cooperate with the oncogenic fusion protein MLL-AF9 to sustain leukemic stem cells (LSCs). LSD1 inhibition impaired the proliferation potential of murine and human AML cells and was accompanied by induction of differentiation. Moreover, LSD1 inhibitors unlocked the ATRA-driven therapeutic response in AML by increasing H3K4me2 level and reactivating the retinoic acid signaling pathway. LSD1 could be an attractive target for cancer therapy because of its deregulation in a number of cancers, including lung, breast, melanoma and hematological malignancies. Despite recent diagnostic and technological improvements, cancer continues to retain its heavyweight status as one of

the most challenging diseases to treat. It is a heterogeneous disease that often results in different clinical outcomes for patients with the same affected tissue. And as such, the disparateness of this disease makes it extremely difficult to fight. The ability to anticipate the clinical behavior of cancers is essential in determining the most suitable therapeutic interventions. Considering that cancer is so diverse and clinical outcome predictions often vary from patient to patient, a considerable amount of effort is being invested to discover molecular biomarkers that can categorize cancer patients with distinct clinical outcomes to expand prognostic capabilities. Given the unsatisfactory clinical outcome associated with standard chemotherapy in acute myeloid leukemia (AML) and melanoma treatment, there is an essential need for new targets. Recently LSD1 have gained great interest for their use as anticancer therapeutics. However, the efficacy of LSD1 inhibitors is limited to a substantial subset of cancer cells. Thus, identification of good predictive biomarkers for sensitivity to treatment with LSD1 inhibitors will be of great value in determining the most suitable therapeutic setting.

Two lines of evidence have provoked our interest in LSD1. First, LSD1 inhibition impaired the proliferation potential of a subset of solid tumors and AML cells. second, LSD1 inhibitors unlocked the ATRA-driven therapeutic response in AML cells.

Our lab, in collaboration with prof. Antonello Mai and prof. Andrea Mattevi, previously developed a new compound working as an LSD1 specific inhibitor, MC2580. By taking advantage of this inhibitor, we have previously shown that LSD1 inhibition sensitizes NB4 cells to retinoic acid (RA) treatment and induces cell growth arrest and differentiation when combined with a physiological concentration of RA (RA low). Starting from these observations, we hypothesized that LSD1 inhibition sensitize UF1 cells, that were established from a patient who was clinically resistant to RA treatment and harbor a point mutation in

ligand binding domain (LBD) of RARα moiety. Surprisingly LSD1 inhibition in UF1 cells led to cell growth inhibition, induced cell differentiation and promoted G1 phase arrest, as a single agent. we performed a genome-wide expression analysis comparing gene expression profiling of the two cell lines (NB4 vs UF1) which differently response to LSD1 inhibitor, before and after MC treatment. We found that p21 highly expressed in UF1 cells and MC-treatment led to further upregulation of p21 in UF1 cells but not in NB4. High level of p21 in UF1 cells, is consistent with the fact that UF1 cells are in higher percentage in G1 phase and lower growth rate. We also showed that induction of p21 by HDAC inhibitors sensitized resistant cells (NB4) to LSD1 inhibitor which further confirmed our observation. Knockdown of p21, rescued UF1 cells from cell growth inhibition, cell differentiation and G1 phase arrest mediated by LSD1 inhibitor. Similar to APL cells, Knock-down of p21 in non-APL AML, SCLC and melanoma cells, rescued cells from the effects of MC. Furthermore, we observed that p21 by binding to CDK leads to G1 cell cycle arrest and sensitizes resistant cells to LSD1 inhibitor. Given modest efficacy of LSD1 inhibitors against a subset of cancer cells, combination therapy with LSD1 inhibitors will be a critical approach for therapeutic intervention. In this study we showed that forced cell cycle inhibition either with p21 induction by HDAC inhibitors or directly by CDK inhibitors (Palbociclib) presents a promising therapeutic strategy in solid and hematologic cancers. In conclusion:

- Inhibition of LSD1 suppresses G1 to S phase transition and cell proliferation in a p21-dependent manner.
- Loss of p21 enables progression of cell cycle and rescues the LSD1 inhibitor phenotypes.

- P21 provoked by LSD1 inhibitor could serves as a biomarker to verify pharmacological activity and a prognostic tool reflecting responsiveness to LSD1 inhibitor.

- Forced cell cycle inhibition either with p21 induction by HDAC inhibitors or directly by CDK inhibitors sensitized tumor cells to LSD1 inhibition.

1. Epigenetic

The field of epigenetics in its current form is relatively new, however the term was established in 1947 by Conrad Waddington, as "the branch of biology which studies the causal interactions between genes and their products which bring the phenotype into being" [Jablonka&Lamb, 2002]. In 2009 this definition was revised as to "An epigenetic trait is a stably heritable phenotype resulting from changes in a chromosome without alterations in the DNA sequence" [Berger, 2009]. As far apart these two definitions might seem they both classify epigenetics as a step beyond classical genetics and closer to how one genotype can be translated into many different phenotypes. Epigenetics now is understood as the study of mitotically and/or meiotically heritable changes in gene expression without changing gene sequence [Bird, 2002; Butler& Dent, 2013]. The word "epi" comes from the Greek and means the same as "over", "above" or "in addition to", so the epigenetic code can be seen as a second layer of information on top of the genetic code. Epigenetics, in a broad sense, is a connection between genotype and phenotype that alters the final outcome of genomes without changing the underlying DNA sequences. This includes covalent and non-covalent modifications of DNA and histone proteins by which the overall chromatin structure is influenced. Epigenetic modifications can be passed from one cell generation to the next (mitotic inheritance) and in some cases between generations of a species (meiotic inheritance). [Kouzarides, 2007; Bannister&Kouzarides, 2011]. It is now well understood that cancer, alone with genetic perturbations, can be characterized by gross alterations within the epigenome. These changes manifest in the nucleus with unique chromatin structure, which in turn leads to global differences in gene expression patterns compared to the normal cell.

2. Mechanisms of epigenetic regulation

The enormous complexity of life even at the cellular level requires a complex traffic of information between external and internal signals and a coordinated response mediated by systems to read the information and execute the response. Probably one of the best examples to understand what epigenetics refers to is found in the heterogeneity of human body itself. Not only do the cells making up different tissues express unique sets of genes that define their characteristics and functions, but we now understand that there are additional levels of control superimposed upon the genome. Although the genetic information that determines the response is contained in the sequence of nucleotides of DNA, the structure of chromatin is crucial in the way this information is read. It has always been amusing that this same genetic information is able to give rise to many diverse cellular phenotypes and specific functions. More important here, cellular differentiation processes are regarded as epigenetic phenomena. Even though cells of a multicellular organism share the same genetic instruction sets, a great diversity of cell types with very different terminal phenotypes is generated from the originally totipotent cell. During this development the cell undergoes changes in its epigenetic state, a fact that has been famously illustrated as the epigenetic landscape by Conrad H. Waddington in 1957 [Goldberg, 2007]. The epigenetic landscape is a metaphor displaying the process of cellular decision-making, with a marble (representing a cell) rolling down a hill into one of several valleys **(Figure 1)**. The cell can follow different permitted trajectories, finally reaching its destination at the bottom of a certain valley, reflecting a terminally differentiated state. From today's point of view, we know that at each point in this slope the cell has a specific epigenetic state which is causal for the cell's gene expression profile.
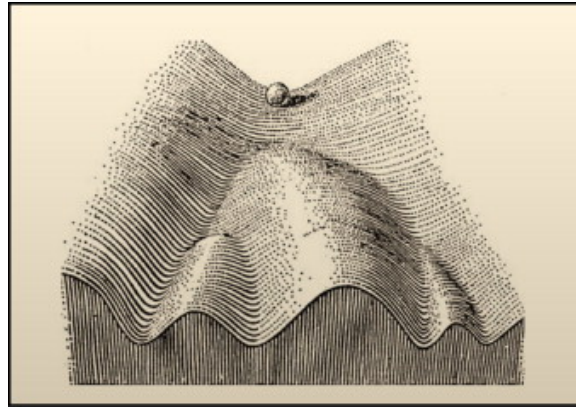
Figure 1. **C.H. Waddington's epigenetic landscape model.** Waddington first proposed the concept of epigenetic landscape in 1957; this figure represents the process of cellular differentiation and different trajectories that the cell (demonstrated by a marble) can undertake toward differentiation. Adapted from Goldberg et al. Cell 2007.

Thus, the epigenetic information of a cell (epigenome) displays a stable, heritable, and changeable, layer of information which instructs cell fates by defining the activity of genes. This is achieved by epigenetic alterations which regulate both chromatin structure and the accessibility of the DNA. The most fundamental epigenetic mechanisms are DNA methylation and histone tail modifications. There are additional epigenetic mechanisms such as the presence of histone variants, and displacement and reposition of nucleosomes. Non-coding RNAs (ncRNAs) among which are the small interference RNA (siRNA) and microRNA (miRNA), are also considered an epigenetic mechanism [Murr, 2010].

The combined effects of these processes define the structure of chromatin at a particular locus and thus, its transcriptional activity. Countless mechanisms involving effectors, players and presenters have been identified in years of intensive research, some of which will be introduced in the following section.

3. DNA methylation

The best known epigenetic mechanism of gene regulation is DNA methylation. DNA methylation does not occur in a stochastic manner. It is targeted to specific bases in the genome. In the mammalian genome DNA methylation takes place at the 5´ position of the pyrimidine ring of a cytosine located adjacent to a guanine (5´-CpG-3´) and is mediated by DNA methyl transferases (DNMTs) [Liyanage, 2014]. Approximately 3–5% of the cytosine residues in the genome of mammalian cells are modified as 5-methyl cytosine, and 70–80% of them are found in CpG residues [Weber, 2007]. The CpG residues are often clustered in the promoter/regulatory regions of the genes as CpG islands. This covalent methylation modification of cytosine residues represents a reversible but heritable change which can alter gene expression and is ultimately responsible for a diverse array of biological responses [Mellen, 2012; Booth, 2012].

Three active DNMTs (DNMT1, DNMT3a, and DNMT3b) have been identified in human. DNMT3a and DNMT3b are responsible for *de novo* methylation whereas DNMT1 is responsible for maintenance of DNA methylation and copies the methylation patterns from the parental to daughter strands of DNA during DNA replication by methylating the hemimethylated strands [Okano, 1998].

Differential DNA methylation at CpG islands has been shown to be associated with regulation of gene expression and is essential for normal embryonic development, X chromosome inactivation, imprinting, chromatin modification, suppression of parasitic DNA sequences, and aberrant silencing of tumor suppressor genes or over-activation of oncogenes in cancer [Jones, 2001]. Having these global functions, it is not surprising that DNA methylation has been implicated in several diseases, especially in cancer. Regarding DNA methylation, two

different phenomena occur in cancer cells: first there is a global DNA hypomethylation that affects mainly repetitive sequences, coding regions and introns and produces chromosomal instability; second there is a DNA hypermethylation at CpG islands that are present at the promoter of many genes. The CpG islands are normally unmethylated in normal cells but become methylated in cancer leading to the repression of tumor suppressor genes [Tuck-Muller, 2000].

4. Chromatin Organization

A high degree of organization is required to confine the eukaryotic genome with more than three billion base pairs and nearly 2 meter of deoxyribonucleic acid (DNA) into the nucleus with an average diameter of 5–10 µ m. In order to achieve this, DNA is associated with proteins that extensively fold and condense it into a highly organized structure, known as chromatin, composed of DNA and its intimately associated histone proteins, non-histone proteins such as High Mobility Group (HMG) proteins and Heterochromatin Protein 1(HP1) and RNAs, such as long ncRNAs. The fundamental unit of chromatin, termed the nucleosome, is composed of 145–147 base pairs (bp) of DNA wrapped nearly twice around an octamer of histone proteins, constructed from two copies of each of the core histones, histone H2A, histone H2B, histone H3, and histone H4 [Kornerber, 1974; Oudet, 1975; Luger, 1997; Kornberg &Lorch, 1999]. Each nucleosome core is connected to an adjacent nucleosome core through a segment of linker DNA to form the chromatin polymer with a repeat length ranging from 160 to 240 bp. Approximately 20 bp of this linker DNA is typically found in association with the linker histone H1 (also H5). The nucleosome core together with the linker histone is called the chromatosome [Robinson, 2006; Kornberg &Lorch, 1999].

Chromatin is generally classified into either euchromatin or heterochromatin, depending on its

level of compaction **(Figure 2, 4)**. Euchromatin is 'open' and poised for gene expression, while heterochromatin is compact and refractory to transcription. Euchromatin is best described by the 'beads on a string' model, which is thought to represent the lowest level of chromatin compaction (10 nm fiber). Heterochromatin is formed by the addition of linker histone H1 (also H5) and various non-histone proteins (such as HP1), which further compact nucleosomes into higher order structures (30 nm fiber and beyond). Finally, chromatin reaches its most condensed state during mitosis **(Figure 2)** [Maresca, 2005; Shogren-Knaak, 2006; Maresca, 2006].

The core histones are well conserved in eukaryotes and are lysine- and arginine-rich proteins (the basic amino acids) that are involved in the formation of nucleosomes. Each core histone has a molecular weight from 11 to 15 kDa and 17~ 20 positive charges at pH 7. All of the four core histones carry the N-terminal tail regions which are rich in lysine residues. These lysine-rich tail regions bind to negatively charged DNA, and play a role in nucleosome-nucleosome interactions. Linker histones (H1, H5) are also major components of metaphase chromosome, and occupy 5.8% of the total protein amount. These linker histones carry more lysine residues than the core histones and have a core domain in the middle part that binds to a nucleosome.

While chromatin plays a structural role, its regulation is highly dynamic that can adopt many different conformations and substructures and allows DNA to be accessed as needed while simultaneously being packaged. This implies that chromatin density plays an important role in regulating gene expression involving a dynamic competition between transcription factors and nucleosomes for critical genomic loci **(Figure 3)**.

Different critical factors contribute to chromatin dynamics, the post-translational modification (PTM) of histones, ATP-dependent chromatin remodeling factors, Poly(ADP-Ribose) Polymerase-1 (PARP-1), histone chaperones, and the incorporation of specialized histone

variants into chromatin.
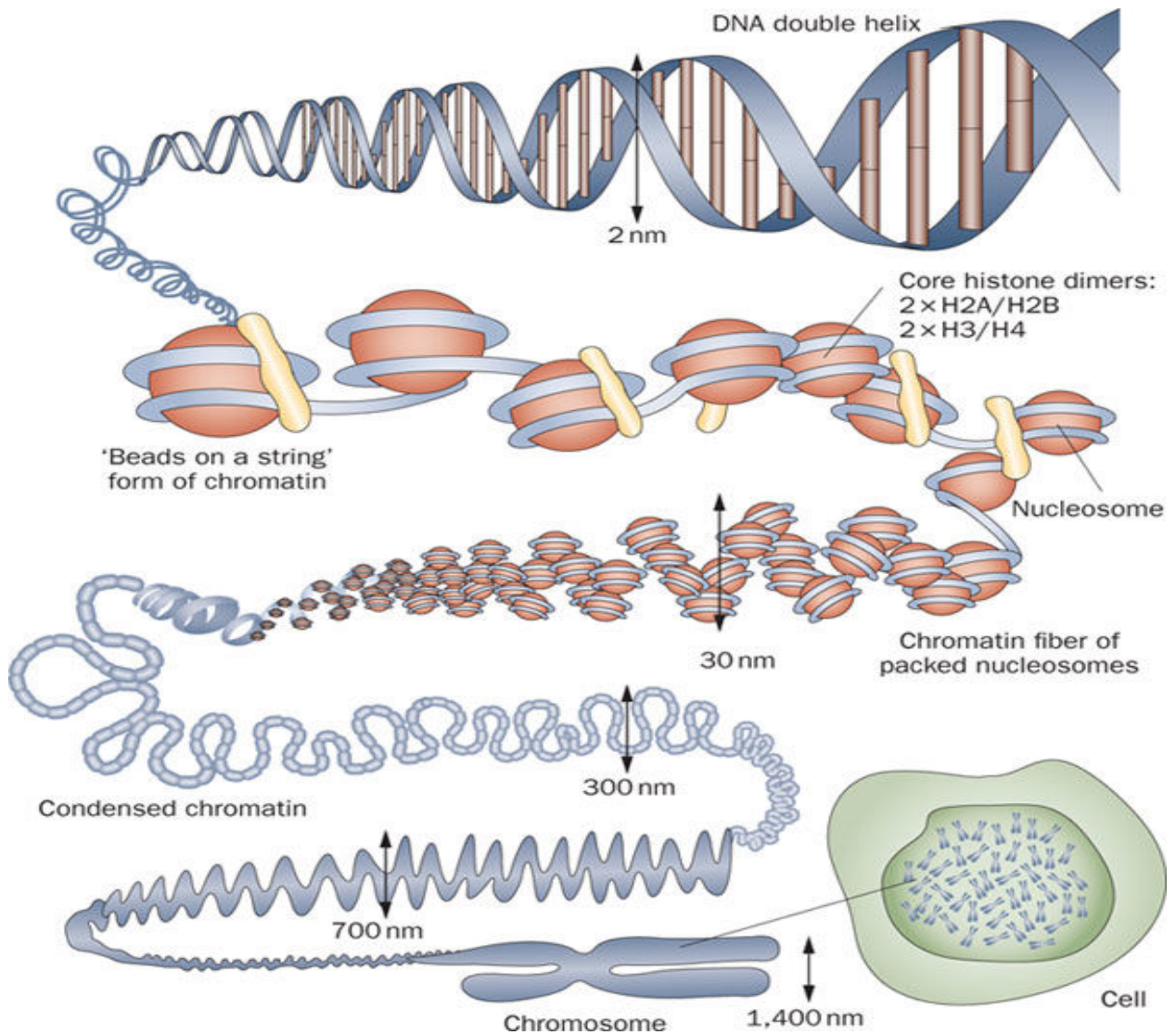
Figure 2. **DNA is packaged into chromatin.** The DNA double helix, which is 2 nm in width, is wrapped around an octamer of histone proteins to form a nucleosome. The nucleosomes are then packaged to form a chromatin fiber of 30 nm in width. Consequently, the chromatin fiber is condensed to ultimately form a chromosome of approximately 1,400 nm in width. Adapted from Tonna et al. Nat Rev Nephrol 2010.

Histone variants, which have a different amino-acid sequence from canonical histone and non-

histone proteins (such as High Mobility Group (HMG) proteins and Heterochromatin Protein

1, HP1) are incorporated to modify the structure and properties of chromatin composition, making chromatin a versatile template that can adapt, and provides a means to regulate various DNA based processes such as replication, transcription, recombination, and repair. Histone variants are classified as either replicative or replacement histones, and exist for the three core histones H3, H2A, and H2B, and for the linker histone H1, but not for the core histone H4. For example, the canonical histone H3 (H3.1) is replaced at the centromere region by the centromere-specific variant CENH3 (CENP-A), which directs the assembly of the kinetochore ensuring proper segregation of the sister chromatids to the daughter cells. Histones H2A.Z and H2A.X are variants of histone H2A. Histone H2A. X plays a role in double-strand break repair, whereas H2A.Z is functional in different processes including gene activation and repression [Tachiwana, 2011; Buschbeck, 2017].

ATP-driven chromatin remodeling complexes that act as molecular machines coupling ATP hydrolysis play an important role in alterations of chromatin structure and so gene regulation. These chromatin remodeling complexes are distinguished from other chromatin factors by their use of the energy of ATP hydrolysis to promote their functions such as (1) phasing and spacing of nucleosomes, (2) altering the path of the DNA wrapped around nucleosomes, (3) transferring the histone octamer to DNA molecules, (4) exchanging the canonical histones of the core with variants (Chromatin Editing) [Clapier, 2017].

Histone chaperones provide another level of complexity of chromatin organization. Histone chaperones are the histone interacting factors that stimulate histone transfer reaction without being a part of the final product. They are involved in the storage of histone pools, transporting the histones from the cytoplasm to the nucleus, histone presentation for histone modification, and nucleosome assembly/disassembly by transiently shielding the positively charged histones to regulate their interaction with negatively charged DNA [Lai, 2017;

Hammond, 2017].
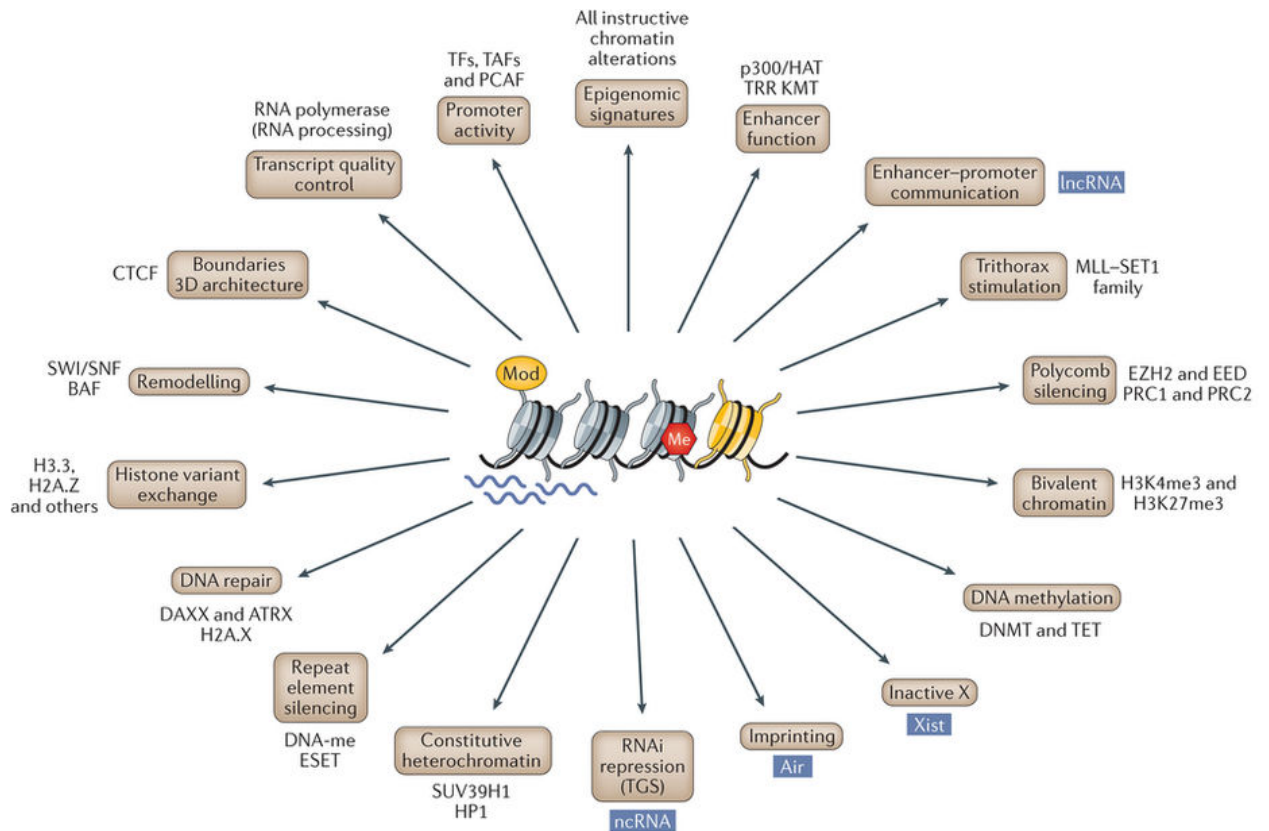
Figure 3. **Chromatin dynamics**. Histone modifications, non-coding RNA, histone variants and remodeling alter chromatin structure. Adapted from Allis et al. Nat Rev Genet 2016.

Poly(ADP-ribose) polymerase-1 (PARP-1) is a ubiquitous and abundant nuclear protein, that by interaction with chromatin and chromatin-modulating proteins alters chromatin structure and nucleosome stability. Although PARP-1 has firstly been studied as a DNA damage detection and repair protein, more recent studies have demonstrated a clear role for PARP-1 as a modulator of chromatin structure. PARP-1catalyze the polymerization of ADP-ribose (ADPR) units from donor NAD+ molecules on target proteins through a process called poly(ADP-ribosyl) ation (or PARylation). Multiple chromatin proteins are targets for PARylation, including histone proteins, especially histones H1 and H2B, some high-mobility

group (HMG) proteins, and other DNA-binding proteins such as DNA ligases and topoisomerases. PARylation may alter the activity of these proteins, thereby changing the way, they interact with chromatin and alter chromatin structure. For example, PARylation of H1, a key target of PARP-1 activity in vivo, may block H1 binding to nucleosomes and inhibit chromatin compaction by H1 [Ray Chaudhuri, 2017].

PTMs are particularly abundant on the N-terminal histone tails, which protrude from the nucleosomal core. However, PTMs also exist within the core and on certain C-terminal tails, for example, H2A. Histone PTMs can result in 'on' or 'off' chromatin states regarding transcriptional status, including acetylation at lysines (K), methylation at lysines and arginines (R), phosphorylation of serines (S) and threonines (T), O -glycosylation of serines and threonines, formylation and crotonylation of lysines, deimination of arginines (R), arginine(R), and proline(P) isomerization, and glutamate poly-ADP ribosylation and hydroxylation of serines but also ubiquitination, citrullination, SUMOylation and ADP ribosylation is observed [Kouzarides, 2007]. All these modifications constitute a complex language that governs the structure of chromatin and the transcriptional status of the genes contained in a particular locus. Whereas acetylation, phosphorylation and ubiquitination are readily reversible, lysine and arginine methylation are comparatively more stable marks. Such modifications could play a direct role in modulating histone-DNA interactions within the nucleosome, thereby determining the ease with which a nucleosome can be translocated along DNA. In terms of transcription, modifications can be grouped in those that correlate with activation of transcription and those that correlate with repression of transcription.

It is thought that specific combinations of modifications in one or more histones form a 'code' which is recognized by particular regulatory proteins and trans-acting factors including ATP-dependent remodelling enzymes. This "histone code" hypothesis states that PTMs can act

through two mechanisms: (1) by structurally changing the chromatin fiber through inter nucleosomal contacts, thus regulating DNA accessibility, and (2) by serving as docking sites for effector molecules (generally referred to as 'readers') that initiate distinct biological processes [Yun, 2011]. However, each modification has its own meaning in a defined context and the same modification can be associated to gene activation or repression depending on the context. Two good examples are methylation of H3K36 and H3K9 that have a positive effect on gene transcription when they are located in the coding region but a negative effect if they are located in the promoter of the gene [Vakoc, 2005].

Histone modification profiles allow the identification of distal enhancer regions, as they show relative H3K4me1 enrichment and H3K4me3 depletion. Interestingly, the chromatin patterns at enhancer regions seem to be much more variable and cell type specific than chromatin patterns at core promoter or insulator regions. Enhancer regions also show enrichment for H3K27 acetylation, H2BK5me1, H3K4me2, H3K9me1, H3K27me1 and H3K36me1, suggesting redundancy in these histone marks.

5. Histone Modifications

Histone PTMs comprise diverse chemical types, primarily acetylation, methylation, phosphorylation, and ubiquitination. Posttranslational modifications to histone tails govern the structural status of chromatin and the resulting transcriptional status of genes within a particular locus. These modifications are reversible and controlled by a group of enzymes. Usually, those enzymes that create histone modifications are called "writers," such as histone acetyltransferases, histone methyltransferases, and kinases, while enzymes that eliminate histone modifications are called "erasers," such as histone deacetylases, histone demethylases, and phosphatases **(Figure 4)**. These counteracting histone-modifying enzymes usually work in

a site- and type-specific manner to establish certain histone PTM patterns along the chromatin fiber. In addition, large families of "reader" modules exist in the cell to specifically recognize histone PTMs or their combinations, by specific PTM-binding domains thereby functioning to translate the "histone code" to particular downstream events. About fifteen distinct structural folds of histone-binding modules have been identified so far. These modules contain various domains, such as chromo, PHD, Tudor, WD40, ADD, MBT, and Zf-CW. Thus, there is an abundance of writers, erasers, and readers that determine the dynamics of histone modifications and subsequently their effects on various processes [Musselman, 2012; Patel, 2013; Wysocka, 2006; Bannister 2001; Taverna, 2007; Vermeulen, 2010; Bartke, 2010 Mujtaba, 2007; Maurer-Stroh, 2003; Champagne, 2009].
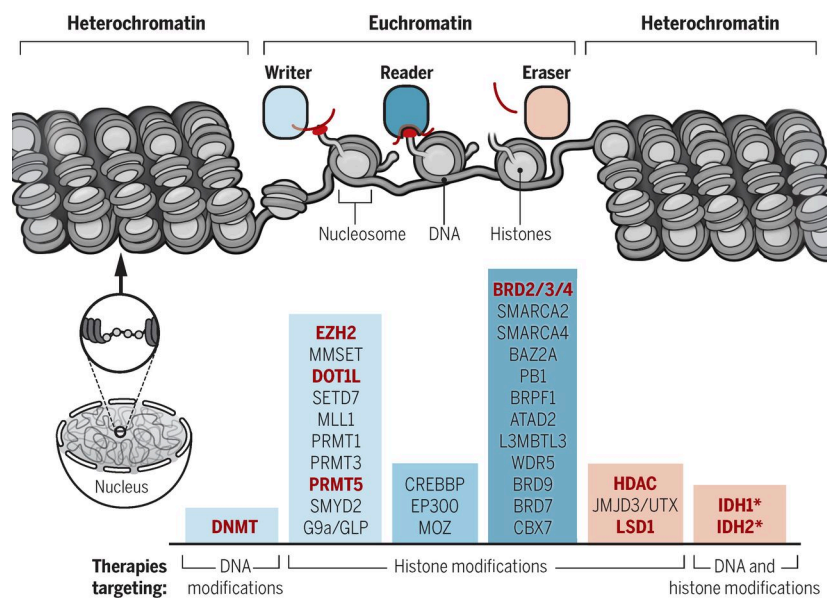
Figure 4. **Writers, erasers, and readers in epigenetics.** Adapted from Dawson. Science 2017.

In contrast to DNA methylation that is generally linked to gene silencing, histone modifications can be associated with either transcriptional repression or activation.

Particularly, variations in acetylation/ deacetylation and methylation/ demethylation patterns at several histone residues (mainly studied those of histones H3 and H4) play essential roles in conferring defined transcriptional potential **(Figure 5)** [Jones, 2005].

The acetylation of histones H3 and H4 mediated by the HATs leads to opening of the chromatin, providing local access of transcription factors and other proteins to the regulatory regions of genes and enabling the active histone code. On the contrary, deacetylation of the lysine residues, mediated by HDACs, results in the compaction of chromatin, rendering it inaccessible to transcription factors and leading to the establishment of a silenced histone code [Thiagalingam, 2003].

Other less well-characterized PTMs, include phosphorylation, SUMOylation, deamination, and ubiquitination. Histone phosphorylation on residues such as serines, threonines, and tyrosines is also a highly dynamic process that is regulated by kinases and phosphatases. Protein kinases, classified into groups based on substrates they act upon, transfer phosphoryl groups from ATP to the hydroxyl groups of the residues, which add negative charges. This ultimately can lead to significant changes in chromatin structure, and consequently has been shown to play roles in processes such as mitosis, apoptosis, and gametogenesis [Perez-Cadahia, 2010; Sawicka&Seiser, 2012]. Phosphorylation of histone H3 on at least two serine residues (Ser10 and Ser28), and on Thr11, is associated with chromosome condensation and segregation during mitosis and meiosis. Phosphatases, also subdivided based upon their substrate specificity, remove phosphate groups, and as a consequence influence chromatin structure [Clayton, 2000; Cerutti&Casas-Mollano, 2009; Khan, 2013; Healy, 2012].

Deimination is a reaction catalyzed by PADI4 that converts arginine, to a citrulline, neutralizing the positive charge of arginine [Cuthbert, 2004].

Another component of the histone code involves the ubiquitination of C-terminal lysine residues of histones H2A and H2B. This modification is added via the sequential action of three enzymes, E1, E2, and E3, and is removed via a de-ubiquitin isopeptidase. It is involved in gene silencing, as well as transcriptional initiation and elongation. Although polyubiquitination targets proteins for degradation by the proteosome, mono-ubiquitination is a stable protein modification that does not affect the half-life of the protein [Cole, 2014; Davie&Murphy, 1990; Wright, 2012].

The small ubiquitin-related modifier (SUMO) can also reversibly modify transcription factors, cofactors, and chromatin-modifying enzymes such as HDACs. SUMOylation of HDAC1 increases both its deacetylase activity and its transcriptional repressor activity. This PTM can prevent the acetylation and ubiquitylation at specific lysine residues, and has been linked to transcriptional repression [Shiio&Eisenman, 2003; Dhall, 2014].

Mono- and poly-ADP ribosylation has been known to occur on histone glutamate and arginine residues. The addition of poly-ADP ribosylation occurs via the poly-ADP-ribose polymerase (PARP) family of enzymes, and the poly-ADP-ribose-glycohydrolase family of enzymes catalyzes the removal of the mark. As this PTM confers a negative charge, it has been generally linked to a relaxed chromatin state, and therefore to transcriptional activation. Histone mono-ADP-ribosylation occurs via the mono-ADP-ribosyltranferases, and has been linked to the DNA damage response as this modification is increased upon DNA damage [Allis, 2007; Messner&Hottiger, 2011; Rouleau, 2010].

Lastly, O-GlcNAc is a histone PTM that occurs on serine and threonine residues. This PTM is added via the O-GlcNAc transferase that utilizes the donor substrate UDP-GlcNAc, and is removed via the β-N-acetylglucosaminidase [Sakabe, 2010].

The large number of histone modifications and the possible interplay between them led to the proposition of the so-called "histone code hypothesis" in which "multiple histone modifications, acting in a combinatorial or sequential fashion on one or multiple histone tails, specify unique downstream functions". There are multiple ways by which cross-talk between modification marks are though to occur. One way is that there could be competition for modifications at one particular residue. Another way cross-talk can occur is if the addition of one modification mark is dependent on the addition of another modification mark. Cross-talk can also occur if a modification mark disrupts or enhances the binding of a protein to another modification mark. Any particular histone modifying enzyme's activity can also potentially be perturbed if a particular modification results in its gene activation or repression. Lastly, cross-talk occurs if modifications work in a cooperative manner in the recruitment of a specific factor. Such cross-talk between histone modifications can be further influenced by the effects of DNA methylation, underscoring the potential for complexity in epigenetics [Bannister, 2011].

Global alterations in histone modifications have been associated with cancer. Global hypoacteylation of H4 in a number of cancer types is mediated by the overexpression of HDACs, leading to the aberrant repression of transcriptional activity [Halkidou, 2004]. Furthermore, histone methylation patterns throughout the genome are often altered during tumorigenesis. Aberrant increases in H3K9 or H3K27 methylation result in the repression of key genes; similarly, cancer specific decreases in promoter H3K4 methylation have also been found at these repressed loci [Valk-Lingbeek, 2004, Cloos, 2008, Fraga, 2005]. These changes are mediated by perturbations to either the HMTs responsible for placing these marks, or the KDMs responsible for removing them. For example, overexpression of the H2K27 methyltransferase EZH2 has been observed in a number of cancers [Valk- Lingbeck, 2004]. Similarly, overexpression of the H3K4 demethylases KDM1A and the KDM5 family of

proteins have also been described in several cancer types **(Figure 5)** [Hosseini&Minucci, 2017]. The role of the KDM1A (LSD1) proteins in tumorigenesis will be discussed in greater detail in the following sections.

6. Histone methylation

6.1. Histone methyltransferases

Histone methylation is due to the action of histone methyltransferases that are divided into two major families based upon their amino acid substrate, the lysine methyltransferases (KMTs) and arginine methyltransferases (PRMTs) [Copeland, 2009; Bedford, 2005]. Methylation is unique among the histone post-translational modifications because up to three methyl groups can be added to a single lysine residue. Arginine can be methylated with one or two groups, and the dimethylated form can occur in a symmetrical and asymmetrical conformation, Lysine, on the other hand, can undergo mono, di and tri- methylation [Barski, 2007]. The functional consequences of the different degree of methylation result in various biological outcomes including transcriptional activation, elongation or repression, imprinting, DNA replication and DNA-damage repair. These enzymes transfer a methyl group, from the cofactor S-adenosyl-L-methionine (SAM) to either the ε-amino group of lysine or to the guanidino group of arginine, and is mainly found on histones H3 and H4.

Enzymes acting on arginine belong to the protein arginine methyltransferases PRMTs family. Nine enzymes that catalyze arginine methylation have been described and include PRMT1, PRMT2, PRMT3, CARM1, PRMT5, PRMT6, PRMT7, PRMT8 and PRMT10 [Di Lorenzo, 2011; Richon, 2011]. Generally, arginine methyltransferases are divided into two different classes: type I and type II. The type II enzymes (PRMT 5, 7, and 9) catalyze mono- and di-symmetric methylation of the arginines (R), whereas, the formation of mono- and di-

asymmetric tails is achieved by type I enzymes (PRMT 1–4, 6, and 8).

KMTs have been grouped in two main different classes: lysine-specific SET domain containing histone methyltransferases, characterized by a 130-amino-acid catalytic domain known as SET [Su(var)3-9, Enhancer of Zeste, Tritorax], and the non-SET-containing lysine methyltransferases (the DOT1 family) [Allis, 2007]. DOT1 methylates lysine-79 within the core domain of H3 only in nucleosomal substrates and not in free histones [Feng, 2002]. The SET domain containing KMTs catalyze mono-, di-, and trimethylation of their target lysine residue localized on histone tails and are classified into six subfamilies: SET1, SET2, SUV39, EZH, SMYD, and PRDM. Of note, a small number of SET-containing KMTs that do not fall into the above six subfamilies due to an absence of conserved sequences flanking their SET domains include Set8/PR-Set7, SUV4-20H1, and SUV4-20H2, Set7/9, as well as MLL5, RIZ (retinoblastoma protein-interacting zinc-finger) and SMYD3 (SET- and MYND-domain containing protein 3) [Allis, 2007].

While histone acetylation generally correlates with transcriptional activation, histone methylation can be either an activating or repressive mark, depending on the location and degree of methylation. The most studied histone lysine methylation sites are H3K4, H3K9, H3K27, H3K36, H3K79 and H4K20. Methylations of histone H3 at lysine 4, 36 and 79 are generally considered as activation marks, whereas methylations on histone H3 lysine 9, 27 and H4K20 are linked to repression **(Figure 5)** [Martin, 2005]. It is worth mentioning that the final effect on transcription and chromatin structure is not strictly dependent in most cases on one single histone modification, but it influenced by the interplay of several histone modifications together [Martin, 2005].
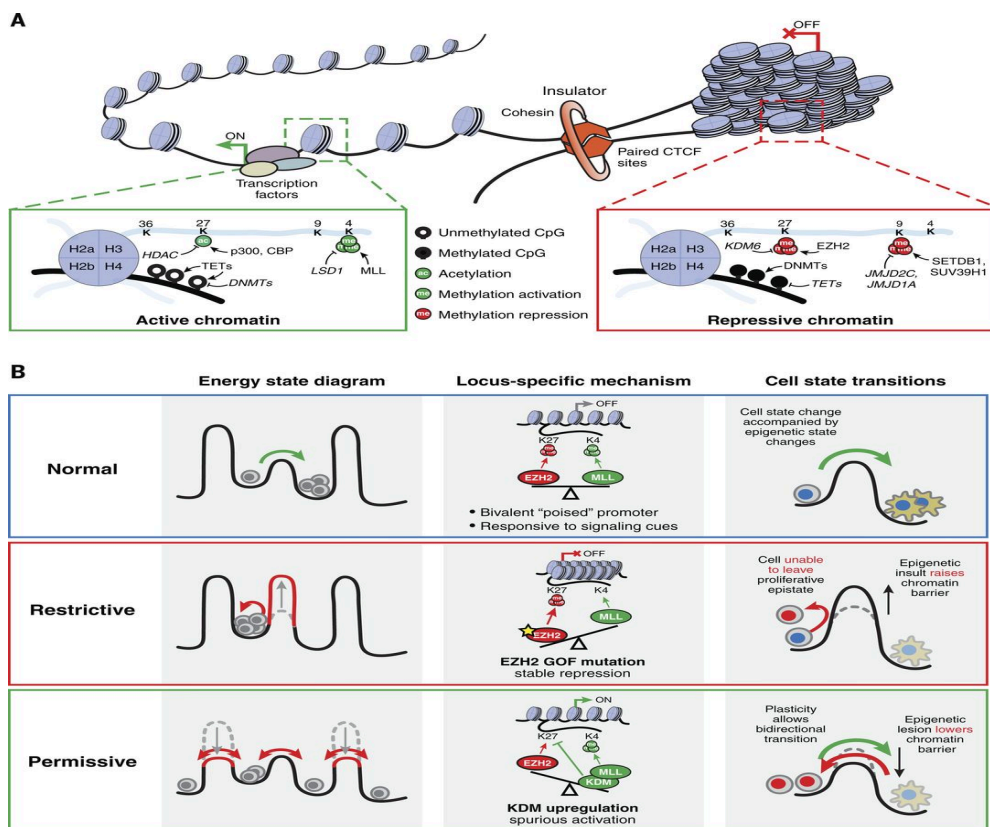
Figure 5. **Histone modifications affect chromatin structure and cellular identity.** (A) Active chromatin are enriched for H3K27ac and H3K4me3. Repressive chromatin are enriched for H3K27me3 and H3K9me3. (B) Chromatin modification reinforce cell states and affect responsive to external and internal signals. Normal chromatin facilitates appropriate responses to development or environmental signal. Genetic, environmental and metabolic insults that disrupt chromatin can lead to either restrictive or overly permissive chromatin states. Adapted from Flavahan et al. Science 2017.

H3K4 methylation is associated with an open chromatin structure which enables access to transcription factors **(Figure 5)** [Sims, 2006]. There are at least 13 H3K4 human methyltransferases (KMT2A (MLL1), KMT2D (MLL2), KMT2C (MLL3), KMT2B (MLL4), KMT2E (MLL5), KMT2H (Ash1), KMT7 (Set7/9), KMT2F (Set1A), KMT2G (Set1B), KMT3D (SMYD1), KMT3C (SMYD2), KMT3E (SMYD3) and KMT8B(PRDM9)) that are activators of gene expression [Hamamoto, 2004; Abu-Farha, 2008; Tan, 2006; Ruthenburg, 2007; Kouzarides, 2007]. H3K4 methylation generally can be found at transcription start sites (TSS) and on genes that are maintained in a transcriptionally poised state [Barski, 2007].

Methylation of histone 3 at Lysine 9 is generally associated with transcriptional silent chromatin. Seven methyltransferases (KMT1C (G9a), KMT1D (, GLP), KMT1A (Suv39H1), KMT1B (Suv39H2), KMT1E (SETDB1), KMT1F (SETDB2), and KMT8 (PRDM2)) known to act upon this mark. Methylation of H3K9 is generally associated with transcriptional repression but monomethyl H3K9 is associated with active promoters surrounding the TSS [Barski, 2007]. H3K9 methylation also is a hallmark of both facultative and constitutive heterochromatin [Krishnan, 2011].

EZH1 and EZH2 are catalytic subunits of polycomb repressive complex 2 (PRC2) deposit methyl group onto H3K27 [Margueron 2008]. The genome-wide analyses of histone modifications in ES cells have identified H3K27me3-enriched gene promoters that are also associated with H3K4me3 marks and are, therefore, called bivalent domains. The genes that have bivalent promoters in ES cells are associated with the developmentally regulated loci which are kept repressed in the pluripotent cells, but their fates are determined in the course of development. This can be achieved by resolving into a monovalent structure in the course of differentiation in which the resolution to H3K4me3 mark results in transcriptional activation and the resolution to H3K27me3 mark results in a more stable repression. Therefore, the chromatin conformation of bivalent promoters keeps them poised for fate determination at the later stages of differentiation [Bernstein, 2006]. Moreover, their dysregulation can cause different types of cancers.

H3K36 methylation is catalyzed by at least six methyltransferases (KMT3B (NSD1), KMT3F (NSD2), KMT3G (NSD3), KMT3C (SMYD2), KMT3A (SETD2), and SETMAR) which is an activating mark [Li, 2009]. Dysregulation of H3K36 methylation has been observed in several cancers [Angrand 2001; Wang 2007].

Unlike other histone modifications that are situated in the N-terminal histone tails, H3K79

methylation which is catalyzed by DOT1L, occurs on the core of histone H3 [Gao, 2007]. H3K79 is supposed to regulate positively gene expression. DOT1L is linked to oncogenic transformation in MLL-rearranged leukemias. MLL fusion proteins, by recruiting DOT1L, increase transcription of MLL fusion target genes [Krivtsov, 2007]. All the histone methyltransferases mentioned above methylate lysine at histone H3 but KMT5A (SETD8), KMT5B (Suv420H1), KMT5C (Suv420H2), and KMT3B (NSD1) methylate histone H4 at lysine 20 which are considered as transcriptional repressors [Kouzarides, 2007].

Histone methylation represents a mechanism of "marking" the histone in order to recruit several effector proteins with recognition domains specific for different methylated lysine residues. For instance, plant homeodomain (PHD) of bromodomain-PHD transcription- factor (BPTF) binds to H3K4 trimethylated/dimethylated (H3K4me3/me2) and recruits the nucleosome remodeling factor (NURF) complex to the target gene leading to gene activation. In contrast, the chromodomain of heterochromatin protein 1 (HP1) binds H3K9 trimethylated (H3K9me3) leading to heterochromatin formation and gene silencing [Yun, 2011].

6.2. Histone demethylases

Histone methylation is a dynamic modification with enzymatic conversion of methylated arginine residues to citrulline and with lysine demethylases that can remove the mono-, di- and tri-methylated groups from lysine.

The peptidyl-arginine deiminases (PADs) catalyse the hydrolysis of the guanidino arginine side chain to the urea group of citrulline. There are two peptidyl-arginine deiminases, PAD2 and PAD4 which catalyse citrulline formation at multiple positions on histone tails [Zhang, 2012; Wang, 2004]. Furthermore, the Jumonji family of histone demethylases is able to

demethylate tri-methylated form of H3 as well as methylated arginine residues.

Lysine demethylating enzymes have been subdivided into two main families: KDM1 (lysine (K) demethylase 1) family which are FAD-dependent amine oxidases, acting only on mono- and dimethylated lysine [Mosammaparast 2010], and the JMJC domain contain proteins which are Fe(II) and 2-oxoglutarate-dependent enzymes able to remove all methylation states [Hausinger, 2004; McDonough, 2010; Klose, 2007].

The first KDM family, lysine-specific demethylase 1 (LSD1) and LSD2 (also known as KDM1B or AOF1), are flavin-dependent amine oxidase domain-containing enzymes [Shi, 2004]. Subsequent to the discovery of LSD1, another family of more than 30 histone demethylases structurally different from LSD1 was described, all of which sharing a motif designated the Jumonji C (JmjC) domain and revealing a substrate specificity [Kooistra, 2012]. These Fe(II) dependent enzymes catalyze the demethylation of mono-, di- and trimethylated lysines using 2-oxoglutarate and oxygen, converting the methyl group in the methyllysine to a hydroxymethyl group, which is subsequently released as formaldehyde [Tao 2014; Pappano 2015; Sun 2014; Rodriguez-Paredes 2014]. The JMJC domain-containing proteins, comprising more than 30 proteins of which 15 have confirmed demethylase activity, are divided into subfamilies based on sequence similarity: KDM2 (FBXL), KDM3 (JMJD1), KDM4 (JMJD2/JHDM3), KDM5 (Jarid1), KDM6(UTX/JMJD6), KDM7 and Jumonji clusters.

KDM1A (LSD1), KDM1B (LSD2), KDM2B (JHMD1B), KDM5A (JARID1A), KDM5B (JARID1B), KDM5C (JARID1C) and KDM5D (JARID1D)) are transcriptional repressors by demethylating K4 at H3.

Seven demethylases (KDM1A (LSD1), KDM3A (JHDM2a), KDM3B (JHDM2b), KDM4A

(JHDM3A), KDM4B (JMJD2B), KDM4C (JMJD2C), and KDM4D (JMJD2D)) known to demethylate Lysine 9 at histone 3.

Demethylation of H3K27 is principally carried out by UTX (KDM6A) and JMJD3 (KDM6B) and results in the activation of gene expression. several mechanisms leading to increased H3K27me3 such as EZH2 overexpression, EZH2 gain of function mutation, UTX loss of function mutations and PRC2 subunit overexpression are associated with many human cancers. Additionally, a close association between H3K27 methylation patterns and DNA methylation have been described, as promoter regions marked by H3K27 methylation, and/or bivalent chromatin in ES cells are commonly aberrantly DNA hypermethylated in cancer.

H3K36 methylation erased by at least 6 demethylases (KDM2A (JHDM1a), KDM2B (JHDM1b), KDM3A (JHDM3A), KDM4B (JMJD2B), KDM4C (JMJD2C), and KDM8 (JMJD5)).

As with the lysine methyltransferases, the histone demethylases possess a high level of substrate specificity with respect to their target lysine and appear sensitive to the degree of lysine methylation. The substrate specificity of histone demethylase can be further influenced by the association of additional proteins. For example, the specificity of LSD1 for H3K9 when in complex with steroid receptors changes to H3K4 when the protein is in a complex with Co-Rest [Metzger, 2005]. Interestingly, this substrate switching also correlates with a switching of the role of LSD1 from activator to repressor of gene transcription.

Identification of these enzymes opened a new era in understanding how chromatin dynamic is regulated and a further understanding of the regulation of these enzymes will provide significant insight into fundamental mechanisms of many biological processes and human diseases including cancers **(Figure 6)**.
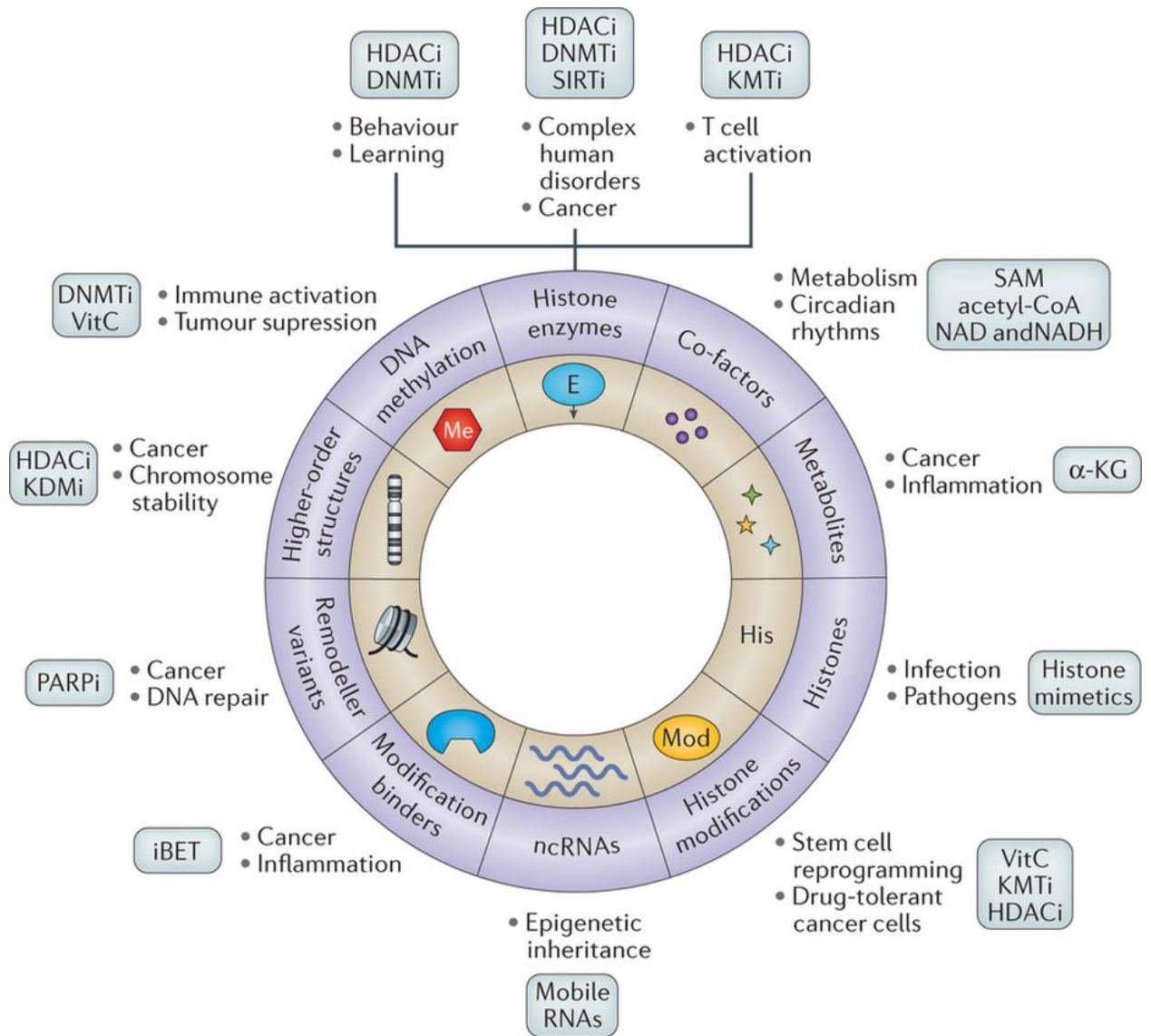
Figure 6. **Molecular hallmarks of epigenetic control.** Deregulation of the epigenome is an important mechanism involved in the development and progression of human diseases such as cancer. Adapted from Allis et al. Nat Rev Genet 2016.

Deregulation of the epigenome is an important mechanism involved in the development and progression of human diseases such as cancer. As opposed to the irreversible nature of genetic events, which introduce changes in the primary DNA sequence, epigenetic modifications are reversible and can be pharmacologically targeted **(Figure 6)**.

7. Lysine-specific demethylase 1 (LSD1)

Discovered a decade ago, lysine-specific demethylase 1 (LSD1) was the first histone demethylase reported. The discovery of LSD1 disproved the notion that histone methylation is a stable and static modification. Since then, other histone demethylases have been identified, such as LSD2. The LSD family is composed of only two members: LSD1(KDM1A, AOF2) and LSD2(KDM1B, AOF1). LSD1 is a flavin-containing amine oxidase that, by reducing the cofactor FAD, catalyzes the cleavage of the α-carbon bond of its substrate to generate an imine intermediate. The imine intermediate spontaneously hydrolyzes to release a formaldehyde molecule resulting in a mono-methylated lysine. This H3K4me1 can also undergo the same reaction to become unmethylated [Forneris, 2005; Edmondson, 2007].
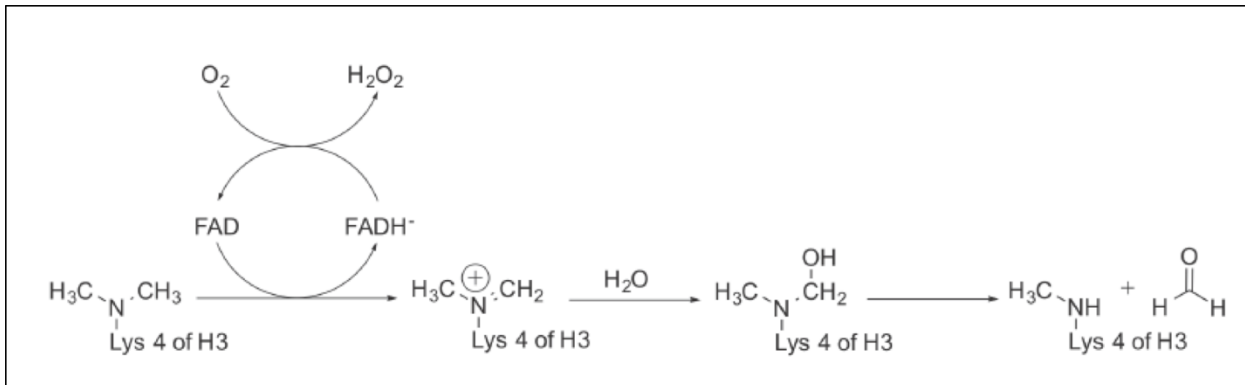
Figure 7. **Mechanism of lysine demethylation catalyzed by LSD1.**

Three methyl groups from H3K4 cannot be cleaved by LSD1 due to a requirement of an electron pair on the lysine amino group in the first step of the LSD1 demethylation reaction, which involves an oxidation by FAD of the amine to an iminium cation intermediate [Højfeldt, 2013].

The second step of the LSD1 demethylation reaction involves the attack of the iminium cation by a water molecule, after which the formed hemiaminal collapses to release the demethylated

substrate and a formaldehyde molecule. The reduced cofactor, FADH, is then re-oxidized back to FAD by molecular oxygen, releasing hydrogen peroxide as a byproduct **(Figure 7)** [Forneris, 2005; Edmondson, 2007].

7.1. Structure of LSD1

LSD1 is highly conserved in organisms ranging from Schizosaccharomyces pombe to human. LSD1 crystal structure consists of three major domains with 852 amino acids: The N-terminal SWIRM (Swi3p/Rsc8p/Moira) domain, a C-terminal AOL (amine oxidase-like) domain, and a central protruding Tower domain **(Figure 8)** [Chen, 2006]. The SWIRM and the AOL domains are tightly knit through hydrophobic interactions, forming the core structure of LSD1 while the Tower domain consists of a pair of long helices that adopts a typical antiparallel coiled-coil conformation. The SWIRM domain is thought to bind LSD1 to the nucleosome through its interaction with DNA [Anand, 2007]. The AOL domain folds into a compact structure which shares structural topologies with other flavin-containing monoamine oxidase(MAO) enzymes [Rotili, 2011]. The AOL domain, separated into two lobes by a 105 aa Tower domain insert, is the catalytic domain. One lobe of the AOL binds FAD, while the other lobe of the AOL binds the substrate. The space between these two sub-modules defines a large and deep pocket where the process of demethylation takes place [Zheng, 2015].

The Tower domain acts as hub for the interaction with other protein, such as the RE1-silencing transcription factor corepressor 1 (CoREST or RCOR1), owing to that LSD1 is able to express its demethylating activity on nucleosomal substrates and to be protected from proteosomal degradation. The Tower domain by itself is sufficient for a stable interaction with CoREST, in fact a deletion mutant of LSD1 (LSD1ΔTower), in which the Tower domain was replaced by a pentaglycine loop, is unable in reducing the methylation level at K4 on histone H3. These evidences indicate that the SWIRM and AOL domains of LSD1 do not significantly

45

contribute to the interaction with CoREST and that the tower domain represents the binding site for it as well as for other molecular partners. In addition to the three domains, LSD1's N-terminal region has recently been found to also play an important role. The N-terminal SWIRM domain seems to be important to localize LSD1 to the nucleus [Hou, 2010; Wang, 2007; Stavropoulos, 2006].
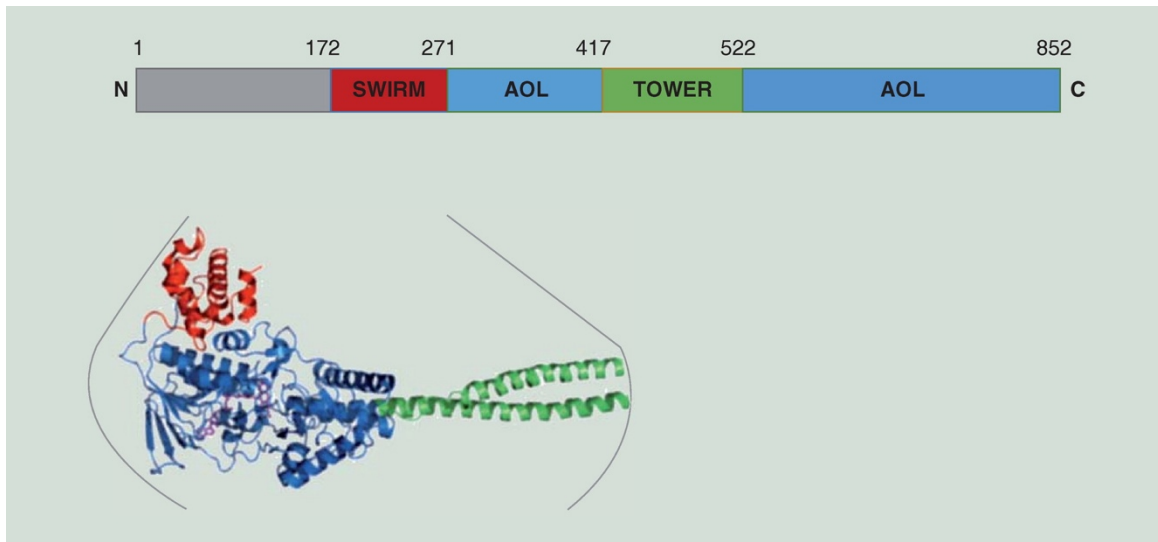
Figure 8.**Structure of lysine-specific demethylase1.** The SWIRM and the AOL domains are tightly knit through hydrophobic interactions, forming the core structure of LSD1. AOL domain (blue), SWIRM domain (red), TOWER domain (green). Adapted from Hosseini&Minucci. epigenomics 2017.

7.2. LSD1 functions as a context-dependent transcriptional co-regulator

LSD1 plays a central role in several key cellular processes in normal and cancer cells such as control of stemness, differentiation, cell motility, epithelial-to-mesenchymal transition and metabolism. To achieve these multiple biological functions, LSD1 through its presence in multi-protein complexes and its association with different partners acts as a context-dependent co-regulator, being able to act as either a co-activator or co-repressor **(Figure 9)**. Additionally, LSD1 has been found to be part of transcription elongation protein complexes that act as both transcriptional activators and repressors, including the MLL and the ELL complexes [Biswas, 2011; Nakamura, 2002].

Four mammalian isoforms of LSD1 have been described as resulting from single or double inclusion of two alternatively spliced exons, E2a and E8a. The inclusion of exon 8a has been reported to generate a docking site that facilitates an interaction between supervillain (SVIL) and LSD1 to convert LSD1 into an H3K9 demethylase during neuronal differentiation [Toffolo, 2014]. A neuronal-specific LDS1 isoform which results from an alternative splicing is associated with altered substrate specificity towards histone H4K20 [Zibetti, 2010; Wang, 2015]. This shows the diversity of different interactions LSD1 can have, all of which are in need of further study to decipher the full extent of LSD1's role in each complex.

In addition, other post translational modifications of histones affect the LSD1 H3K4 demethylase activity: in fact, H3K9 acetylation and H3S10 phosphorylation negatively affect the H3K4 demethylase activity of LSD1 [Lee, 2006; Shi, 2005].
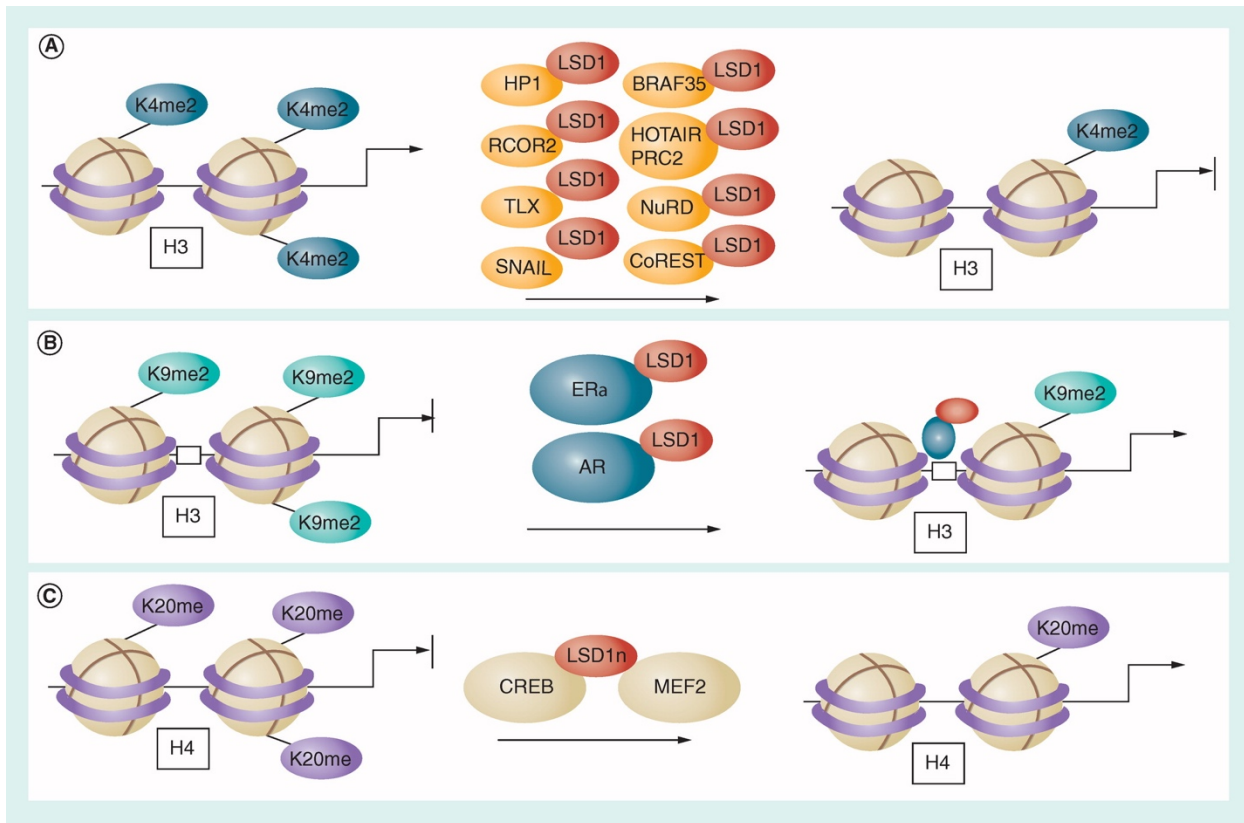
Figure 9. **LSD1 functions as a context-dependent transcriptional co-regulator.** (A) LSD1 act as a co-repressor. (B) LSD1 act as a co-activator. (C) A neuronal-specific LSD1 isoform. Adapted from Hosseini&Minucci. epigenomics 2017.

7.3. LSD1 as a transcriptional co-repressor

Complexes containing LSD1 that act as repressors of transcription include CoREST and NuRD. Originally LSD1 was identified as a component of transcriptional repressor complexes comprising transcriptional co-repressor protein (CoREST) and HDAC1/2 [Klose, 2007; Hakimi, 2003]. Several other transcription factors have been described that recruit LSD1 to their target genes. Recruitment of LSD1 is mediated by its ability to bind to the SNAG domain of the transcription factors such as GFI1, GFI1b, SNAI1, SNAI2 and INSM1. The sequence of the SNAG domain mimics that of the N-terminus of histone H3 for binding to the catalytic

cavity of LSD1 [Lin, 2010]. LSD1 regulates specific cell processes such as control of stemness, differentiation, cell motility, epithelial-to-mesenchymal transition and metabolism through its co-repressor function. Such studies show the extensive range of roles LSD1 can participate in, as well as potential use of LSD1 inhibitors against various serious diseases.

7.3.1. Role of LSD1 in hematopoietic differentiation

LSD1 plays many roles in hematopoiesis, mainly by binding to the regulatory regions controlling the expression of key hematopoietic factors and regulating their expression, depending on the differentiation stage. Mechanistically, LSD1 and its CoREST partners control differentiation of various hematopoietic lineages in association with growth factor independence (Gfi)-1, (Gfi)-1b and TAL1. These transcription factors (TFs) control hematopoietic-restricted gene expression by interacting with several co-repressors. In hematopoietic cells, two other CoREST (RCOR1) paralogs have been found to bind LSD1 including RCOR2 and RCOR3. RCOR2 acts as CoREST where it facilitates LSD1-mediated demethylation of H3K4. On the other hand, RCOR3 competitively inhibits LSD1 demethylation of H3K4, ultimately inhibiting differentiation of the hematopoietic cells, indicating that LSD1 and RCOR1/3 levels play a role in differentiation [Upadhyay, 2014].

7.3.2. Role of LSD1 in development and stem cell maintenance

LSD1 plays a crucial role in higher eukaryotes as genetic deletion of LSD1 from mice has been shown to result in embryonic lethality, with the arrest of embryonic development at or before embryonic day 6. Embryonic stem cells derived from LSD1 knockout mice revealed severe growth impairment due to increased cell death, impaired cell cycle progression and defects in differentiation [Wang, 2009; Wang, 2007]. LSD1 is highly expressed in undifferentiated human embryonic stem cells (ESCs) and is down regulated during

differentiation. LSD1 contributes to repression of lineage specific developmental programs and is involved in the maintenance of pluripotency by regulating the critical balance between H3K4 and H3K27 methylation at the regulatory regions of key genes such as *BMP2* and *FOXA2* [Adamo, 2011; Foster, 2010]. Moreover, LSD1 regulates the expression and appropriate timing of key developmental regulators during early embryonic development. LSD1 also serves as a key regulator of neural stem cell proliferation via modulation of TLX signaling and demethylation of TLX target gene promoters including the *PTEN* tumor suppressor gene and cell cycle-related factors such as p21, a cyclin-dependent kinase inhibitor [Sun, 2010; Hakimi, 2002; Ballas, 2005]. The constitutive transrepressor TLX forms a complex with LSD1-CoREST-HDAC1 via interactions with the amine oxidase and SWIRM domains of LSD1, and this interaction is indispensable for Y79 retinoblastoma cells proliferation through regulation of PTEN expression [Yokoyama, 2008]. In addition, LSD1 is required for stem cell maintenance and proper differentiation of several other cell types, such as skeletal muscle, adipogenesis, anterior pituitary gland, and for normal function of oocytes and bone marrow cells [Kim, 2015; Musri, 2010; Choi, 2010].

7.3.3. Role of LSD1 in epithelial–mesenchymal transition (EMT)

The process of epithelial–mesenchymal transition (EMT), that is the acquisition by epithelial cells of the phenotype of mesenchymal cells, is required for cancer cell invasion and metastasis [Lamouille, 2014]. It has been proposed that LSD1 is involved in the regulation of EMT in breast cancer. By binding to SNAI1, LSD1 represses the expression of E-cadherin, via H3K4 demethylation [Ferrari-Amorotti, 2013]. NURD regulates several cellular signaling pathways that are critically involved in cell proliferation, survival, and epithelial-to-mesenchymal transition. In the NuRD complex, or the nucleosome remodeling and deacetylation complex, LSD1 is clustered with HDAC1/2, a chromodomain containing DNA-

binding helicase protein (CHD3 or CHD4), a metastasis tumor antigen (MTA) relative called MTA2, BRCA2, and a few other proteins. Such complexes have been shown to protect LSD1 from degradation, bind it to chromatin, and allow LSD1 to recognize nucleosomes as substrates, as in vitro, LSD1 is efficiently able to demethylate core histones but not nucleosomes [Lee, 2005; Shi, 2005].

7.3.4. Role of LSD1 in cell metabolism

Regarding metabolic control, inhibiting LSD1 has been shown to stimulate de novo glucose synthesis and reduce intracellular glycogen regulation. Cancer cells undergo a metabolic shift from mitochondrial to glycolytic metabolism, in order to maintain their proliferative potential [Pan, 2013]. In pancreatic cancer and hepatocellular carcinoma (HCC) cells, LSD1 is required for the glycolytic shift [Sakamoto, 2015; Qin, 2014].

In lipid homeostasis, Prospero-related homeobox (Prox1) can interact with LSD1 to recruit LSD1 to repress CYP7A1 gene expression. As CYP7A1 is responsible for catalyzing the first step in bile acid synthesis in the liver, targeting LSD1 can impact lipid regulation [Ouyang, 2013]. In addition, blood pressure sensitivity to dietary salt intake was found to be affected by LSD1 by the alteration of renal Na^+ handling [Krug, 2013]. Additionally, it was found that feeding mice a high-fat diet increased levels of LSD1 in the white adipose tissue and induced mitochondrial activity to regulate metabolism, ultimately limiting weight gain. This has linked LSD1 to metabolic adaptation in white adipose tissues as there was LSD1- dependent expression of genes, such as those involved in oxidative phosphorylation, which promoted the formation of islets of metabolically active brown-like adipocytes in white adipose tissue [Duteil, 2014].

7.4. LSD1 as a transcriptional co-activator

Complexes containing LSD1 that act as activators of transcription include androgen or estrogen receptor complexes. In such complexes, LSD1 has been proposed to change its substrate specificity from H3K4me2 to H3K9me2, activating gene transcription, as unmethylated H3K9 is usually associated with active transcriptional states [Garcia-Bassets, 2007; Metzger, 2005]. To change the substrate specificity of LSD1, the hormone receptors have been suggested to induce a change in the structure of the active site of LSD1. How this might happen is puzzling as structures of LSD1 and H3K4 substrate analogs show well-defined molecular recognition for the major H3K4 substrate. One protein that has been hypothesized to influence LSD1's substrate specificity is the proline glutamic acid and leucine-rich protein 1, PELP1, which was reported to bind concurrently to an estrogen receptor, ERα, and LSD1, facilitating LSD1-catalyzed demethylation of H3K9 [Yang, 2006; Nair, 2010]. Metzger et al. demonstrated that, following hormone treatment, AR and LSD1 colocalize on promoters in both normal human prostate and prostate tumor and stimulate H3K9 demethylation without altering the H3K4 methylation status, and promote ligand dependent transcription of AR target genes thus resulting in enhanced tumor cell growth [Metzger, 2005]. Another mechanism that has been reported to switch LSD1 demethylation specificity from H3K4me2 to H3K9me2 involves the action of protein kinase C, which is recruited to the androgen nuclear receptor target promoters, and is then able to phosphorylate Thr6 of histone H3 after hormone treatment [Wissmann, 2007; Hu, 2009]. Additionally, LSD1 actions release hydrogen peroxide, that in turn drive the recruitment of base excision repair enzymes that can loop chromatin and allow LSD1 to access H3K9me2 [Perillo, 2008]. This is an underexplored mechanistical aspect of LSD1 function that deserves further analysis. Other H3K9-specific histone demethylases could be recruited by LSD1. For example, JMJD2C

colocalizes with androgen receptor and LSD1 in normal prostate and in prostate carcinomas. JMJD2C and LSD1 interact and both demethylases cooperatively stimulate androgen receptor-dependent gene transcription [Wissmann, 2007].

7.5. Nonhistone substrates of LSD1

LSD1 also demethylates non-histone proteins, including P53, DNA methyltransferase 1 (DNMT1), transcription factors like E2F1 and STAT3, the myosin phosphatase MYPT1, modulating their cellular activities [Huang, 2007; Kontaki, 2010; Yang, 2010; Cho, 2011]. LSD1 can directly interact with P53 to confer P53-mediated transcriptional repression. These findings reveal that LSD1 is targeted to chromatin by P53 in a gene-specific manner, and define a molecular mechanism by which P53 mediates transcriptional repression. LSD1 blocks the pro-apoptotic activity of P53 and represses P53-mediated transcriptional activation by demethylating the dimethylated lysine 370 residue which is required for efficient binding to the transcriptional co-activator p53-binding protein-1(53BP1). This activity of LSD1 implies the involvement of LSD1 in the DNA damage response pathway via modulation of P53 activity [Huang, 2007]. LSD1 also regulate DNA damage induced cell death in P53-deficient tumor cells via protection of E2F1 (E2F transcription factor 1) from ubiquitination and degradation [Kontaki, 2010]. LSD1 controls DNA methylation by regulating the methylation status of DNMT1 and modulating its stability. Thus LSD1 coordinates not only histone methylation but also DNA methylation to regulate chromatin structure and gene activity [Wang, 2009]. It has been shown that LSD1 promoted cell cycle progression through Demethylation of MYPT1 at Lys 442 which in turn enhances RB1 phosphorylation [Cho, 2011].

7.6. Role of LSD1 in Cancer

LSD1 could be an attractive target for cancer therapy because of its high level of expression in neuroblastomas, retinoblastoma, prostate, breast, lung, pancreatic, bladder cancers and hematological malignancies.

7.6.1. LSD1 in hematological malignancies

Epigenetic changes are linked to many hematopoietic malignancies, such as acute leukemias, which are disorders where there is an uncontrolled self-renewal, proliferation, and impaired differentiation of leukemic stem cells (LSCs). LSD1 was shown to be essential in regulating LSC by activating LSC associated oncogenic target genes [Somervaille, 2006; Harris, 2012]. Higher expression level of LSD1 in c-kit$^+$ (a marker enriching for cells endowed with self-renewal) AML in comparison with c-kit$^-$ AML cells suggested its down regulation with differentiation and preferential expression in LSCs.

This was further verified by showing that knockdown of LSD1 resulted in AML cell impairment of differentiation and apoptosis, as well as the inability to form colonies and transplanting leukemia in secondary mice recipients *in vivo*, which is consistent with LSC potential loss. Thus, LSD1 inhibition may have promise in combating AML.

The re-expression of genes as a result of LSD1 inhibition in cancer cell lines may antagonize LSD1's role in tumorigenesis, and several studies have investigated these mechanisms. For example, E-cadherin has been shown to re-expressed by chemically inhibiting LSD1 in several human acute myeloid leukemia cell lines [Murray-Stewart, 2014]. Such changes in gene expression show that inhibiting LSD1 may result in the re-expression of important genes that may have the ability to inhibit cancer cell growth. Finally, other reports showed that depletion and inhibition of LSD1 impairs proliferation in Myelodysplastic syndrome (MDSs), acute

erythroleukemia (AEL) and acute megakaryoblastic leukemia (AMKL) by induction of cell differentiation [Sugino, 2017; Ishikawa, 2017].

7.6.2. LSD1 in solid tumors

High levels of LSD1 expression has been proposed as a biomarker for aggressive in hepatocellular carcinoma (HCC), prostate cancer, bladder carcinomas and ER-negative breast cancers. LSD1 is highly expressed in ER-negative breast cancers, and that inhibiting LSD1 results in growth inhibition of breast cancer cells by induction of p21[Lim, 2010]. The bladder cancer cell proliferation was proposed to be due to LSD1 co-localizing with bladder cancer stem cells in the basal layer of bladder carcinoma tissue, ultimately playing a role in maintaining the pluripotency. Lan et al found that LSD1 to be elevated in bladder cancer, and that knockdown of LSD1 suppressed bladder cancer cell lines proliferation [Lan, 2013].

The re-expression of genes as a result of LSD1 inhibition in cancer cell lines may antagonize LSD1's role in tumorigenesis, and several studies have investigated these mechanisms. For example, Knockdown of LSD1 increased E-cadherin expression resulting in suppressed proliferation of non small cell lung cancer (NSCLC) [Nair, 2010]. Additionally, in the HCT116 (colon carcinoma) cell line, tumor suppressors SFRPs and GATA have been implicated [Huang, 2007].

In prostate cancer specimens, LSD1 expression was correlated with known mediators of prostate cancer progression such as VEGF-A. Both siRNA depletion and chemically inhibiting of LSD1 in prostate cancer cells decreased VEGF-A, which blocked androgen induced PSDA and Tmprss2 expression and reduced proliferation of both androgen (LnCaP) and androgen-independent cells (LnCaP: C42, PC3) [Kashyap, 2013].

Consistent with the role of LSD1 in the epithelial-to-mesenchymal transition (EMT), LSD1

expression correlated with metastasis in colon and ovarian cancer. The knockout of LSD1 in colorectal cancer cells (HCT116) resulted in an increased population of cells in the G1-phase of the cell cycle, as well as reduced cell proliferation and tumorigenicity [Jin, 2013; Huang, 2013].

Qin et al found pancreatic cancer patient tissue samples to have increased levels of LSD1 protein levels, and that Knock-down of LSD1 not only repressed proliferation and tumorigenicity of pancreatic cancer cells but also arrested glycolysis, which is critical to sustain the growth of cancer cells. The growth of the pancreatic cancer cells was shown to be due to LSD1 synergizing with the Hypoxia Inducible Factor-1alpha (HIF1alpha), which together maintain the glycolytic process that contribute to increased proliferation [Qin, 2014].

It has been shown that LSD1 plays a role in carcinoma and sarcoma pathology and its elevated level is associated with tumor size, pathological grade, and reduced survival of patients.

Yu et al found high expression of LSD1 to correlate with the severity of esophageal squamous cell carcinoma (ESCC) in patients, as well as dose dependent attenuation in migration of ESCC cells in vitro after LSD1 inhibition [Yu, 2013]. LSD1 was also found to be overexpressed in tongue squamous cell carcinoma samples, rhabdomyosarcoma, synovial sarcoma, chondrosarcoma, Ewing's sarcoma, and osteosarcoma [Yuan, 2014; Bennani-Baiti, 2012]. Taken together, these results are consistent with an oncogenic role of LSD1 in solid tumors as well as hematological tumors, and therefore LSD1 is an intriguing target for novel therapeutics.

7.7. Targeting LSD1

Synthetic inhibitors of LSD1's catalytic activity are predicted to reactivate gene expression of silenced genes, such as tumor suppressors, and thus to be beneficial in the treatment of diseases, including cancer. Motivated by the similarities in the enzymatic properties of LSD1 and MAO-A/B, McCafferty and coworkers screened a focused group of irreversible MAO inhibitors against LSD1. The antidepressants TCP were found to weakly inhibit recombinant LSD1 demethylation of nucleosomes, whereas the propargylamines tested were inactive. Subsequent studies validated that TCP is a covalent, FAD-directed inhibitor of LSD1 and LSD2 with a mechanism of the formation of TCP-FAD adducts, and provided insight to rational design of TCP analogs [Lee, 2006; Schmidt, 2007]. TCP was reported to inhibit the colony forming activity of AML cells in mouse models of MLL-AF9 leukemias. OG86, A TCP derivative, impaired the proliferation potential of murine and human AML cells, accompanied by induction of differentiation. Harris et al. by using two analogs of tranylcypromine which were more potent and selective inhibitors of LSD1, found that these compounds phenocopied both LSD1 KD and TCP treatment [Somervaille, 2009; Somervaille, 2006; Harris, 2012].

The amine oxidase domains of LSD1/2 and MAO-A/B are homologous (37-45% sequence identity). The active sites of LSD1/2 feature an open cleft that accommodates the H3 N-terminal tail and other large substrates, whereas MAO-A/B feature internal cavities that are gated by surface loops. These structural differences have been exploited to design TCP analogs with improved potency and selectivity for LSD1 over MAO-A/B, which is paramount for studies of LSD1 function in diseases. There have since been many different tranylcypromine analogs developed as LSD1 inhibitors. In 2009, Ueda et al first synthesized tranylcypromine analogs that linked a homoserine with the phenyl ring of tranylcypromine

through an ether bond. Such compounds gave IC50 values of 1.9 to 22 μM and showed various cancer cell line growth inhibitory effects [Ueda 2009]. In 2010, Binda et al also synthesized tranylcypromine analogs with additional phenyl rings added to the tranylcypromine phenyl ring through an amide bond. The compounds displayed Ki values as low as 1.1 μM, and showed growth inhibition of acute promyelocytic leukemia cells that acted synergistically with retinoic acid. This cotreatment in NB4 acute promyelocytic leulemia (APL) cells resulted in synergistic inhibition of proliferation through induction of differentiation and apoptosis [Binda, 2010]. TCP also unlocked the ATRA-driven therapeutic response in non-APL AMLs by increasing H3K4me2 level and expression of myeloid-differentiation–associated genes such as CD11b and LY96 [Schenk, 2012]. The combination of TCP, ATRA and cytarabine (a chemotherapic drug) is in phase I/IIa study in AML and MDS patients. By using both reversible(GSK90) and irreversible(RN-1), LSD1 inhibitors in a panel of all AML subtype cell lines, McGrath et al. found cells bearing RUNX1-RUNX1T1(AML-ETO) translocation were especially among the most sensitive. Both inhibitors did not change global level of H3K4me2 and H3K9me2 but dispossess LSD1 from chromatin specially at promoter of myeloid-differentiation-associated gene [McGrath, 2016].

TCP and its derivatives are irreversible inhibitors, and reversible LSD1 inhibitors have attracted considerable interest since they may alleviate some of the possible side effects of irreversible inhibitors, though it is not clear whether efficacy will be maintained. GlaxoSmithKline has disclosed a reversible LSD1 inhibitor (GSK354 or GSK690) with both high selectivity and cellular activity [Vankayalapati, 2014]. GSK2879552 induces differentiation and inhibits cell growth in AML and small cell lung cancer (SCLC), and entered phase trials in AML and SCLC. By testing GSK2879552 on small cell lung carcinoma cell lines (SCLC), Mohammad et al. found a correlation of DNA hypomethylation of a signature set of probes with sensitivity to LSD1 inhibitors [Mohammad, 2015]. Sugino et al

recently demonstrates that a novel LSD1 inhibitor, NCD38, exert an anti-tumor effect not only in AMLs harboring MLL-AF9 but also in erythroleukemia, megakaryoblastic leukemia and MDS overt leukemia cells. Mechanistically, NCD38 treatment and LSD1 inhibition increases H3K27ac levels at super enhancers of LSD1 target genes, such as GFI1 and ERG, thus inducing differentiation and an anti-leukemic effect [Sugino, 2017].

Drug combination therapies have many advantages, including lowering doses of toxic agents, reducing the potential for drug resistance, and inhibiting multiple independent pathways that converge on a single essential molecular process. Histone modifying enzymes are great candidates for drug combinations as they work close together in changing chromatin structure, and consequently gene expression. Additionally, it has been previously shown that affecting one histone modifying enzyme can have effects on others. For example, Meng et al showed that treating ovarian cancer cells (SKOV3) with trichostatin A (TSA) and decitabine, HDAC and DNMT1 inhibitors respectively, lowered the expression levels of LSD1 and increased H3K4me2 levels [Meng, 2013]. Vasilatos et al also showed that knockdown of LSD1 in breast cancer cells decreased mRNA levels of HDAC isozymes. Thus, targeting LSD1 and other epigenetic enzymes simultaneously offers therapeutic promise [Vasilatos, 2013]. As mentioned, LSD1 and HDAC1/2 are found in cellular complexes, thus inhibiting both LSD1 and HDACs simultaneously has potential to yield additive or synergistic pharmacologic impact. In fact, previous studies have shown that targeting both LSD1 and HDAC1/2 in cells results in synergistic cell proliferation inhibition. For example, it was found that treating triple-negative breast cancer cells with both pargyline, a potential LSD1 inhibitor, and SAHA, an established HDAC inhibitor, lead to synergistic growth inhibition and apoptosis [Vasilatos, 2013]. Additionally, Fiskus et al. found that the combination of a reversible LSD1 inhibitor (SP2509) and of the pan-HDAC inhibitor panobinostat was synergistically lethal against cultured primary AML blasts with low toxicity [Fiskus, 2014]. Other combination therapies

59

targeting LSD1 have also been shown to have promise. For example, Xu et al looked at the combined effect of retinoic acid and LSD1 siRNA inhibition on cell death in a human neuroblastoma cell line, SH-SY5Y [Xu, 2013]. It was found that combined treatment led to higher rates of cell death than single agent targeting, implying that neuroblastoma can be better treated with the addition of an epigenetic drug inhibitor, such as an LSD1 inhibitor [Xu, 2013]. Targeting two different enzymes with one compound is another interesting strategy that has shown promise. Rotili et al synthesized compounds that combine the moiety of an LSD1 inhibitor, tranylcypromine, with that of JMJD2 inhibitor 2- oxoglutarate templates [Rotili, 2014]. The compounds were able to in fact target both LSD1 and JMJD2 enzymes in vitro, and showed significant inhibition of both LNCaP and HCT116 cell proliferation. Such a strategy has potential to be applied to other drug combinations, such as by combining moieties of LSD1 inhibitors with those of various HDAC inhibitors.

Recently, compounds targeting lysine-specific demethylase 1 (LSD1) have entered in clinical trials for cancer treatment, and the results will help to further validate the multiple roles of LSD1 in cancer. Further work will be necessary to find biomarkers for sensitivity to treatment with LSD1 inhibitors in determining the most suitable therapeutic setting.

8. Acute Myeloid Leukemia (AML) and Acute Promyelocytic Leukemia(APL)

Acute myeloid leukemia (AML) is a hematopoietic malignancy characterized by a block in the differentiation of progenitor cells and an accumulation of immature cells in the bone marrow and blood [Henderson, 2002]. Rather than a single disorder, AML represents a set of related malignancies. The French-American-British (FAB) classification recognizes 8 major subtypes of AML, based on cellular morphology and cytochemical staining [Bennett, 1976]. Although the system is widely accepted internationally, an exclusively cytogenetic/molecular analysis-based classification of acute leukemias, could be better define biologic and prognostic groups [Harris, 1997; Vardiman, 2002]. The majority of patients present with a hypercellular bone marrow due to the proliferation of malignant blasts or promyelocytes. According to the original FAB classification scheme, a diagnosis of acute leukemia is made when immature blasts count for at least 30% of all nucleated marrow cells. The recent World Health Organization (WHO) Classification system requires that blasts account for higher than 20% of all nucleated marrow cells to render a diagnosis of acute leukemia [Jaffe, 2001]. A marrow containing increased blasts, but accounting for less than 30% of all nucleated marrow elements (or less than 20% in the WHO Classification), usually indicates the presence of a myelodysplastic syndrome (MDS), a diverse group of related disorders characterized by clonal stem cell proliferation, ineffective hematopoiesis, and increased risk to evolve into AML.

Clonal cytogenetic abnormalities are identified in 60 - 80% of AMLs and can frequently be of clinical value [Mrozek, 1997]. This is particularly true of cases with the t (15;17) translocation that is consistently associated with acute promyelocytic leukemia (APL) and often has distinct clinical and morphologic features [Bitter, 1987]. The reciprocal translocation involves the PML gene on chromosome 15 and the retinoic acid receptor-alpha (RARα) gene on

chromosome 17, and the resulting fusion mRNA product inhibits maturation of the affected cells leading to a proliferation of atypical promyelocytes [Grimwade, 1999].

The fusion product, PML-RARα, encodes a functionally altered transcription factor that is the initiating event in APL leukemogenesis. As such, it represents a unique opportunity for modeling the development of leukemia.

8.1. PML-RARα fusion protein

PML-RARα fusion protein contains the N-terminus of PML fused to the DNA and hormone-binding domain of RARα [de Thé, 1991; Kakizuka, 1991]. The breakpoint on chromosome 17 is located at the second intron of RARα while those on chromosome 15 are found at two different introns of PML, intron 3 and 6. PML-RARα mRNA is found in almost all (>95%) of the APL cases while the reciprocal RARα-PML is observed in about two thirds of APL patients [Grimwade, 1999]. The detection of specific fusion transcripts of PML-RARα and RARα-PML by reverse-transcriptase polymerase chain reaction (RT-PCR) hence allows for precise diagnosis of APL and identification of residual or recurrent disease [Lo Coco, 1999]. A dominant-negative function of the PML-RARα fusion protein on PML and RARα pathways has been proposed. The individual moieties of PML-RARα retain their abilities to heterodimerise with PML and RXR respectively. The PML moiety of PML-RARα binds to PML through its homodimerisation domain while the RARα moiety dimerises with RXR and binds to DNA and its ligand. PML-RARα can also homodimerise. These homodimers can bind to the RAREs in the regulatory region of target genes required for differentiation of granulocytes and repressed transcription of these genes by recruiting corepressors such as N-CoR and SMRT. PML-RARα also recruits methylating enzymes and hypermethylates promoters of RA target genes resulting in transcriptional repression [Lo Coco, 2006]. In contrast to previously held belief of its dominant-negative function, a gain-of-function has

been described for PML-RARα. PML-RARα acquires aberrant DNA binding activity through the PML moiety, allowing PML-RARα homodimers to bind to DNA consensus sites that are not recognized by RARα/RXR heterodimer, thus allowing the repression of genes not regulated by RARα **(Figure 10)** [Kamashev, 2004].

PML-RARα has domains that allow protein-protein interactions in both the RARα and PML portions. Like wild-type RARα, PML-RARα can recruits the NCor/SMRT/HDAC corepressor complex [Grignani, 1998; Guidez, 1998; He, 1998; Lin, 1998]. Histone deacetylation causes chromatin to adopt a "closed" conformation that is less accessible to the transcriptional machinery, therefore silencing gene expression. In contrast to RARα, PML-RARα does not dissociate from the corepressor complex in the presence of physiological concentrations of ATRA, but requires pharmacological doses to relieve transcriptional repression. This strong association of PML-RARα with the co-repressors and the ability to retain the deacetylase complex, enable the fusion protein to maintain the repression of myeloid gene expression at physiological doses of ATRA. In fact, the affinity of PML-RARα for the co-repressors is much higher than wild-type RARα, requiring an ATRA concentration of 10^{-6}mol/L for dissociation. Binding of ATRA to the PML-RARα homodimer results in a conformational change, thus allowing the HDAC-containing complex to dissociate, thereby opening the chromatin structure and relieving transcriptional repression. PML-RARα, unlike RARα, can self-dimerize and form higher order oligomers; it has been suggested that oligomerization allows for increased corepressor binding **(Figure 10)** [Grignani, 1999].

Of interest, a NB4 resistant cell-line, NB4-R4, containing a mutation in PML-RARα that impairs ligand binding, is able to partially differentiate in response to ATRA when exposed to TSA, a histone deacetylation inhibitor. TSA also restores ATRA-induced transactivation of an RARE-containing reporter [Lin, 1998]. Restoration of differentiation in PML-RARα

expressing cells, NB4 cells, is achieved by overexpressing specific N-CoR fragments. Interaction of overexpressed fragments with the fusion proteins blocks their interaction with N-CoR/SMRT, disrupts HDAC1 complex formation and targets the fusion protein for degradation. The investigators confirmed that the induced differentiation is not due to degradation of PML-RARα. Addition of proteasome inhibitors to restore PML-RARα does not inhibit the differentiation [Racanicchi, 2005]. Also, it has been shown that demolishing the N-CoR/HDAC3 complex using siRNA against HDAC3 in PML-RARα-expressing 293T cells can re-activate the expression of RA responsive genes [Atsumi, 2006]. Lastly, N-CoR/HDAC3 complex has been proposed to help in silencing of PML-RARα targeted genes by recruiting MBD1, a methyl-CpG binding protein which is able to methlyate DNA [Villa, 2006].

A report demonstrated that PML-RARα can also recruit the polycomb repressor complex 2 (PRC2) to target genes [Villa, 2007]. PRC2 includes the proteins EZH2, SUZ12 and histone binding proteins. PRC2 recruitment results in H3K27 histone methylation by EZH2, another epigenetic modification associated with transcriptional repression. It is not yet known whether PRC2 recruitment is essential for PML-RARα induced leukemogenesis or immortalization. Additionally, there is evidence that PML-RARα can recruit histone methyltransferases directly [Carbone, 2006]. In summary, PML-RARα appears to drive repression through three distinct mechanisms: histone deacetylation, DNA methylation, and histone methylation. Accordingly, PML-RARα bound regions undergo epigenetic modification, including decreases in histone H3 acetylation and increases lysine 9 trimethylation. Upon ATRA treatment, H3 acetylation increases in most PML-RARα bound regions as well as globally [Martens, 2010]. The global DNA methylation profile of APL samples is also distinct from that of other AMLs [Figueroa 2010]. Since PML-RARα target genes include chromatin modifying enzymes such as JMJD3 (H3K27 demethylation), SETDB1 (H3K9 methylation), and DNMT3a (DNA methylation)

[Martens, 2010; Wang, 2010], it is likely that the global changes reflect both direct recruitment of modifying enzymes by PML-RARα and effects on expression of the enzymes.

8.2. APL treatment

Prior to the development of targeted therapies, the prognosis of APL was among the worst of all AML subtypes, with a 5-year survival of only 25-30 percent [Soignet, 2001]. Death occurred in up to 15 percent of patients undergoing induction chemotherapy, and those who achieved a complete remission invariably relapsed within 2 years [Fenaux, 2007]. However, in the mid 1980s, based on the observation that retinoic acid could induce differentiation of APL cells *in vitro*, Huang et al performed a small trial of all ATRA alone or in combination with traditional chemotherapy in 24 APL patients [Huang, 1988]. The success of this study and subsequent trials [Castaigne, 1997; Tallman, 1997; Warrell, 1991] led to the adoption of ATRA therapy in combination with anthracycline based chemotherapy as the standard treatment for APL. Currently, the 5-year disease free survival of APL patients treated with combination chemotherapy and ATRA is approximately 75 percent [Tallman, 2007].

ATRA releases the transcriptional repression exerted by PML-RARα. This allows the activated receptors to bind to the RAREs, leading to differentiation in APL **(Figure 10)** [Warrell, 1993]. Another effect of ATRA in APL is to induce the degradation of PML-RARα through caspase-mediated cleavage [Nervi, 1998]. Arsenic trioxide (ATO) is an effective therapy in some of the relapsed patients previously treated with the ATRA/chemotherapy [Chen, 1996; Soignet, 2001; Niu, 1999]. Combination therapy of ATRA/ATO shows excellent results when used on newly diagnosed patients, achieving complete remission (CR) at a shorter time with faster recovery of white blood cell count [Shen, 2004]. ATO shows different responses at different concentrations in cell culture conditions. It promotes differentiation of APL cells at low concentrations while inducing mitochondria-mediated intrinsic apoptotic

pathway at high concentrations [Chen, 1997]. PML-RARα and wild-type PML are degraded in APL cells *in vitro* and *in vivo* after ATO treatment [Chen, 1997].
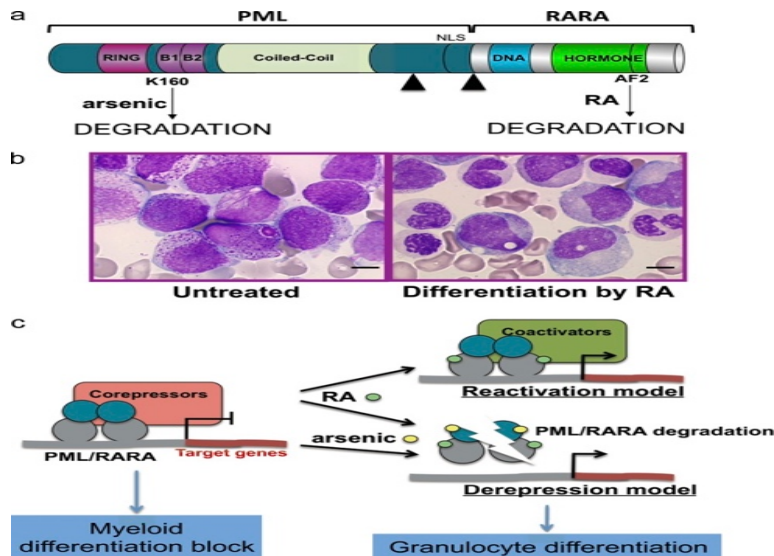
Figure 10. **PML-RARα, ATRA and ATO treatment.** (A) PML-RARα fusion protein. (B) RA treatment in vivo elicits the differentiation of leukemia cells. (C) mechanism of ATRA and ATO action in treatment of APL. Adapted from de Thé et al. J Cell Biol 2012.

8.3. Rationale for novel therapeutics for APL

Despite the success of ATRA therapy of APL, many challenges remain in the treatment of APL patients. Up to 30 percent of APL patients will eventually experience a relapse of their leukemia despite ATRA and chemotherapy treatment [Tallman, 2007]. Relapsed APL is frequently resistant to ATRA [Gallagher, 2002]. Relapsed or refractory APL may be treated with chemotherapy in combination with arsenic trioxide, histone deacetylase (HDAC) inhibitors, hematopoeitic stem cell transplantation and various experimental drugs currently in clinical trials [Tallman, 2007; Tallman, 1997; Soignet, 2001]. Despite these advances,

approximately 40-50 percent of patients will die within 2 years of relapse [Sanz, 2006]. These facts underscore the need for development of novel therapeutic agents.

ATRA resistance can also be a result of mutations in the DNA binding domain [Ding, 1998] or the ligand binding domain (LBD) of the RARα gene [Zhou, 2002]. ATO is also implicated in the leukocyte activation syndrome [Camacho, 2000] and in arrhythmia [Unnikrishnan, 2001]. New therapeutic agents which specifically target APL cells, but work by different pathways to those of current commonly used therapeutic agents might give us a breakthrough in finding a cure for APL.

9. Melanoma

Melanoma is a skin cancer arising from the uncontrolled proliferation and invasion of melanocytes. Melanoma is an aggressive disease, but if metastasis is limited to local invasion of the skin, surgical resection is adequate. However, if distant metastasis has occurred, prognosis is poor and only 5 -22 % of patients survive beyond 5 years. Melanoma is largely attributable to somatic mutations caused by ultraviolet (UV) radiation exposure [Bandarchi, 2010]. More than 80 % of melanomas arising in the skin have activating mutations in either B-RAF or N-RAS, highlighting the importance of MAPK pathway in melanoma [Curtin, 2005]. However, these mutations are always mutually exclusive [Gray-Schopfer, 2005]. In addition, genetic polymorphisms in the Cdkn2a (p16), MC1R, PTEN, EGFR and MITF genes can result in a predisposition to the disease [Yokoyama, 2011; Hussussian, 1994; Beaumont, 2005; Garraway, 2005]. Initially dysplastic nevi are formed, the nevi proliferate within the epidermis. Then the lesion switches to a vertical growth phase and invades into the lower epidermis, dermis and underlying basement membrane **(Figure 11)**. As the disease progresses, angiogenesis increases vascular density and promotes spread to distant organs, resulting in

metastatic melanoma [Miller&Mihm, 2006]. Distant metastases are subsequently initiated through the motility and invasion of melanoma cells into lymphatic or blood vessels and growth at secondary organs.

In addition to gene deletion and mutational alteration of protein activity, epigenetic alterations in DNA and histones have recently become a part of melanoma genetic aberrations. Epigenetic alterations are regarded to be related to transcriptional deregulation leading to loss of tumor suppressor genes expression and/or up-regulation of oncogenes [Howell, 2009; Klose, 2006]. Epigenetic regulation of gene expression has been associated with silencing of tumor suppressor genes in melanoma, more prominently genes like CDKN2A, RASSF1A and PTEN [Woodman, 2012; Hocker, 2008, Garraway, 2005]. The transcriptional silencing by aberrant promoter methylation is associated with di-methylated lysine 9 in histone 3 (H3K9me2), resulting from activity of H3K9 histone methyltransferases like SETDB1 and EHMT2 and counteracted by H3K9 histone demethylase LSD1 [Miura, 2014]. The transcriptional repression is believed to require for binding of methyl CpG binding protein 2 (MECP2) and methyl CpG domain binding protein 1 and 2 (MBD1 and MBD2) activity [Klose, 2006].

Loss of gene regulation in melanoma may be association to epigenetic regulation or as a result of mutations in genes coding for epigenetic regulators. Alterations in EZH2 or SETDB1 are found in 37% of all cutaneous malignant melanoma (CMM) tumors accounting increased mRNA transcription, gene amplification and mutation.
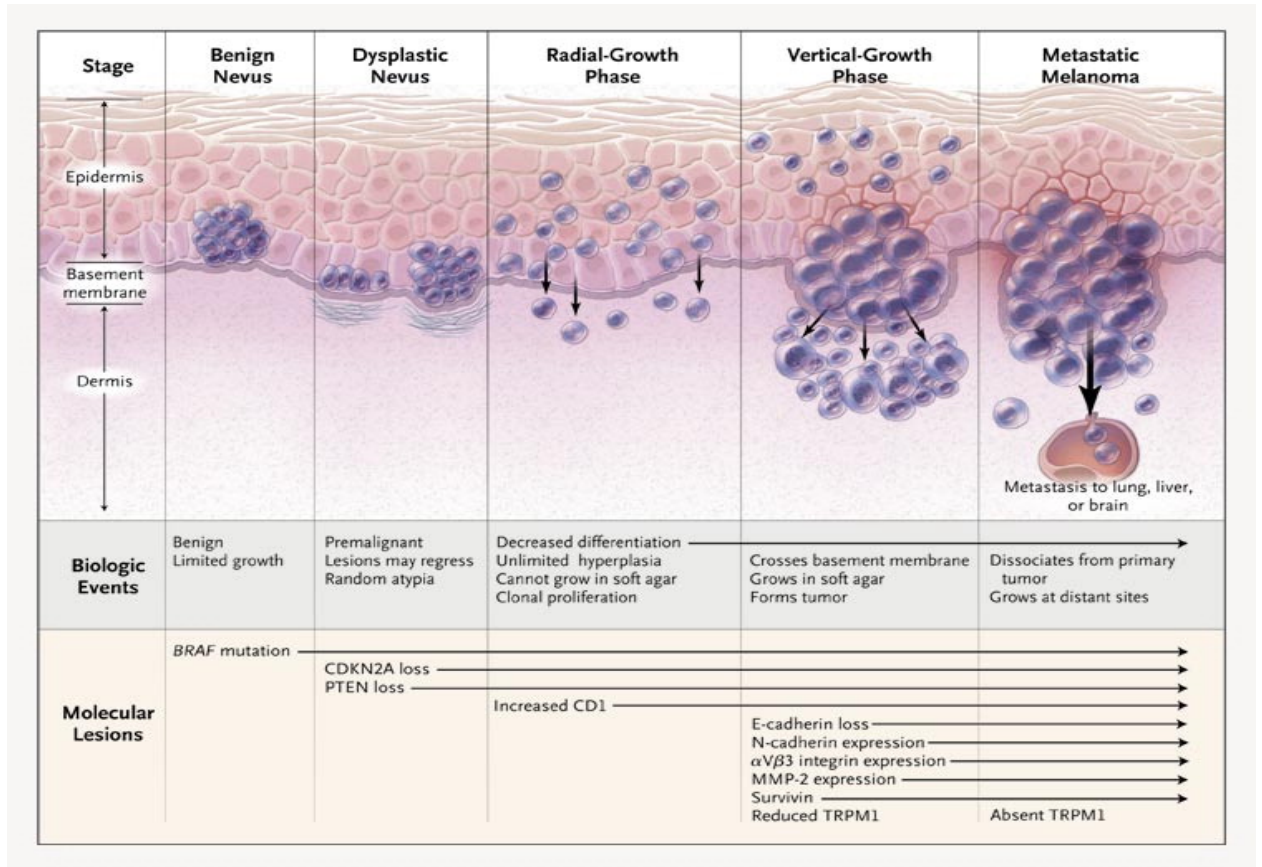
Figure 11. **The steps of melanoma progression**. Adapted from Miller&Mihm. N Engl J Med 2006.

9.1. Melanoma treatment

Although early detection and surgical removal of melanoma does, in almost 90% of diagnosed cases, when surgery is not sufficient to remove the melanoma cells, risk for metastatic spread of the disease is high. Six drugs have been approved by the US Food and Drug Administration (FDA); Dacarbazine (1975), Ipilimumab (2011), Vemurafenib (2011), Dabrafenib (2013), Trametinib (2013) and Pembrolizumab (Keytruda) (2014) for the treatment of patients with advanced melanoma [Palathinkal, 2014].

Recently, approval of two promising more specifically targeted therapeutic approaches, ipilimumab and vemurafenib, have led to increasing understanding of melanoma characteristic

and biology. Ipilimumab is a monoclonal antibody that blocks cytotoxic T-lymphocyte-associated antigen 4 (CTLA4) on lymphocytes and thereby stimulating the immune system against the cancer cells. Vemurafenib and Dabrafenib are inhibitors of V600E mutant BRAF that limit the activity of the MAPK/ERK signalling pathway. Treatment with Vemurafenib has resulted in complete or partial tumor regression in the majority of melanoma patients carrying B-RAF V600E mutations [Hamid, 2013; Finn, 2012]. Trametinib is an inhibitor against MEK1/2 that has been approved as a single agent treatment of B-RAF V600E or V600K mutation-positive metastatic melanoma.

The therapeutic alternatives for patients with N-RAS mutations have so far been limited, since designing drugs that directly target N-RAS has been a challenge. Likewise, finding eligible strategies to treat melanomas that are B-RAF/N-RAS wild type have proven even more elusive [Fedorenko, 2015]. Clinical trials are assessing the treatment potential of MEK inhibitors in these patient groups; however, the responses appear to be sub-optimal. Aiming to improve the response, combined inhibition of MEK and PI3K, Akt, cyclin D/CDK4 and cyclin D3/CDK6, are currently being investigated (ClinicalTrials.gov).

9.2. Rationale for novel therapeutics for melanoma

Although targeted treatment and immunotherapy have in many cases led to promising antitumor effect, development of resistance and adverse effects are a major problem. In general, the high mutational rate observed in malignant melanoma cells is a potential source of therapy resistance. The heterogeneity inducers other than diversity in genetic aberrations may include hypoxia, tumor microenvironment, selection by therapeutic agents and may be executed by reversible alterations of epigenetic changes in histone modifications and be seen as adaptations [Siegel, 2013]. Despite initial response, resistance to B-RAF and MEK inhibitors develops at a median time of 6 months after treatment initiation, and have been

70

associated with reactivation of the MAPK signaling pathway, or activation of compensatory pathways such as the PI3K network. For traditional chemotherapy, therapy resistance has been shown to largely depend on loss of p16 and alterations in p53 pathway. Conventional chemotherapies and radiotherapies target proliferating cells and require active cycling for induction of apoptosis. The slow-cycling nature of many cancer stem cell (CSC) pools is therefore an inherent mechanism for resistance and cell survival in response to conventional therapies. The connections between therapy resistance and quiescence and slow cycling rate of CSCs was explored in the work conducted by Roesch et al. in melanoma [Roesch, 2010].

The transition from general cytotoxic therapies (chemotherapies) to targeted therapies has led to a change in therapy-associated resistance: from intrinsic resistance to acquired resistance. Whether the recent advances in combination therapy and novel epi-drug can help to avoid the acquired therapy resistance is to be seen.

Aims of the project

Post-translational modification of histone tails plays a critical role in chromatin regulation, gene activity and nuclear architecture. The addition or removal of post-translational modifications from histone tails is fairly dynamic and is achieved by a number of different histone modifying enzymes. Given the fundamental roles of histone modifications in gene regulation and expression, it is not surprising that aberrant patterns of histone marks are found in cancer. Such modifications include histone lysine methylation, which can either promote or repress gene activity depending on the extent of methylation and its context. Histone lysine methylation is maintained by dynamic opposition of methyltransferase and demethylase enzymes, both of which are implicated in normal embryonic development and tumorigenesis. LSD1 is a flavin-containing amine oxidase that, by reducing the cofactor FAD, demethylates H3K4me1/2 and H3K9me1/2 at target loci in a context-dependent manner. In cancer cells, it has been shown that LSD1 is required for the development and maintenance of acute myeloid leukemia (AML) and cooperate with the oncogenic fusion protein MLL-AF9 to sustain leukemic stem cells (LSCs). LSD1 inhibition impaired the proliferation potential of murine and human AML cells and was accompanied by induction of differentiation. Moreover, LSD1 inhibitors unlocked the ATRA-driven therapeutic response in AML by increasing H3K4me2 level and reactivating the retinoic acid signaling pathway. LSD1 could be an attractive target for cancer therapy because of its deregulation in a number of cancers, including lung, breast, melanoma and hematological malignancies. Despite recent diagnostic and technological improvements, cancer continues to retain its heavyweight status as one of the most challenging diseases to treat. It is a heterogeneous disease that often results in different clinical outcomes for patients with the same affected tissue. And as such, the disparateness of this disease makes it extremely difficult to fight. The ability to anticipate the clinical behavior of

cancers is essential in determining the most suitable therapeutic interventions. Considering that cancer is so diverse and clinical outcome predictions often vary from patient to patient, a considerable amount of effort is being invested to discover molecular biomarkers that can categorize cancer patients with distinct clinical outcomes to expand prognostic capabilities. Given the unsatisfactory clinical outcome associated with standard chemotherapy in acute myeloid leukemia (AML) and melanoma treatment, there is an essential need for new targets. Recently LSD1 have gained great interest for their use as anticancer therapeutics. However, the efficacy of LSD1 inhibitors is limited to a substantial subset of cancer cells. Thus, identification of good predictive biomarkers for sensitivity to treatment with LSD1 inhibitors will be of great value in determining the most suitable therapeutic setting.

Three lines of evidence have provoked our interest in LSD1. First, LSD1 could be an attractive target for cancer therapy because of its deregulation in a number of solid and hematological malignancies. Second, LSD1 inhibition impaired the proliferation potential of a subset of solid tumor and AML cells. Third, LSD1 inhibitors unlocked the ATRA-driven therapeutic response in cancer cells. In this study we aim to:

- Identify predictive biomarkers for sensitivity to LSD1 inhibition by using resistant vs. sensitive APL cells.

- Broaden our observation to other type of cancers such as non-APL AML, small cell lung carcinoma (SCLC) and melanoma.

- Explore the synergistic potential of LSD1 inhibitors in combination with other inhibitors (HDACi and Palbociclib (CDK4/6i)) based on identified biomarkers.

Cell lines and growing conditions.

NB4 cells, were established from an APL patient by Lanotte and colleagues, have characteristics similar to APL blasts [Lanotte, 1999]. NB4 cells were grown in RPMI-1640 medium with 10% of (FBS) fetal bovine serum, 2mM glutamine and 1% Penicillin/Streptomycin.

UF1 cells were established from a patient who was clinically resistant to RA and were grown in RPMI-1640 medium with 15% of (FBS) fetal bovine serum, 2mM glutamine and 1% Penicillin/Streptomycin [Kizaki, 1996].

Kasumi AML (FAB M2) cells with an 8;21 chromosome translocation (AML-ETO chromosomal translocation), were established from the peripheral blood of a 7-year-otd boy suffering from acute myeloid leukemia (AML). Kasumi cells were grown in RPMI-1640 medium with 10% of (FBS) fetal bovine serum, 2mM glutamine and 1% Penicillin/Streptomycin [Asou, 1991].

NCI-H69 small cell lung carcinoma (SCLC) cell line was grown in Iscove MDM with 10% of (FBS) fetal bovine serum, 2mM glutamine, 1mM Sodium pyruvate (NaP).

293T cells are human embryonic kidney cells, which was originally established by stable transfection with Ad5 sheared DNA and carry a temperature sensitive mutant of SV-40 large T-antigen (tsA1609neo) [Graham, 1977; DuBridge, 1987]. 293T cells used for the production of lentiviruses due to their high transfection efficiency [Pear, 1993]. The 293T cells were cultured in DMEM (Lonza) supplemented with 10% FBS, SA (Microgem), 2 mM L-Glutamine (Lonza), 100 U/ml penicillin and 100 U/ml streptomycin (Pen/Strep stock, Lonza).

These cells were used to generate pLKO Lentiviral vectors. All cells were grown in a humidified incubator at 37 °C with 5% CO_2 environment.

Cell culture of Human Primary melanoma cells

Human primary melanoma cells were grown in RPMI-1640 medium with 10% of (FBS) fetal bovine serum, 2mM glutamine and 1% Penicillin/Streptomycin. Confluent cells were first washed with 1X phosphate buffered saline (PBS) (8.0 mg/mL NaCl, 1.4 mg/mL Na2HPO4, 0.2 mg/mL KCl, 0.2 mg/mL KH2PO4, pH 7.2(Lonza)). Trypsin/EDTA (0.025% trypsin, 0.05% EDTA, 1XPBS, pH7.6 (Lonza)) was next added to cells and incubated for 5 to 10 minutes inside cell culture incubator until cells were detached from culture dish. 10% serum supplemented culture medium was added to trypsinized-cells to inactivate trypsin. Cells were resuspended thoroughly for further passaging at ratio of 1:5 in new dish with fresh culture medium.

Stocking and thawing cells

Cells were centrifuged at 1,200 rpm for 5 minutes and cell pellets were resuspended in anti-freezing medium (10% DMSO and 90% FBS). 1mL anti-freezing medium was added per $12x10^6$-$2x10^6$ cells. Resuspended cells were placed in 1 mL cryogenic vials in cryogen box filled with isopropanol and frozen at -80^oC for 24 hours prior to storage in liquid nitrogen. To thaw cells from frozen stock, cells in cryogenic vials were thawed in 37^oC water bath for 30 seconds. Thawed cells were washed with 1XPBS and centrifuged. Cell pellets were lastly resuspended in appropriate culture medium for plating in culture dish.

Lysine-specific demethylase1 inhibitor (LSD1i)

We have previously characterized a novel LSD1 inhibitor, MC2580, showing high specificity (100 fold more than TCP) and acting at relatively low concentrations [Binda, 2010]. Despite similarity in the catalytic and structural properties with other FAD-dependent amine oxidases, the ligand-binding subdomain of LSD1 is much larger than in MAO-A and MAO-B. This compound is an analog of tranylcypromine/Parnate (TCP) with increasing larger substituents that contained a mix of hydrophobic and hydrophilic group. By taking advantage of this inhibitor we have been able to investigate the mechanistic role of LSD1 in different kind of cancers. Compounds were dissolved to 10mM in dimethyl sulfoxide (DMSO).

Assay of cell proliferation

Approximately 400,000 of cell lines were plated in triplicates in the presence of compound at day 1, and the number of cells were counted using the hemocytometer every day. Three cell suspension samples were prepared for triplicate independent counting and average of three readings represented the cell count. Medium containing the compound was refreshed every 2-3 days, and the cell concentration was kept under 1-2 million per ml as recommended.

10,000 primary melanomas cells/well were plated in triplicate in 12 well-plates in the presence of compound at day 1, and the number of cells were counted using the hemocytometer every two days. Three cell suspension samples were prepared for triplicate independent counting and average of three readings represented the cell count.

Cell suspension was diluted with Trypan Blue dye (Sigma) at 1:1 ratio and incubated for 5 minutes. 10 μL of stained cell mixture was gently loaded into the hematocytometer to avoid air bubbles. Viable cells (non-stained) were counted in each of the five 1mm^2 squares in the center, on top right, bottom right, top left and bottom left of the hematocytometer under phase

76

contrast microscope. Cell concentration (number of cells per mL) was calculated with the following equation: Number of cell count in 5 square units /5 x 10^4.

Colony Forming Unit (CFU) Assay

Approximately 1000-5000 cells were initially plated in triplicates in the methylcellulose medium (MethoCult^{TM} GF H4435 Enriched; StemCell Technologies) and (MethoCult^{TM} GF H3434; StemCell Technologies) pre-added with DMSO or compound. For serial replating, cells isolated from colonies in the previous plating were seeded again in the same semi-solid medium. CFUs were scored and the cells were used for immunoblotting and morphological analysis by direct quantification every 7 to 10 /days' post seeding.

Morphological characterization (Wright-Giemsa staining)

The cells collected from methylcellulose or culture plates were spun onto a cytological slide by using a cytospin centrifuge (Cytospin™ 4 Cytocentrifuge). Cytospins were stained using the May-Grünwald-Giemsa staining method. The fixed cells were stained for 8 minutes in May-Grünwald stain, then slides were sequentially washed 6 times in deionized water and then incubated for 30 min with Giemsa stain and diluted with 19 volumes of distilled water. After this step the cytological slides were rinsed again 3 times in distilled water and air-dried. For long time storage, a cover slip was attached to the slides by Eukitt ® mounting medium, which is an adhesive and specimen preservative that can be used manually and in automated cover slipping equipment.

This method of coloration represents the most common way to stain peripheral blood and bone marrow smears. The two solutions contain a basic dye (methylene blue) and an acid dye (eosin). The first carrying a basic net positive charges stain nuclei because of the negative charges of phosphate groups of DNA and RNA molecules, basophil granules and RNA

molecules within the cytoplasm varying shades of blue to purple. The eosin carries a net negative charge and stains red blood cells and granules of eosinophil granulocytes an orange to pink color. Mature populations were defined based on their morphology: (1) a reduced nucleus-to-cytoplasm ratio; (2) the dark blue cytoplasm became lighter and often contained granules; and (3) segmented/multi-lobular nuclei.

Annexin V and Propidium Iodide (PI) staining

Indicated cells were subjected to cell cycle and apoptosis analysis by means of Fluorescence Activated Cell Sorting (FACS) taking advantage of specific dye intercalating the DNA (Propidium Iodide) and phosphatidylserine (Annexin V). PI is used as a DNA stain or DNA content in cell cycle analysis. PI is membrane impermeable and can be used for identifying dead cells. Annexin V can be used to detect and measure early apoptosis by binding to phosphatidylserine residues. During apoptosis, phosphatidylserine is translocated from the cytoplasmic face of the plasma membrane to the cell surface.

Annexin V analysis of cells was performed using annexin V-FITC (annexin V- fluorescein isothiocyanate). Briefly, cells were treated as indicated, pelleted, washed with PBS, and counted. Then 500,000 cells were resuspended in 50μl annexin V binding buffer (HEPES 10mM, NaCl 150mM, $MgCl_2$ 1mM, $CaCl_2$ 3.6mM, KCl 5mM) labled with annexin V-FITC and incubated for 1 hour at room temperature. Cells were resuspended in 500 μl PBS and 1 μl PI (50 μg/ml0 and then analyzed by flow cytometry using BD FACSCalibur instrument. Here propidium iodide (PI) is used as a dye for detecting apoptotic events.

Lentiviral shRNA costructs

ShRNA-based lentiviral plasmids were generated by ligating synthetic oligo nucleotides targeting the indicated mRNA into a modified pLKO vector in which the cDNA for

puromycin selection had been replaced with that encoding for enhanced GFP. The shRNA sequences are in the format: target sequence sense (underlined)–loop-target sequence antisense (underlined). The target sequences, added with specific oligonucleotides allowing the insertion and the formation of the hairpin structure, were cloned into pLKO backbone previously co-digested by AgeI and EcoRI restriction enzymes by means of T4 DNA ligase (Invitrogen).

shRNAs sequences used in this study:

LSD1-shRNA-1,

5'-CCGGGCCTAGACATTAAACTGAATACTCGAGTATTCAGTTTAATGTCTAGGCTTTTTG-3'

LSD1-shRNA-2,

5'- CCGGGCTACATCTTACCTTAGTCATCTCGAGATGACTAAGGTAAGATGTAGCTTTTTG-3'

P21-shRNA-1,

5'- CCGG GTCACTGTCTTGTACCCTTGT CTCGAG ACAAGGGTACAAGACAGTGACTTTTTG-3'

P21-shRNA-2,

5'-CCGGCGCTCTACATCTTCTGCCTTACTCGAGTAAGGCAGAAGATGTAGAGCGTTTTTG-3'

P21-WT, P21-PCNAm, P21-CDKm expression plasmid

P21 wild-type, PCNA mutant and CDK mutant expression pWPI vector kindly provided by prof. Pelicci. In p21-CDK mutant, amino-acids W49, F51 and D52 were changed to R49, S51 and A52 while in p21-PCNA mutant, residues M147, D149 and F150 were changed to A147, A149 and A150. A triple hemagglutinin (HA) tag has been introduced in frame with p21

coding sequence at the carboxy-terminus. All constructs were sequenced to verify that the triple HA tag had been correctly inserted and that the desired mutations had been introduced with no additional mutations. P21 wild-type, PCNA mutant and CDK mutant expression vector in vector pWPI have been described previously [Cayrol, 1998].

Transformation & Mini-, midi-, maxi-preparation of plasmid DNA

The plasmids were heat-shock transformed into competent Stbl3 cells by adding the plasmids into 100 µL competent cells, ice incubated for 15 minutes and heat shocked at 42^oC for 20 seconds. The transformed competent cells were further snap-cooled on ice for 2-4 seconds and inoculated with 1 mL Luria Bertani (LB) broth for incubating at 42^oC with gentle shaking. Transformed cells were spread on LB agar plate containing Ampicillin. Agar plates were placed in 37^oC incubator overnight. single bacterial clone was picked for further culture expansion.

For minipreparation of plasmid DNA, single bacterial clone was expanded by inoculating with 1.5 mL LB broth containing appropriate antibiotic and cultured at 37^oC shaking incubator for 8 hours. The culture was centrifuged at 13,000 rpm for 3 minute at room temperature to pellet the bacteria. Minipreparation of plasmid was performed using NucleoSpin plasmid Kit (MACHEREY-NAGEL) according to manufacturer's protocol. Bacterial pellet was resuspended completely in 250 µL cold buffer A1 (RNAse A added) and lysed with 250 µL buffer A2 (alkaline lysis buffer) by gentle inversion of tubes several times for 5 min in room temperature. 300 µL buffer A3 was added to completely stop the lysing and the lysis mixture was centrifuged at 11,000 x g for 10 minutes. Supernatant was transferred to new spin column and washed with 500 µL Buffer AW and 600 µL Buffer A4. Plasmid DNA was eluted in 50 µL water or AE.

For midipreparation of plasmid DNA, 2 mL bacterial starter culture was inoculated with 150 mL LB broth containing appropriate antibiotic and cultured at 37°C shaking incubator overnight. The culture was centrifuged at 6,000 x g for 5 minutes at 4°C to pellet the bacteria. Midipreparation of plasmid was performed using NucleoSpin plasmid Kit (MACHEREY-NAGEL) according to manufacturer's protocol. Bacterial pellet was resuspended completely in 8 mL buffer RES-EF, lysed with 8 mL buffer LYS-EF by gentle inversion of tubes and incubation at room temperature for 5 minutes. 8 mL buffer NEU-EF was added to stop lysing completely. The lysis mixture was loaded on pre-wet column during column equilibration. Then the column and the filter washed in three subsequent washing step with buffer FIL-EF, buffer ENDO-EF and buffer WASH-EF. Finally, plasmid eluted with 5 mL of buffer ELU-EF into a clean centrifuge tube containing 3.5 mL of isopropanol. Plasmid DNA was pelleted by centrifugation at 15,000 x g for 30 minutes at 4°C. The DNA pellet was washed with 70% ethanol, air-dried and dissolved in 150 μL H2O. Quantity and quality of plasmid DNA was determined by spectrophotometer, verified by restriction enzyme digestion and sequencing.

For maxipreparation of plasmid DNA, 2 mL bacterial starter culture was inoculated with 500 mL LB broth containing appropriate antibiotic and cultured at 37°C shaking incubator overnight. The culture was centrifuged at 6,000 x g for 5 minutes at 4°C to pellet the bacteria. Midipreparation of plasmid was performed using NucleoSpin plasmid Kit (MACHEREY-NAGEL) according to manufacturer's protocol. Bacterial pellet was resuspended completely in 15 mL buffer RES-EF, lysed with 15 mL buffer LYS-EF by gentle inversion of tubes and incubation at room temperature for 5 minutes. 15 mL buffer NEU-EF was added to stop lysing completely. The lysis mixture was loaded on pre-wet column during column equilibration. Then the column and the filter washed in three subsequent washing step with buffer FIL-EF, buffer ENDO-EF and buffer WASH-EF. Finally, plasmid eluted with 15 mL of buffer ELU-EF into a clean centrifuge tube containing 3.5 mL of isopropanol. Plasmid DNA was pelleted

by centrifugation at 15,000 x g for 30 minutes at 4°C. The DNA pellet was washed with 70% ethanol, air-dried and dissolved in 500 μL H2O. Quantity and quality of plasmid DNA was determined by spectrophotometer (ND1000 NanoDrop).

Calcium phosphate transfection

The day before transfection the packaging cells (293T cells) were plated at the density such that the day of transfection they were 50% to 60% confluent. Co-transfection of the lentiviral expression vector with packaging plasmids encoding the gag, pol and rev proteins were necessary for the assembly of infectious lentivirus in 293T cells. For the transfection two solutions were prepared: Solution A: DNA of packaging plasmid (pCMV-dR8.2 8μg/10 cm plate), DNA of envelope plasmid (pCMV-VSV-G 5 μg/10 cm plate), DNA (10 μg/10 cm plate), 625 μl CaCl2 and water in a final Volume of 500 μl; Solution B: 500 μl of 2x HBS (HEPES (4-(2-hydroxyethyl)-1-piperazineethanesulfonic acid). pCMV-VSV-G expresses the G glycoprotein of the vesicular stomatitis virus (VSV-G) under the control of the CMV immediate-early promoter. pCMV-dR8.2 provides all of the proteins essential for transcription and packaging of an RNA copy of the expression construct into recombinant pseudoviral particles. The solution A was slowly added drop wise to the 2X HBS while bubbling air through it with a Pasteur pipette. After 10- 20 minutes the formed DNA-calcium precipitates were added to the media of the 293T cells. The cells were incubated at 37°C in a humidified CO2 incubator for 12-16 hours, and then the media was removed and replenished with fresh one. Forty-eight and 72 hours' post-transfection the first and second viral supernatant were filtered and collected.

Viral concentration

In order to concentrate lentivirus -based particles, 48 hours and 72 hours' post-transfection the

first and second viral supernatant respectively were filtrated through 0.45 μm Millipore syringe filters and transferred into sterile 50mL falcons, and 1 volume of cold 5x PEG solution (System Bioscience) was added to every 4 volumes of lentivirus-containing supernatant. Then it was refrigerated overnight at 4˚C, and the next day it was centrifuged at 1500x g for 30 minutes at 4˚C. After centrifugation the lentivirus particles appeared as a white pellet at the bottom of the falcon all traces of fluid were removed by aspiration and the retroviral pellet was resuspended 1:100 of original volume using cold, sterile PBS, aliquoted into cryogenic vials and immediately stored at -80˚C.

Infection of the cells

Cells were put in 24 well-plates and plated at a density 500,000 cells in 500 μl of medium per well. Virus was diluted in RPMI 10% serum pen/strep in order to add 500 μl to the cells. Two rounds of infection were carried out in the presence of 5ug/mL of polybrene (Sigma). Cells were infected simply by adding the concentrated rentivirus supernatant (20-35μL/well) onto the cells; the plate was centrifuged for 45 minutes at 4˚C in 1800rpm and then incubated at 37˚C overnight. Eight hours later 500 μl virus-free medium were added to the virus incubations to dilute the polybrene. The second round of infection was performed the day after by adding (20-35μL/well) of concentrated retroviral supernatant to the cells and centrifugation for 45 minutes at 4˚C in 1800rpm. At the end of the two cycles, the medium with viral particles was removed and substituted with virus-free medium. Infected cells expressed shRNA against the mRNA of the protein of interest and GFP as the selection marker. Therefore, the selection of cells expressing the shRNA was done by sorting of GFP positive cells by fluorescence-activated cell sorting (FACS) instrument (FACSVantage instrument, BC). Cells were also collected for RNA and protein extraction to confirm the successful knockdown of target gene.

Protein extraction

This method allows the detection of protein of interest and relative post translational modification in a sample extract. Protein extracts were obtained from cell pellets after lysis with 100μL to 200μL of sodium-dodecyl-sulfate (SDS) lysis buffer (2% SDS, 10% glycerol, 50mM of Tris HCL) plus protease inhibitor cocktail. Cell lysate was then sonicated for 30 seconds by Branson Sonifier 250. After sonication, samples were centrifuged for 15 min at 4°C, 13000 rpm. Protein was quantified by a Bio-rad Bradford assay. 1X volume of Bradford reagent was diluted with 4X volume of MilliQ water to prepare a working Bradford solution. For measuring protein concentration of sample at absorbance 595 nm, SDS buffer was first measured as blank, and 1 μL sample in 999 μl Bradford (dilution factor 1: 20) was measured.

Western blot analysis and Antibodies

Proteins can be separated based on their molecular size, net charge and shape in a polyacrylamide gel electrophoresis (PAGE). Acrylamide can be polymerized under the presence of bis-acrylamide into chains to form meshwork of polyacrylamide and by adjusting the concentration of acrylamide, polyacrylamide gel with different resolution can be casted to obtain efficient separation of protein molecules. The polymerization is catalyzed by addition of ammonium persulfate (APS) as source of free radicals and N,N,N',N'-tetramethylethylenediamine (TEMED) to form and stabilize the free radicals. Proteins are denatured by detergent such as sodium dodecyl sulfate (SDS) to become negatively charged. SDS binds to hydrophobic regions of the proten molecules, causing them to unfold. During PAGE, denatured proteins are separated primarily by their molecular size but not structure and isoelectric charges. A stacking gel is casted on top of the resolving gel in the PAGE system. The purpose of stacking gel, which is usually of lower acrylamide concentration and pH than

the resolving gel, is to focus all protein molecules of various molecular sizes into the same thin layer for entering into another gel boundary. Separated proteins in the PAG can then be transferred for Western blotting or visualized by direct staining.

50-80 μg of proteins were mixed with Laemmli (b-mercaptoethanol and bromophenol blue) and denatured for 10 min at 95°C. Cell lysates were loaded onto each lane of an acrylamide, bis-acrylamide gel, and a sodium dodecyl sulfate-polyacrylamide gel electrophoresis (SDS-PAGE). 10 μL of dual-color Pre-stained Protein ladder (BIO-RAD) was also loaded per gel for reference of protein molecular size.

Gel-separated proteins were transferred to a nitrocellulose membrane (Whatman) in a 1X transfer buffer containing 20% methanol, at 100V for 1 hour at 4°C. The gel/membrane was compressed with layers of filter papers and sponge to ensure close contact between the gel and the membrane. Protein molecules, which were negatively charged, were transferred to the membrane in 1X transfer buffer (25 mM Tris base, 192 mM glycine, 20% methanol) at constant voltage of 100 volts for 1 hour.

Ponceau S was used for staining of membrane, which allows the visualizing of proteins and thus the quality of the transfer. After a brief wash in water and 1% Tris-buffered Saline-Tween (TBS-T), Membranes were blocked with a solution of in TRIS-buffered saline (TBS: 20mM TRIS/HCl, pH 7.4, 137 mM NaCl, 2.7 mM KCl) plus 0.1% Tween (TBS-T) containing 5% non-fat dried milk. Pre-blocking of the membrane can prevent non-specific binding of antibodies which may result in a high background or false positive detection.

The same milk/TBS-T solution was prepared to dilute primary antibodies, which were incubated for one hour at room temperature or overnight at 4 °C. The next day, after 3 washes with 1% TBS-T (each wash 10 minutes), membrane was incubated with the proper

horseradish peroxide (HRP)-conjugated secondary antibody or secondary antibodies labeled with IRDye near-infrared (NIR) fluorescent dyes, diluted in 5% milk, for 30-60 minute at room temperature. Following three further washes in TBS-T, the bound secondary antibody was revealed by ECL method (enhanced chemiluminenscence, Amersham) or ECL-plus (Amersham) or fluorescence Detection (Odyssey, Licor).

The antibodies used in the study were anti-LSD1 Antibody (Cell signalling #2139); anti-PML (H-238) (Biotechnology Inc, Santa Cruz, CA); anti-Tubulin T8328 Sigma; anti-P21 (C-19) (Biotechnology Inc, Santa Cruz, CA).

Total RNA Extraction and Complementary DNA (cDNA) Synthesis

For Total RNA extraction, 1 mL TRIZOL reagent was added to cell pellet harvested from confluent cells grown. Cells were gently pipetted up and down for complete cell lysing in TRIZOL. TRIZOL/cell mixture was next transferred into clean microcentrifuge tube and total RNA was purified using RNeasy Mini Kit (QIAGEN, Valencia, CA) and quantified by spectrophotometer (ND1000 NanoDrop). RNA quantity and quality was assessed by A260 (1 OD260 = 40 μg/ml for single stranded RNA), A260/A280 ratio (> 1.6). RNA sample was stored at -80°C for later use.

Then RNA reverse transcribed to cDNA with one script plus reverse trascriptase (abm) according to the manufacturer's instructions. Briefly, 1 μg RNA was mixed with 1 μl random primer (10 μM), 1 μl dNTP mix (10mM) and reachet to 14.5 μl with nuclease-free H_2O and denatured at 65^oC for 5 minutes and snap-frozen on ice for 5 minutes. Reverse transcription (RT) was performed in a 20 μl-reaction mixture containing 4 μl 5X RT buffer, 0.5 μl RNaseOFF Ribonuclease inhibitor(40u/μl) and 1μl EasyScript Plus RTase (200U/μl). The denatured RNA was incubated with the RT reaction mixture for 10 minutes at 25^oC. The

reaction was stopped by heating it at 85°C for 5 min. cDNA sample was stored at -20 °C for later use.

Quantitative polymerase chain reaction (qPCR)

From 5 to 10 ng of cDNA were used to perform quantitative polymerase chain reaction using SYBR Green Reaction Mix (Perkin Elmer, Boston, MA). mRNA levels were normalized against GAPDH mRNA. All the qPCR amplifications were performed in the CFX96™ real-time system (BIO RAD): 95°C hold for 10 minutes followed by 40 cycles of 95°C for 15 seconds and 60°C for 60 seconds. The sequences of the primers used in this study are listed in the table 1.

Table 1.Primers for quantitative PCR used in this study.

Primer name	Forward primer (Fw)	Reverse primer (Rv)
GAPDH	GCCTCAAGATCATCAGCAATGC	CCACGATACCAAAGTTGTCATGG
ITGAM	AACCCCTGGTTCACCTCCT	CATGACATAAGGTCAAGGCTGT
LSD1	AGACGACAGTTCTGGAGGGTA	TCTTGAGAAGTCATCCGGTCA
P21	TCACTGTCTTGTACCCTTGTGC	GGCGTTTGGAGTGGTAGAAA
Ccl5	CCTCATTGCTACTGCCCTCT	GGTGTGGTGTCCGAGGAATA
BMP2	CGGACTGCGGTCTCCTAA	GGAAGCAGCAACGCTAGAAG

RNA-seq protocol

RNA-Sequencing (RNA-Seq) allows for quantitative measurement of expression levels of genes and their transcripts. RNA-seq was performed according to the True-seq Low sample

protocol selecting only polyadenylated transcripts. In brief, before starting mRNA isolation and library preparations the integrity of the total RNA was evaluated by running samples on a Bioanalyzer instrument by picoRNA Chip (Agilent), then converted into libraries of double stranded cDNA appropriate for next generation sequencing on the Illumina platform. The Illumina TruSeq v.2 RNA Sample Preparation Kit was used following manufacturer's recommendations. Briefly, 0.1-1 μg of total RNA were subjected to two rounds of mRNA purification by denaturing and letting the RNA bind to Poly-T oligo-attached magnetic beads. Then fragmentation was performed exploiting divalent cations contained in the Illumina fragmentation buffer and high temperature. First and second strand cDNA is reverse transcribed from fragmented RNA using random hexamers. First strand cDNA was synthesized by SuperScript II (Invitrogen) reverse transcriptase transcriptase and random primers and second strand cDNA synthesized by DNA polymerase I and Rnase H. The subsequent isolation of the cDNA was achieved by using AMPure XP beads (depending on the concentration used, these beads can efficiently recover PCR products of different sizes). The product recovered contained overhanging strands of various length due to the fragmentation procedure. The 5' and 3' ends of cDNA are repaired by the 3'-5' exonuclease activity and the polymerase activity and adenylated at 3' extremities before ligating specific Illumina oligonucleotides adapters followed by 15 cycles of PCR reaction using proprietary Illumina primers mix to enrich the DNA fragments. Prepared libraries were quality checked and quantified using Agilent high sensitivity DNA assay on a Bioanalizer 2100 instrument (Agilent Technologies).

RNA sequencing data analysis

RNA-seq analysis was performed with the TopHat and Cufflinks algorithm [Trapnell, 2010]. Cufflinks is able to re-assemble transcripts to give a quantitative estimation of their presence

and to calculate differential gene regulation among several samples. The number of reads obtained was comparable among the samples. The values considered to quantify the relative expression of a given gene correspond to the number of reads aligned per kilobases of the transcript per million map able fragment detected (FPKM, fragment per kilobase of exon per million fragments mapped). These values were used for all the comparative analysis. The threshold set to consider a gene as being regulated was FDR$\leq$ 0.05, FPKM $\geq$ 0.5 and Fold change greater than absolute Log2(1.5).

ChIP-Seq and ChIP- qPCR

ChIP (chromatin immunoprecipitation) technique is used to investigate protein-DNA interaction studies. The fundamental principle is the cross-linking between DNA and DNA-associated proteins that can be achieved by fixing cells with formaldehyde. Cross-linked chromatin is sheared by sonication to generate fragments of 300-1000 base pairs (bp) in length. Through immunoprecipitation, proteins of interest coupled to DNA are isolated by specific antibodies. Antibodies that recognize a protein or protein modification of interest can be used to determine the relative abundance of protein or modification. Chemical cross-linking is reversible, thus DNA can be separated from associated proteins and analyzed, both by high throughput sequencing and real time quantitative PCR.

Cells were cross-linked in culture medium by adding 37% formaldehyde to a final concentration of 1% and the reaction was stopped after 10 min at RT by adding 2M glycine to a final concentration of 0.125M for 5 min. The cells were washed twice with cold PBS and collected by centrifuge for 5 min at 1500rpm. At this step the Pellets can be stored at -80° in SDS buffer (50 mM Tris•HCl pH 8.1, 0.33% SDS, 150mM NaCl, 5 mM EDTA, and protease inhibitor cocktail) or directly processed with sonication in IP buffer (100mM tris ph 8.6 0.3% SDS 1.7% TRITON x-100 and 5mM EDTA).

Chromatin was then fragmented to obtain 200-500 bp in length by using a Branson Sonifier 250.

Then protein A sepharose beads (GE Healthcare, cat. 170780-01; 30 µl slurry per milligram of sonicated chromatin; 0.5-1 mg of chromatin was used for each precipitation; 100 µl were used for histone PTMs) were added and incubated 2 h at 4°C, to remove DNA or proteins which might bind non-specifically to the Protein G beads. This was followed by three washes with "low salt" wash buffer (20 mM TRIS/HCl pH8.0, 2 mM EDTA, 150 mM NaCl, 0.1% SDS, 1% TRITON X-100), and one in "high salt" wash buffer (20 mM TRIS/HCl pH8.0, 2 mM EDTA, 500 mM NaCl, 0.1% SDS, 1% TRITON X-100) were performed. Then, the supernatant was immunoprecipitated overnight in the presence of 30-50 microL of protein G magnetic beads. For histone modification 1 ml corresponding to 3×10^6 cells per each IP and 4ug/ml primary antibody were used while for LSD1 Chip-Seq 40×10^6 cells per each IP and 10ug/ml of LSD1 antibody were used. Before IP 2.5% of input was stored at 4% prior to the decrosslinking procedure. We used anti-IgG as mock antibody (negative control) of the ChIP assay. Decrosslinking was performed for all the IP samples and corresponding inputs, over night in 0.1%SDS and 0.1% NaCOH3. The day after, the enriched DNA was treated with proteinase K at 56°C for 40 min and purified with QIAquick PCR purification kit (Qiagen). The obtained DNA was then quantified by picogreen and 5-10ng were processed for ChIP-Seq library preparation or used for quantitative real-time PCR (qPCR). The DNA retrieved from ChIP experiments were used for ChIPseq libraries preparation with the Illumina ChIPSeq Sample Prep kit (IP-102-1001) and multiplexing oligonucleotide kit (PE-400-1001) by our internal genomic facility. DNA libraries were quantified using a high sensitivity DNA Chip on Bioanalyzer instrument (Agilent) and used for cluster generation and sequencing using the HiSeq 2000 pltaform (Illumina) following the protocol of the manufacturer.

For the validation of specific regions, ChIP-qPCR were performed as follows. Immunoprecipitated DNA was diluted in 9,6μl of H2O per reaction, plus 400 nM primers in a final volume of 20μl in SYBR Green. Each ChIP experiment was performed at least three times with biological replicates.

Abs used for ChIP qPCR/Seq: anti-LSD1 antibody (Abcam – ab17721), anti- H3K4me2 antibody (Abcam-ab32356) and anti- H3K27ac antibody (Abcam-ab4729), IgG sc-2027.

PicoGreen(pcg) quantification of ChIP DNA.

This protocol was established with a Glomax fluorometer. PicoGreen dsDNA Quantitation Reagent is an ultra-sensitive fluorescent nucleic acid stain for quantitating double-stranded DNA (dsDNA) in molecular biological procedures, allows the detection and quantitation of DNA concentrations as low as 25pg/mL of dsDNA. PicoGreen 2x solution was prepared by diluting 200x stock in TE (final volume 200μL). A standard DNA curve was performed by using genomic DNA as a reference. ChIP DNA generally has a low concentration; therefore, standard DNA dilutions should range from 25pg/ml up to 25ng/ml. We prepared a reference sample of 2μg/ml of genomic DNA, which was then diluted 40x in TE this stock to get a final 50ng/ml solution. This is further diluted and then by serial dilution you may obtain 1/10-1/100-1/1000 the last of which corresponds to a 25pg/ml concentration. Briefly, we routinely took 2μl from ChIP samples, brought the volume to 200μL TE - to have a replica - including total control and mock. We then added 100 μL/ml of pcg to each well and incubated 2-5 minutes, mixed and further incubated for 2 to 5 minutes at RT, protected from light. After reading, we plot a low-range standard curve corrected against the reagent blank fluorescence value.

ChIP-Seq analysis

Sequencing data generated from the Illumina platforms were aligned were mapped to Human NCBI36/hg18 using Bowtie version 0.12.7 [Langmead, 2009]. Only sequences showing unique alignment were used for peak detection, allowing for a maximum of two mismatches. Peaks calling was performed with MACS with the threshold of -log10(p)=5 for all the ChIP-seq except LSD1 both in NB4 and UF1, for which we perform ChIP- qPCR and set a more stringent threshold. For the validation of LSD1 positive regions we selected regions with several p-values (obtained with MACS peak calling) and perform ChIP-qPCR assay. For LSD1 ChiP-Seq in NB4 and UF1 cells according to our validation analysis we set a stringent threshold; pvalue $\leq$ 0.017, while for the all other ChIP-seq p-value $\leq$ 0.05. Using intergenic region negative for LSD1 as control and anti-IgG antibody as mock control we set the minimum value for positive true enrichment as the enrichment of negative control plus three times the relative SD. 26 out of 30 regions tested were considered as validated and thus we set as MACS score threshold the minimum score among these 26 validated regions. With this new threshold of -log10(p)=16.9 we obtained 15187 and 33515 LSD1 peaks in NB4 and UF1 respectively. Reads from each sample were normalized to the respective input. Peaks were associated to Refseq annotated genes according to GIN (Cesaroni et al. Bioinformatics 2008) while intergenic regions were considered as having more than 22kb of distance from the nearest gene. UCSC Genome tracks were generated normalizing each sample to the same sequencing depth. The intersection among the peaks datasets was performed with bedtools intersect tool, peaks are considered overlapping if they share at least 1bp.

Statistical analysis:

Statistical analyses were performed using the unpaired sample 2-tailed Student t test (GraphPad software) unless otherwise specified.

Contents of general buffers used in this study:

Phosphate-Buffered Saline (PBS), pH 7.4:

137 mM NaCl

2.7 mM KCl

8.1 mM Na_2HPO_4

1.76 mM KH_2PO_4

Tris-Buffered Saline (TBS)-Tween:

150 mM NaCl

2.7 mM KCl

25 mM Tris base

0.1% Tween 20

Tris-Acetate-EDTA (TAE):

40 mM Tris acetate

1 mM EDTA pH 8.

Urea lysis buffer:

8 M Urea

25 mM Tris-HCL pH 6.8

1 mM EDTA

10% glycerol

<u>Resolving gel mix (1 gel at 12%):</u>

Acrilamide/Bis-acrylamide solution 30 %: 2.52 mL for 12% gel

Tris-HCl, pH 8.8 (1.5 mL)

ddH_2O (1.7 mL)

SDS 10% (60 μL)

APS 10% (50 μL)

TEMED (2 μL)

<u>Stacking gel mix (1 gel):</u>

Acrilamide/Bis-acrylamide stock solution – 30%: 0.8 ratio at 30% (0.52 mL)

Tris-HCl, pH 6.8 (1.25 mL)

ddH_2O (3.10 mL)

SDS 10% (50 μL)

APS 10% (50 μL)

TEMED (5 μL)

<u>Laemmli loading buffer (5X):</u>

100mM Tris-HCl pH 6.8

20% Glycerol

2% SDS

5% β-mercaptoethanol

<u>Western blot transfer buffer:</u>

25 mM Tris base

192 mM Glycine

20% Methanol

Western blot Stripping buffer:

62.5 mM Tris-HCl, pH 7.6

2% SDS

100 mM β-mercaptoethanol

SDS buffer:

50 mM TRIS-Cl

0.5% SDS

100 mM NaCl

5mM EDTA pH 8

0.02% NaN3

Triton dilution buffer:

5% Triton X-100

100 mM TRIS-Cl PH 8.6

100 mM NaCl

5mM EDTA pH 8

0.02 % NaN3

Mixed Micelle wash buffer:

5.2% Sucrose

1% Triton X-100

20 mM TRIS-Cl PH 8.1

150 mM NaCl

5mM EDTA pH 8

0.02 % NaN3

0.2% SDS

Li/Cl detergent buffer:

250mM LiCl

0.5% Deoxycholic acid

10 mM TRIS-Cl PH 8

0.5% NP-40

1mM EDTA pH 8

0.02 % NaN3

Decrosslinking solution:

0.1M NaHCO3

1% SDS

LSD1 inhibition in APL cell lines

We have previously characterized a novel LSD1 inhibitor, MC2580, showing high specificity (100 fold more than TCP) and acting at relatively low concentrations [Binda, 2010]. By taking advantage of this inhibitor (we will refer to this as MC) we have been able to investigate the mechanistic role of LSD1 in APL. As a model system we used two APL cell lines: i) NB4 cells, isolated from an APL patient, that have characteristics similar to APL blasts and are sensitive to RA; and ii) UF1 cells, that were established from a patient who was clinically resistant to RA [Lanotte ,1999; Kizaki, 1996].

We have previously shown that LSD1 inhibition sensitizes NB4 cells to retinoic acid (RA) treatment and induces cell growth arrest and differentiation when combined with a physiological concentration of RA (RA low) [Binda, 2010] **(Figure 12A, B)**. We hereafter refer to physiological (0.01 μM) and pharmacological (1 μM) dose of RA with RA low and RA high respectively.

To strengthen our observations, we performed colony forming unit assay (CFU) as a surrogate read-out for the self renewal ability of leukemic cells. NB4 cells were treated with the LSD1 inhibitor also in combination with RA low and RA high. Both co-treatment and RA high significantly reduced the number of colonies and led to differentiation in 1st plating. While RA high-treated colonies gave rise to higher number of secondary colonies, co-treatment maintained the reduction when they were cultured in the absence of the drugs, suggesting that co-treatment more efficiently reduce clonogenic activity of NB4 cells **(Figure 13)**.
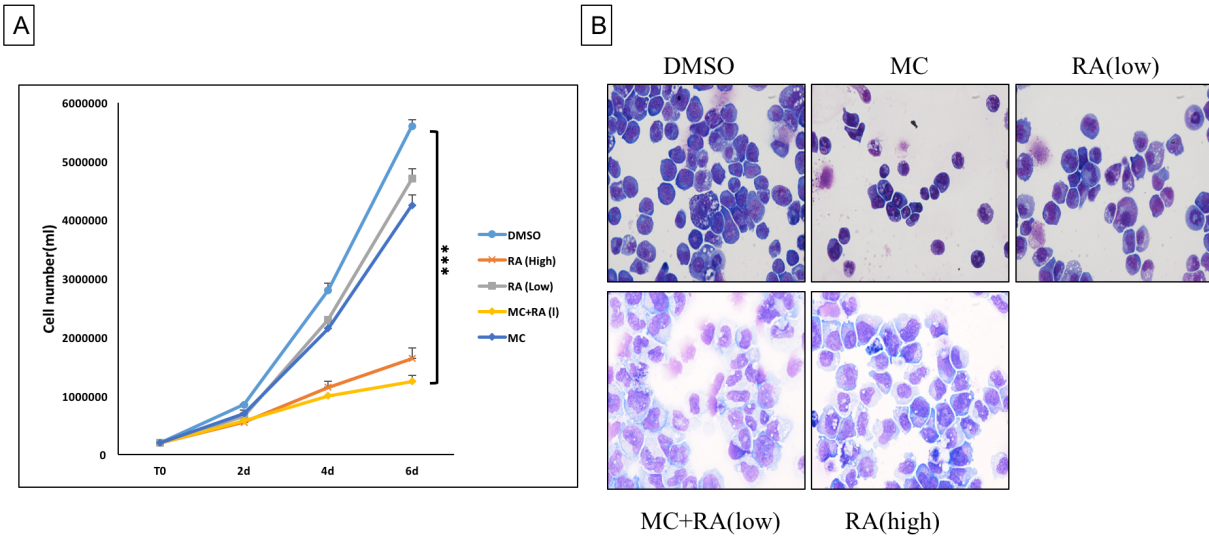
Figure 12. **LSD1 inhibition sensitizes NB4 cells to physiological dose of retinoic acid (RA).** (A) Relative proliferation of NB4 cells treated with MC and/or RA low (10nM) and RA high (1µM). Data are presented as mean of triplicates ± SD. (B) Representive light micrograph show Wright-Giemsa staining of NB4 cells treated with indicated inhibitors for 6 days. P value < 0.05 (*****), P < 0.01 (*** ***) and P <0.001 (*** * ***).
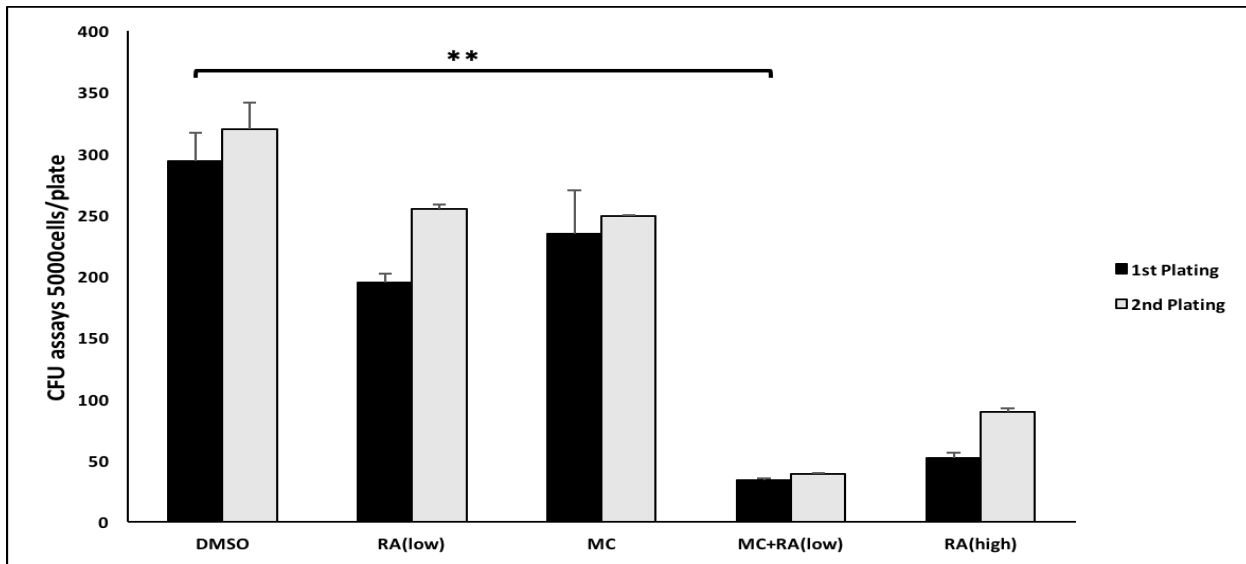

Figure 13. **LSD1 inhibition sensitizes NB4 cells to physiological dose of retinoic acid (RA).** Analysis of the proliferative potential of treated NB4 cells with indicated inhibitors by serial replating assay. Data are presented as mean of triplicates ± SD. P value < 0.05 (*****), P < 0.01 (*** ***) and P <0.001 (*** * ***).

These results prompted us to evaluate whether LSD1 inhibitor sensitizes RA-resistant cell line, UF1 cells, to RA. To this end, UF1 cells were treated with MC also in combination with RA low. Surprisingly MC as a single agent inhibited UF1 cell proliferation and as expected, RA had no effect on cell proliferation **(Figure 14)**.
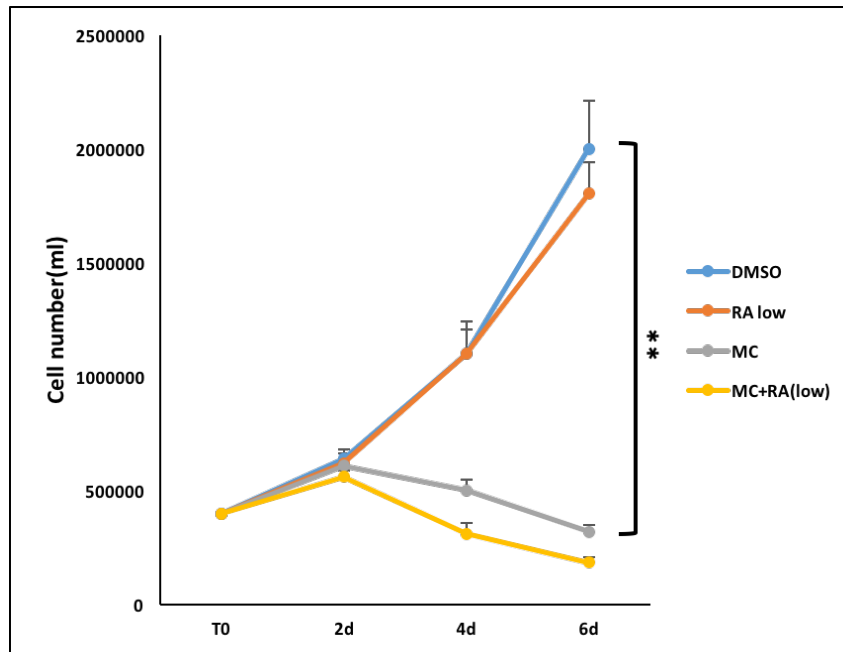

Figure 14. **LSD1 inhibition inhibits proliferation of UF1 cells.** Relative proliferation of UF1cells treated with MC and/or RA low (10nM). Data are presented as mean of triplicates ± SD. P value < 0.05 (*****), P < 0.01 (*** ***) and P <0.001 (*** * ***).

We next evaluated the effect of MC in UF1 cell differentiation. Cell differentiation was evaluated in all samples after Wright-Giemsa staining. Relative to DMSO, MC and co-treated cells display a more mature morphology as observed by several features: 1) they contained a reduced nucleus to cytoplasm ratios and 2) nuclear lobulation **(Figure 15A)**. This induction of differentiation was further confirmed by induction of CD11b expression, a surface marker belonging to the integrin family that is expressed specifically in differentiated granulocytes **(Figure 15B)**. As expected RA low had no effect on UF1 cells differentiation.
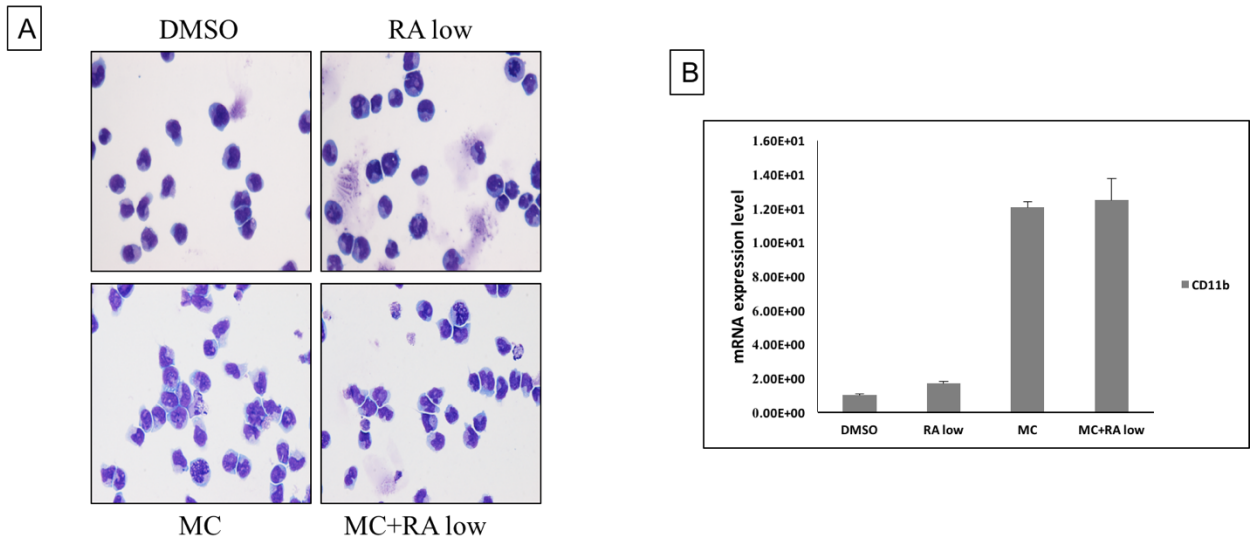
Figure 15. **LSD1 inhibition promotes differentiation in UF1 cells.** (A) Representive light micrograph show Wright-Giemsa staining of UF1 cells treated with indicated inhibitors for 6 days. (B) LSD1 inhibition induces expression of the CD11b gene. Values were normalized against GAPDH.

It has been shown that pharmacological doses of RA (RA high) induces differentiation of APL cells by PML-RARα fusion protein degradation, which has been proposed as a crucial goal in order to eradicate APL. We observed that LSD1 inhibition induces cell differentiation without inducing PML-RARα degradation **(Figure 16)**. Thus LSD1 inhibition can overcome PML-RARα expression to reach differentiation and growth arrest of APL-UF1 cells.
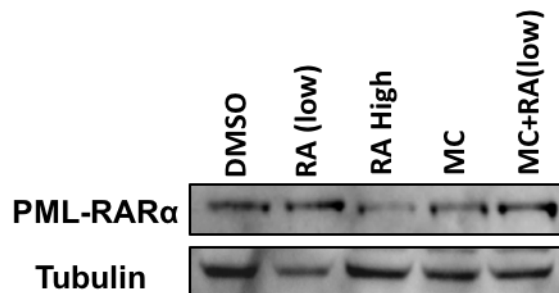
Figure 16. **LSD1 inhibition promotes differentiation of UF1 cells without PML-RARα degradation.** Western blot analysis of PML-RARα and tubulin (serves as loading control) in UF1 cells after 6 days treatment with indicated inhibitors.

To further understand the basis of the observed decrease in cell growth caused by MC treatment, we studied cell death in control and MC-treated UF1 cells. We performed trypan blue staining, which is incorporated specifically in dead cells, and found an increased rate of cell death in MC-treated cells as compared to control cells. We next used Annexin V / PI staining followed by FACS analysis to study whether this increase in basal cell death was caused by apoptosis. During apoptosis, phosphatidylserine is translocated from the cytoplasmic face of the plasma membrane to the cell surface. Annexin V can be used to detect and measure early apoptosis by binding to phosphatidylserine residues. PI is used as a DNA stain or DNA content in cell cycle analysis. PI is membrane impermeable and can be used for identifying dead cells. MC-treatment for 6 days increased the G1 cell cycle arrest and induced apoptosis **(Figure 17A, B)**. The increased number of cells in G1 phase was accompanied by reduced proportion of cells in S phase.
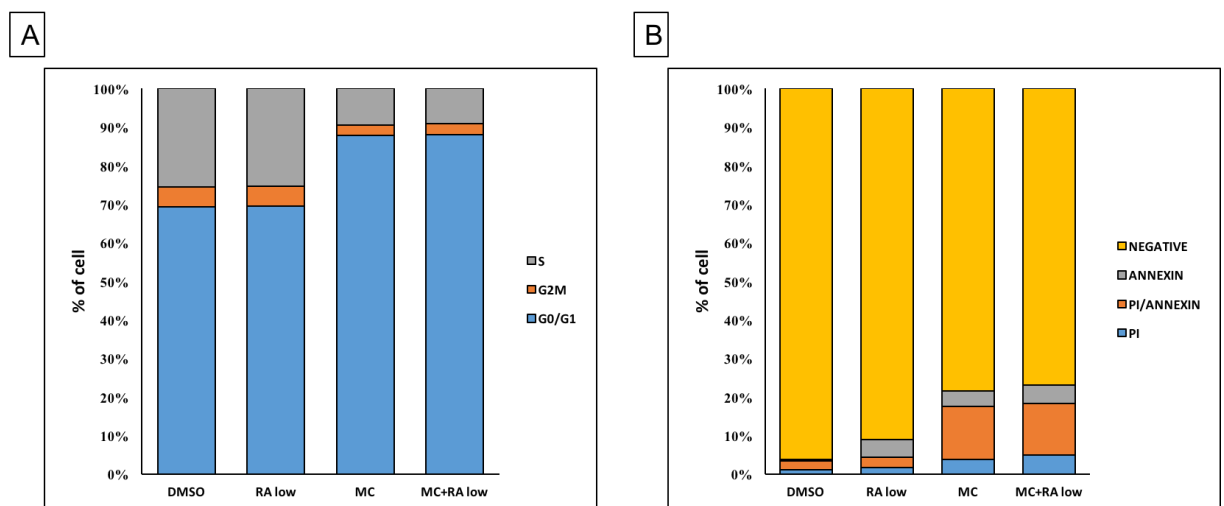

Figure 17. **LSD1 inhibition in UF1 cells, induces cell cycle arrest and apoptosis.** (A) Summary of cell-cycle status of UF1 cells after 6 days treatment with indicated inhibitors. (B) Percentage of live and apoptotic UF1 cells after 6 days treatment with indicated inhibitors.

To corroborate these cell viability data, we took advantage of two other LSD1 inhibitors which are reversible and irreversible LSD1 inhibitors. Both inhibitors inhibited cell proliferation in a time and dose-dependent manner **(Figure 18A, B)**.
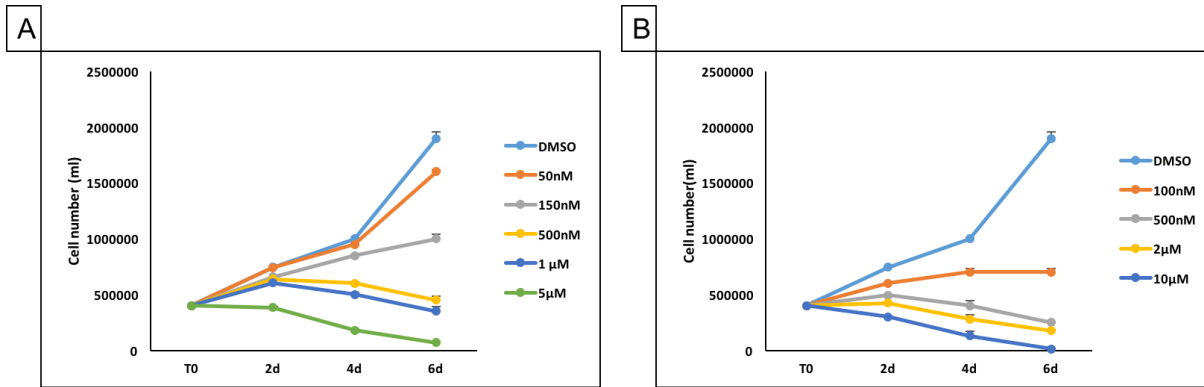
Figure 18. **LSD1 inhibitors inhibit UF1 cell proliferation in a time and dose-dependent manner.** (A) Growth inhibition in response to reversible LSD1 inhibitor. (B) Growth inhibition in response to irreversible LSD1 inhibitor. Data are presented as mean of triplicates ± SD.

Mirroring the results in liquid culture, treatment with MC drastically reduced the number of colonies and this reduction was maintained in 2nd plating. Following treatment with MC, and not DMSO, UF1 cells exhibited a dramatic morphologic alteration from the primarily large and compact colonies to the small and diffuse one, characteristic of differentiated cell clusters **(Figure 19A, B)**.

Taken together, LSD1 inhibitor as a single agent in UF1 cells in contrast to NB4 cells leads to cell growth inhibition, induced cell differentiation without PML-RAR degradation. Treatment of UF1 cells with MC promoted G1 cell cycle arrest and apoptosis.
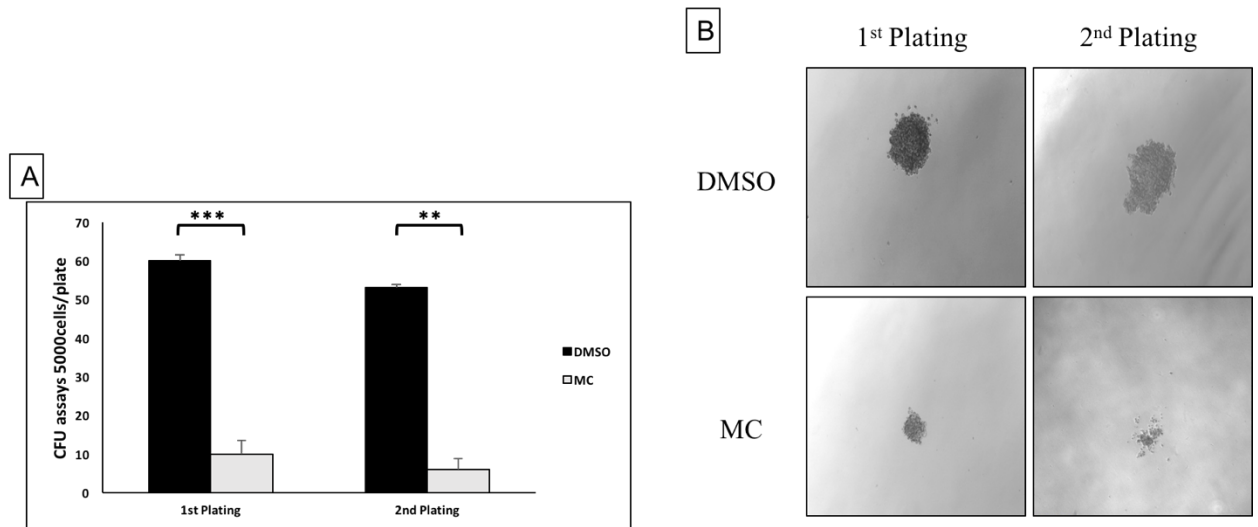
Figure 19. **LSD1 inhibition efficiently inhibits clonogenic activity of UF1 cells.** (A) Analysis of the proliferative potential of treated UF1 cells with indicated inhibitors by serial replating assay. Data are presented as mean of triplicates ± SD. (B) Colony morphology of treated UF1 cells with indicated inhibitors. P value < 0.05 (*****), P < 0.01 (*** ***) and P <0.001 (*** * ***).

LSD1 depletion mimics the effect of LSD1 inhibition

To modulate levels of LSD1 protein, we transfected LSD1-directed short hairpin RNA (shRNA) constructs into UF1 cells and monitored knockdown by western blot and qPCR. We used two independent shRNA constructs that efficiently downregulated LSD1 mRNA and protein levels.

As shown in Figure 20, both shRNAs effectively reduced the protein and mRNA levels of LSD1 compared with control shRNA **(Figure 20A, B)**.

Knock-down of LSD1 led to a significant cell growth inhibition of UF1 cells **(Figure 21)**.
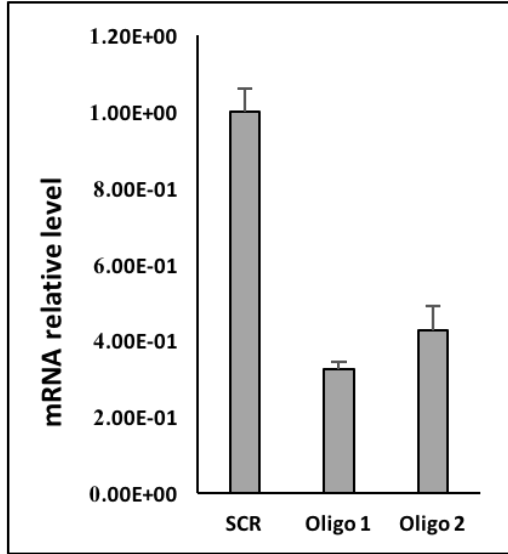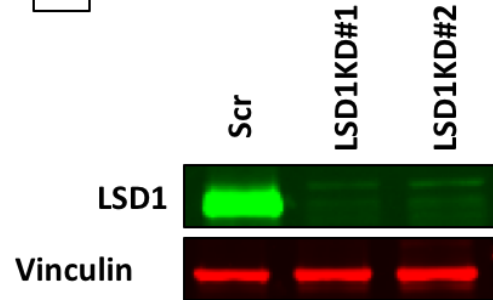
Figure 20. **LSD1 depletion in UF1 cells.** (A) Analysis of LSD1 mRNA relative levels in UF1 cells, transduced with the indicated lentiviral vectors. Values were normalized against GAPDH and referred to SCR. (B) Immunoblot analysis of LSD1 expression in UF1 cells. Vinculin was used as a loading control.
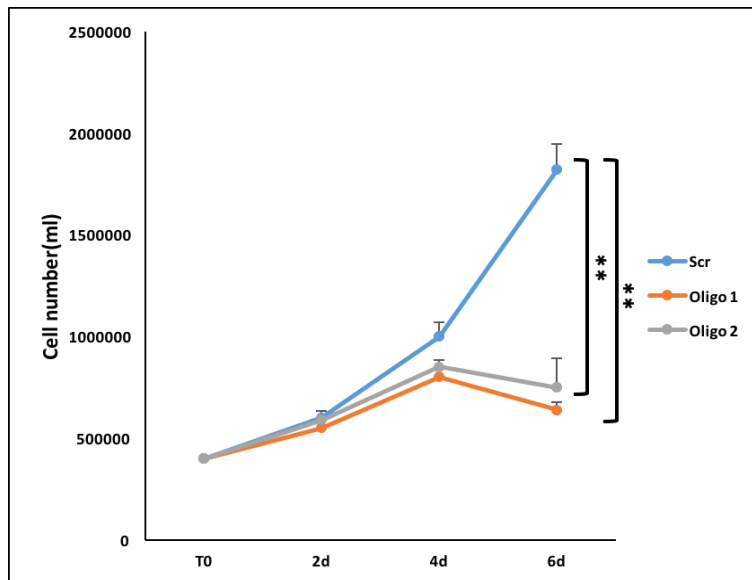

Figure 21. **LSD1 depletion inhibits proliferation of UF1 cells.** Relative proliferation of UF1cells infected with SCR or LSD1 shRNAs. Data are presented as mean of triplicates ± SD. P value < 0.05 (*), P < 0.01 (**) and P <0.001 (***).

We next investigated the effect of LSD1 depletion in cell differentiation. Wright-Giemsa staining revealed alteration by LSD1 depletion in cell morphology from leukemic myeloblasts to differentiated cells which was concurrent with the increased expression of differentiation marker **(Figure 22A, B)**.
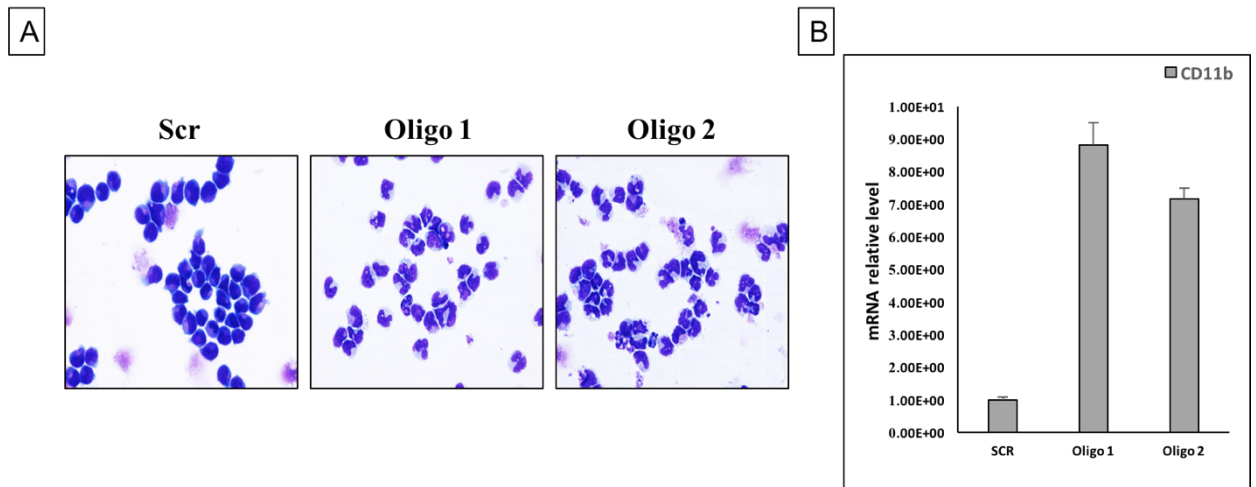

Figure 22. **LSD1 depletion promotes differentiation in UF1 cells.** (A) Representative light micrograph show Wright-Giemsa staining of UF1 cells infected with indicated shRNA. (B) LSD1 depletion induces expression of the CD11b gene. Values were normalized against GAPDH and referred to SCR.

Like MC-treated cells, KD of LSD1 led to G1 cell cycle arrest **(Figure 23A)**. PI and annexin V binding assays also demonstrated that some LSD1-KD cells underwent apoptosis **(Figure 23B)**.
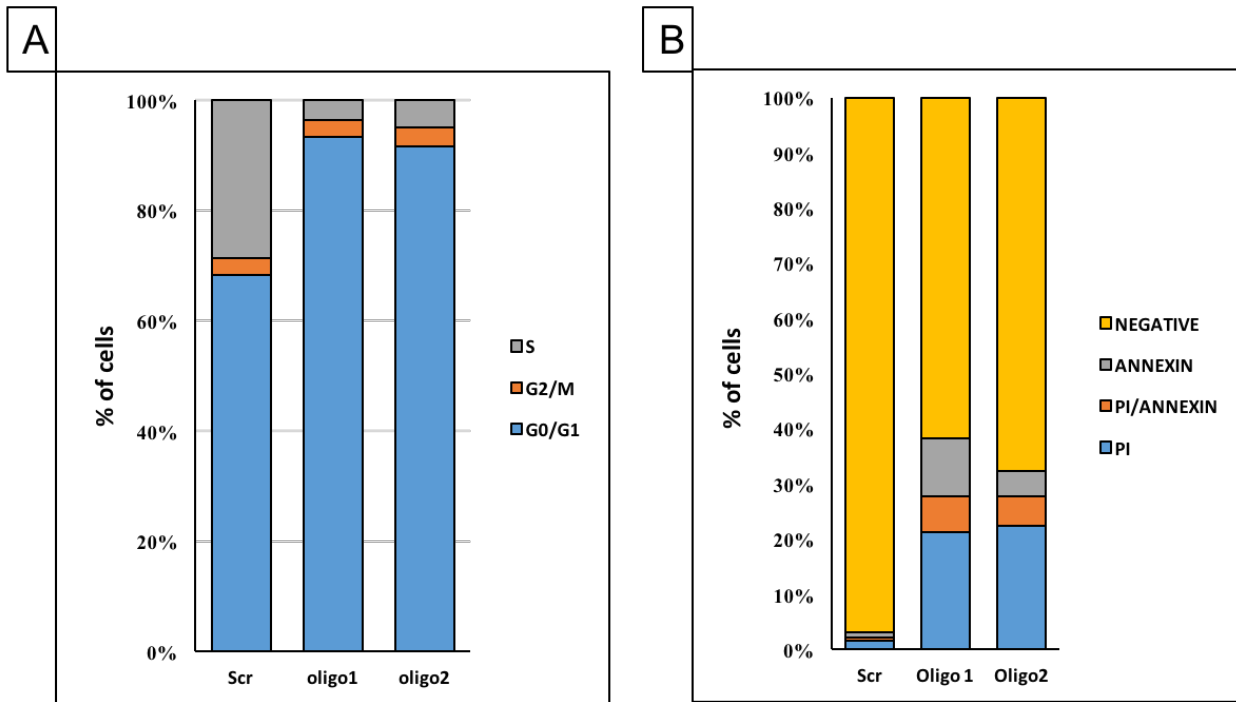
Figure 23. **LSD1 depletion in UF1 cells, induces cell cycle arrest and apoptosis.** (A) Summary of cell-cycle status of UF1 cells infected with indicated shRNA. (B) percentage of live and apoptotic UF1 cells infected with indicated shRNA.

Together these data demonstrate on-target effects of MC as LSD1 depletion effectively mimics the effect of LSD1 inhibition.

Underlying molecular mechanism for the different responses of NB4 and UF1 APL cell lines to LSD1 inhibition

To dissect underlying molecular mechanisms for different response to LSD1 inhibition in NB4 and UF1 cells, we performed a genome-wide expression analysis comparing basal gene expression profiling of the two cell lines. While RNA-seq results showed high correlation in gene expression profiling in both APL cell lines, 86 genes and 101 genes were found up and down-regulated respectively in UF1 cells in comparison with NB4 cells **(Figure 24, 25)**.
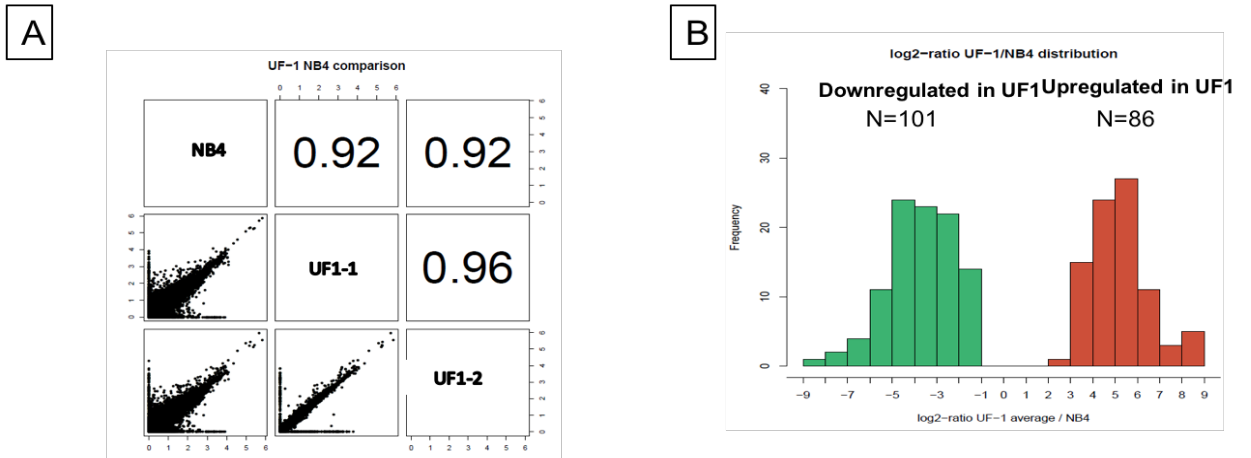
Figure 24. **Gene expression profiling in UF1 and NB4 cells.** (A) high correlation in gene expression profiling in UF1 and NB4 cells. (B) There are 86 genes and 101 genes up and down-regulated respectively in UF1 cells compared with NB4 cells.
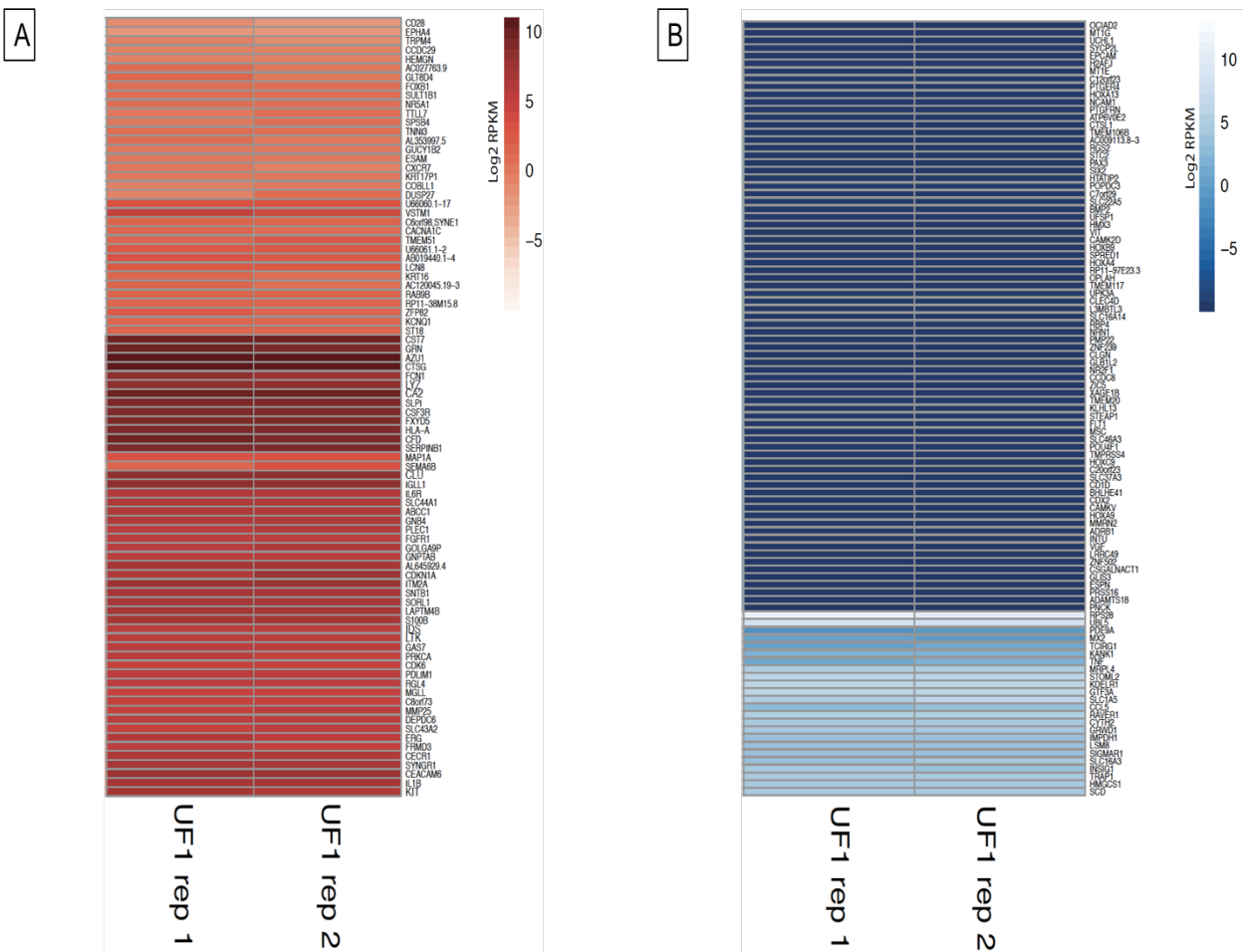
Figure 25. **86 and 101 genes up and down-regulated respectively in UF1 cells compared with NB4 cells.** Heatmap representation of gene expression in UF1(2 replicates) compared with NB4 cells. The data are presented as the average log$_2$ fold change. The magnitude of the changes is indicated by a color scale, with shades of red indicating increase and shades of blue indicating decrease in expression.

Additionally, we validated the RNA-seq results by qRT-PCR for two upregulated genes, KIT,

p21 and two downregulated genes, CCL5 and BMP2 **(Figure 26)**.
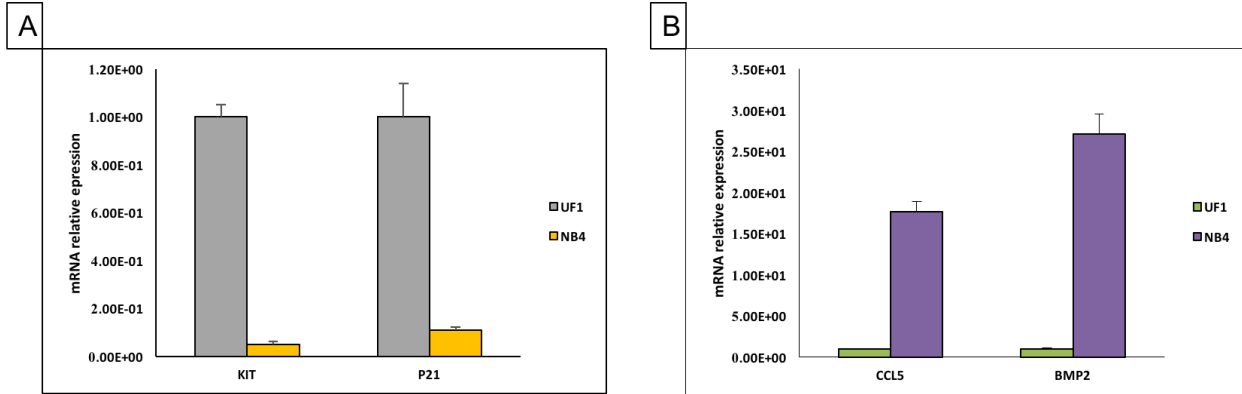
Figure 26. **Validation of the RNA-seq results by qRT-PCR.** (A, B) Expression of KIT, p21, CCL5 and BMP2 were measured in UF1 and NB4 cells by real-time RT-qPCR. Values were normalized to GAPDH.

One of those up-regulated genes was CDKN1A (p21) **(Figure 27)**, and this high level of p21

was further confirmed by qRT-PCR **(Figure 26)**. In addition, as illustrated in Figure 27, p21

were further upregulated in UF1 cells but not in NB4 cells after treatment with MC **(Figure

27)**.
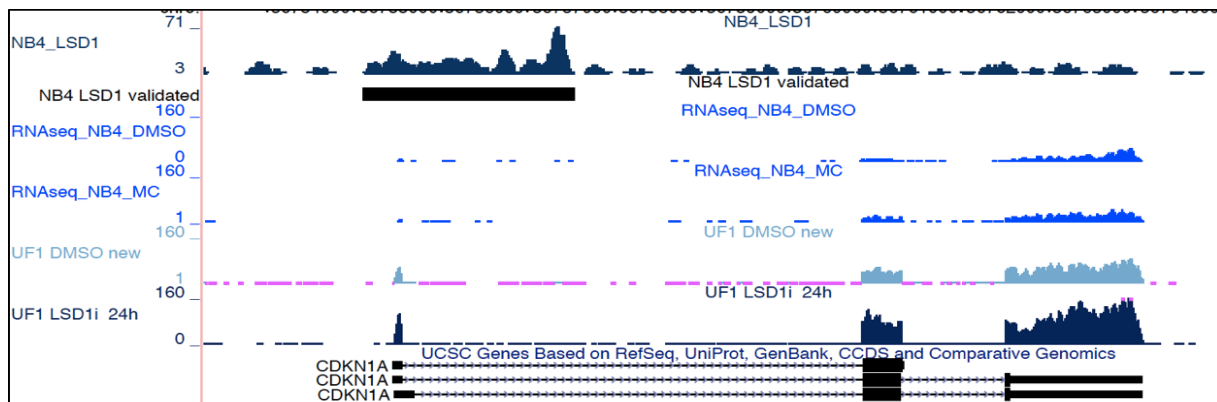
Figure 27.**UF1 cells expressed high level of p21 compared with NB4 cells.** Snapshot of the p21 gene and its expression (RNA-Seq tracks in blue) in UF1 and NB4 cells treated with DMSO (control) or MC for 24 hours. Tracks were obtained using MACS and scaled to the same sequencing depth using custom scripts.

High level of p21 in DMSO-treated UF1 cells, is consistent with the fact that UF1 cells are in higher percentage in G1 phase and lower growth rate compared with NB4 cells. Furthermore, we observed that LSD1 inhibition leads to further p21 expression in UF1 cells, suggesting that the induction of p21 was associated with the induction of G1 phase arrest and inhibition of cell growth.

LSD1 inhibition induced expression of myeloid differentiation markers

To investigate the transcriptional changes caused by LSD1 inhibition, we performed RNA-sequencing in UF1 cells in the absence or presence of the LSD1 inhibitor MC. Treatment with MC for 24 hours results in a number of genes that were consistently and significantly altered (>2-fold change). Consistent with the role of LSD1 in transcriptional repression, almost all genes that expression changes upon LSD1 inhibition were upregulated (**Figure 28A**) and 90% of thease genes were LSD1 target genes. LSD1 inhibition markedly downregulated the expression of proteinas 3 (PRTN3), which is involved in the differentiation arrest of leukemic cells and are highly expressed under undifferentiated conditions. PRTN3 also is one of the tumour-associated antigens (TAAs). It has been reported that the expression of TAAs might play a critical role in the control of minimal residual disease (MRD) in acute myeloid leukemia (AML).

Given the potentiation of differentiation observed upon treatment with MC; one prediction would be that LSD1 is involved in controlling the expression of genes required for hematopoietic differentiation. LSD1 inhibition increased expression of genes involved in myeloid differentiation, such as CD86, CD53, CD34, CD11b and LY96 (**Figure 28B-E**).
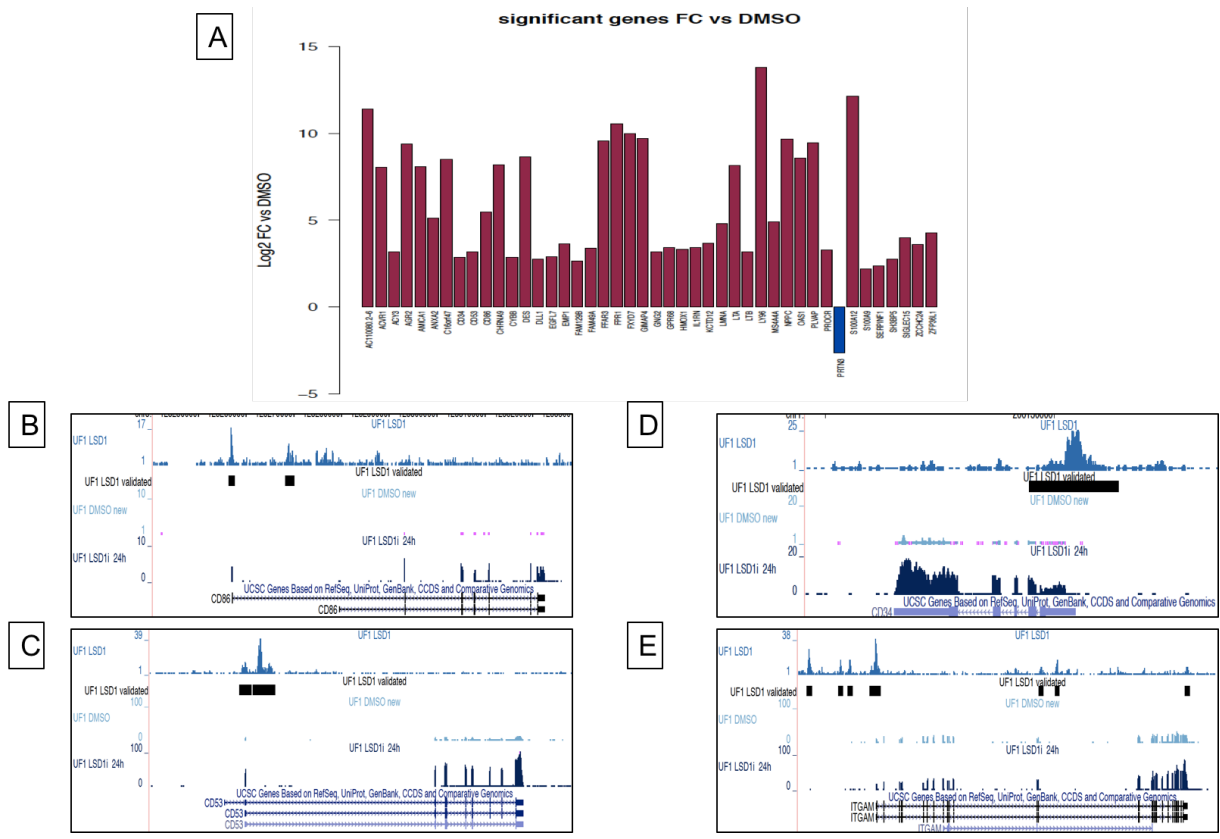
Figure 28. **LSD1 inhibition induced expression of myeloid differentiation markers.** (A) gene expression changes in UF1 cells upon treatment with MC for 24 hours. (B, C, D,E) Snapshot of the CD86 gene (B), CD34 gene (C), CD53 gene (D) and CD11b gene (E) and their expression (RNA-Seq tracks in blue) in UF1 cells treated with DMSO (control) or MC for 24 hours. Tracks were obtained using MACS and scaled to the same sequencing depth using custom scripts.

To further investigate the mechanisms of LSD1 efficacy in UF1 cells, epigenetic changes in response to MC were evaluated. LSD1 inhibition is predicted to be associated with increase in H3K4 methylation and since it has been shown that there is interplay between histone acetylation and methylation; therefore, changes in the levels of H3K4me2 and H3K27ac were evaluated by ChIp-sequencing studies in the absence and presence of MC. Although we found no genome-wide increase in H3K4me2 in response to LSD1 inhibitor, we found unique increase in H3K4me2 and specially H3K27ac at promoter of myeloid-differentiation associated genes (**Figure 29A, B**). Overall, these results suggest that LSD1 inhibition

110

increases the H3K4me2 and H3K27ac at promoter of myeloid-differentiation-associated genes and increases their expression.
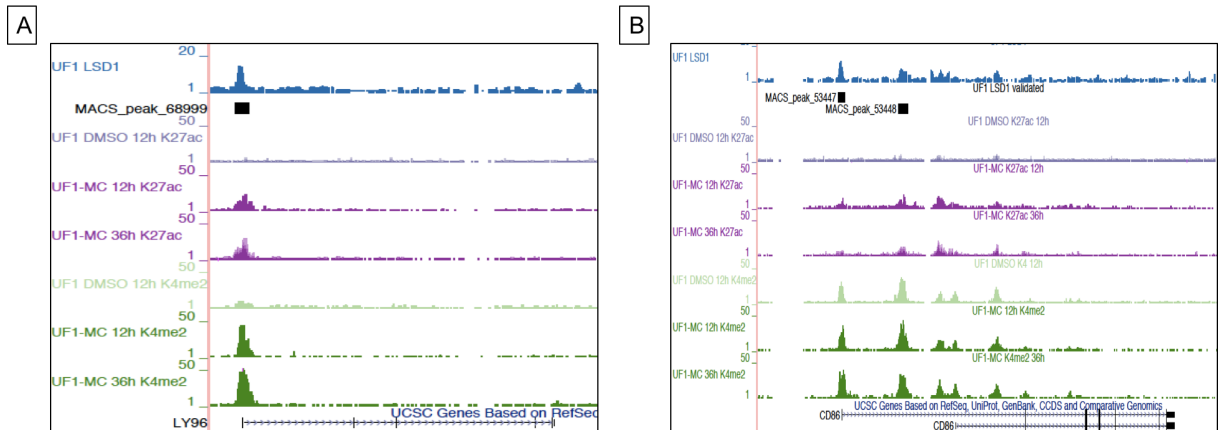
Figure 29. **Gene-specific increases in H3K4me2 and H3K4ac induced by treatment with MC.** (A) Increases in H3K4me2 and H3K27ac at promoter of LY96 gene upon MC treatment. (B) Increases in H3K4me2 and H3K27ac at promoter of CD86 gene upon MC treatment. SE is indicated by horizontal bars.

Growth inhibition and cell differentiation mediated by LSD1 inhibition is P21-dependent in UF1 cells

To evaluate the direct role of p21 expression on cell growth inhibition and differentiation in UF1 cell treated with MC, knockdown of p21 was performed by using two specific shRNA constructs. As shown in Figure 30, p21 RNA and protein levels were reduced by 80% and 60% in UF1 cells infected with shRNA #1 and shRNA #2 respectively, compared with control **(Figure 30A, B)**. ShRNA #1 was used for further experiments because of its greater effectiveness.
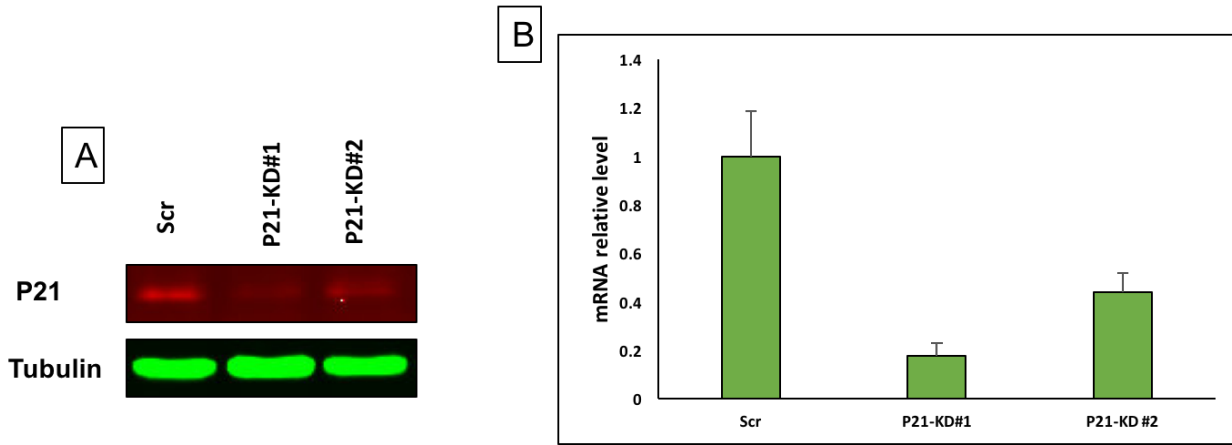
Figure 30. **P21 depletion in UF1 cells.** (A) Immunoblot analysis of p21 expression in UF1 cells infected with indicated shRNA. Tubulin was used as a loading control. (B) Analysis of p21 mRNA relative levels in UF1 cells, transduced with the indicated lentiviral vectors. Values were normalized against GAPDH and referred to SCR.

In p21KD-UF1 cells, there was a decrease in the G1 phase population when compared with control cells, with an increase of S phase cells, suggesting that the presence of p21 at its constitutive levels exerts a modest inhibitory effect regulating G1/S transition in UF1 cells **(Figure 31)**. This effect was corroborated by a trend toward increased cell proliferation in p21-KD UF1 cells **(Figure 32)**.
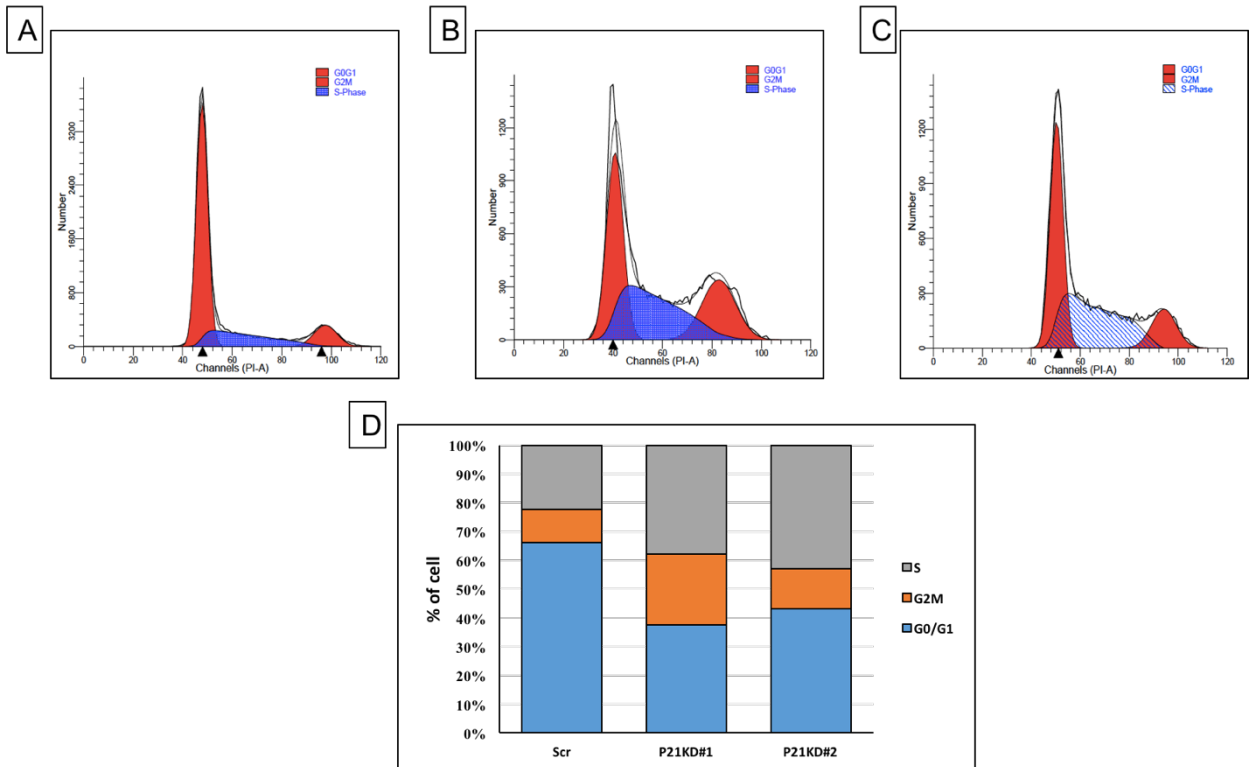
Figure 31. **Suppression of p21 decrease the G1 phase population.** (A, B, C) Cell cycle analysis of UF1 cells infected with control siRNA (SCR), and siRNA targeting p21. (A) SCR siRNA (B) 1st p21-siRNA (C) 2nd p21-siRNA. (D) Summary of cell-cycle status of UF1 cells infected with indicated shRNA.

The results of cell viability demonstrated that p21 acts as a key regulator of the MC-induced cell growth inhibition since knockdown of p21 reversed the antiproliferative activity of LSD1 inhibitor **(Figure 32)**.
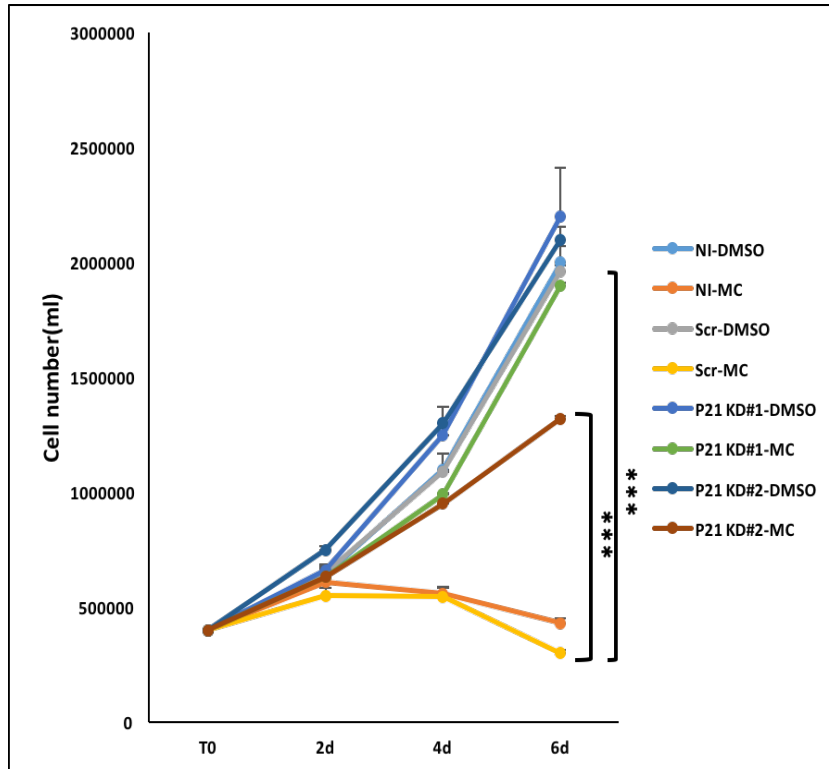
Figure 32. **Suppression of p21 rescued UF1cells from cell growth inhibition induced by inhibition of LSD1.** Relative proliferation of UF1cells stably transduced with either control shRNA (SCR) or shRNA targeting p21 following treatment with MC or DMSO. Data are presented as mean of triplicates ± SD. P value < 0.05 (*****), P < 0.01 (*** ***) and P <0.001 (*** * ***). (NI: Not Infected).

Cell cycle and morphologic analysis in UF1 cells showed that MC induced a G1 phase arrest and cell differentiation but knockdown of p21 rescued UF1 cells from these effects induced by LSD1 inhibitor **(Figure 33A, B)**.
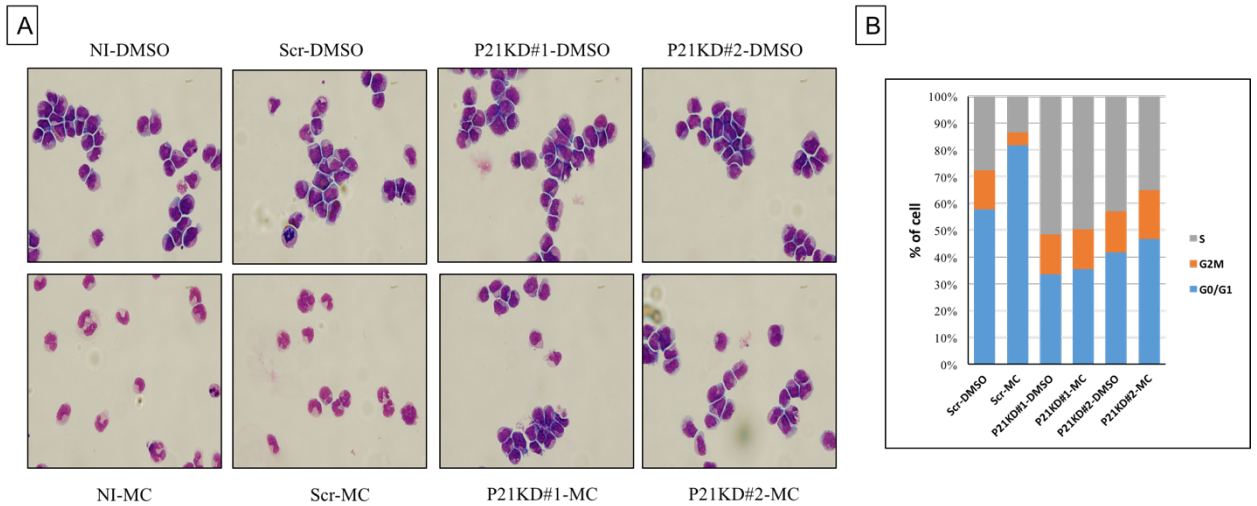
Figure 33. **Suppression of p21 rescued UF1cells from induction of differentiation and cell cycle arrest induced by inhibition of LSD1.** (A) Representive light micrograph show Wright-Giemsa staining of UF1 cell stably transduced with either control shRNA (SCR) or shRNA targeting p21following treatment with MC or DMSO. (B) Summary of cell-cycle status of UF1 cells stably transduced with either control shRNA or shRNA targeting p21 following treatment with MC or DMSO. (NI: Not Infected).

Together, these results indicate that suppression of p21 inhibits the G1 cell cycle arrest caused by MC. This finding of inhibition was supported by the higher rate of proliferation observed in p21KD cells treated with MC compared with corresponding control cells. Hence, repression of p21 by LSD1 promotes cell cycle progression.

LSD1 inhibition led to further upregulation of P21 protein level but not in p21KD cells and p21 shRNA could suppress p21 induction under these conditions **(Figure 34A)**. This upregulation was further confirmed by comparing RNA-seq results before and after LSD1 inhibition **(Figure34B)**.
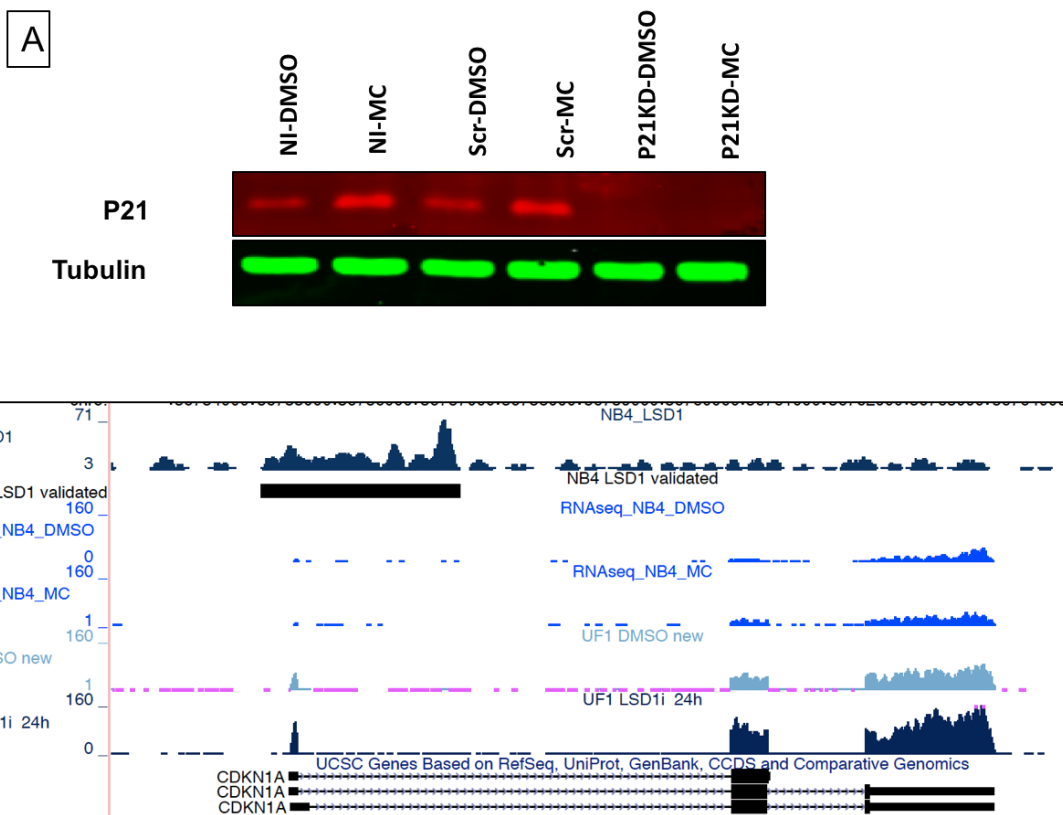
Figure 34. **Suppression of p21 inhibits the p21 induction induced by inhibition of LSD1.** (A) Immunoblot analysis of p21 expression in UF1 cells stably transduced with either control shRNA (SCR) or shRNA targeting p21 following treatment with MC or DMSO. Tubulin was used as a loading control. (B) Snapshot of the p21 gene and its expression (RNA-Seq tracks in blue) in UF1 and NB4 cells treated with DMSO (control) or MC for 24 hours. Tracks were obtained using MACS and scaled to the same sequencing depth using custom scripts.

Overall these results suggest that p21 expression and its induction is associated with cell growth inhibition, cell differentiation and G1 phase arrest mediated by LSD1 inhibitor and knockdown of p21 notably suppressed these phenotypes.

Overexpression of p21 sensitizes resistant cells to LSD1 inhibition

Parallel to the knockdown experiments in UF1 cells, gain of function studies were also carried out to verify the role of p21. We thus generated a p21KD-UF1 cells that stably overexpressed p21 and the corresponding control cell line (infected with an empty vector). Since our p21-HA

116

plasmid contained GFP as a reporter, we were able to evaluate the effect of MC in the cells expressing the highest levels of p21 by sorting out the GFP positive population. We then performed cell growth and differentiation assays by treating control and p21-overexpressing cells with MC. Restored expression of p21 increased cell growth inhibition and G1 cell cycle arrest following MC administration **(Figure 35)**.
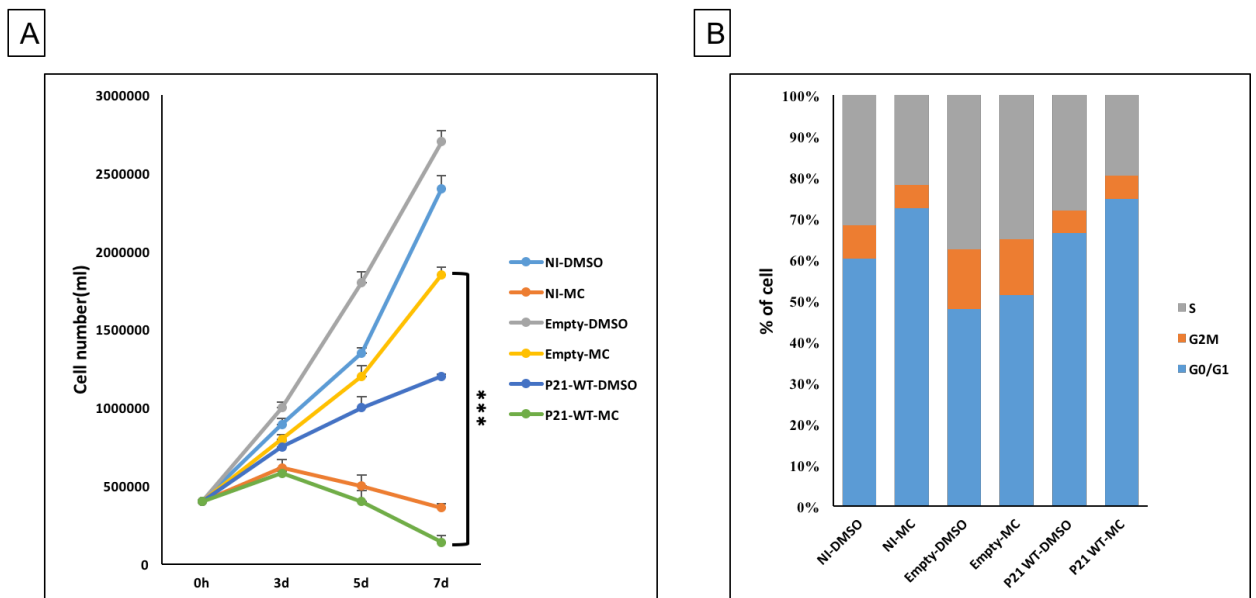
Figure 35. **Suppression of p21 rescued UF1cells from cell growth inhibition and cell cycle arrest induced by inhibition of LSD1 and these effects reversed by restored expression of p21.** (A)Relative proliferation of UF1cells stably transduced with shRNA targeting p21 following transfection with empty or p21 expression vector following treatment with MC or DMSO. Data are presented as mean of triplicates ± SD. (B) Summary of cell-cycle status of UF1 cells stably transduced with shRNA targeting p21 following transfection with empty or p21 expression vector following treatment with MC or DMSO. P value < 0.05 (*****), P < 0.01 (*** ***) and P <0.001 (*** * ***). (NI: Not Infected).

Morphology evaluation of treated cells showed that p21 overexpression increased the cell differentiation potential following MC administration. On the other hand, p21 overexpression did not change the differentiation status in basal conditions. It should be noticed that, in the absence of MC, the amount of differentiated cells in cells infected with empty plasmid is already low **(Figure 36)**.
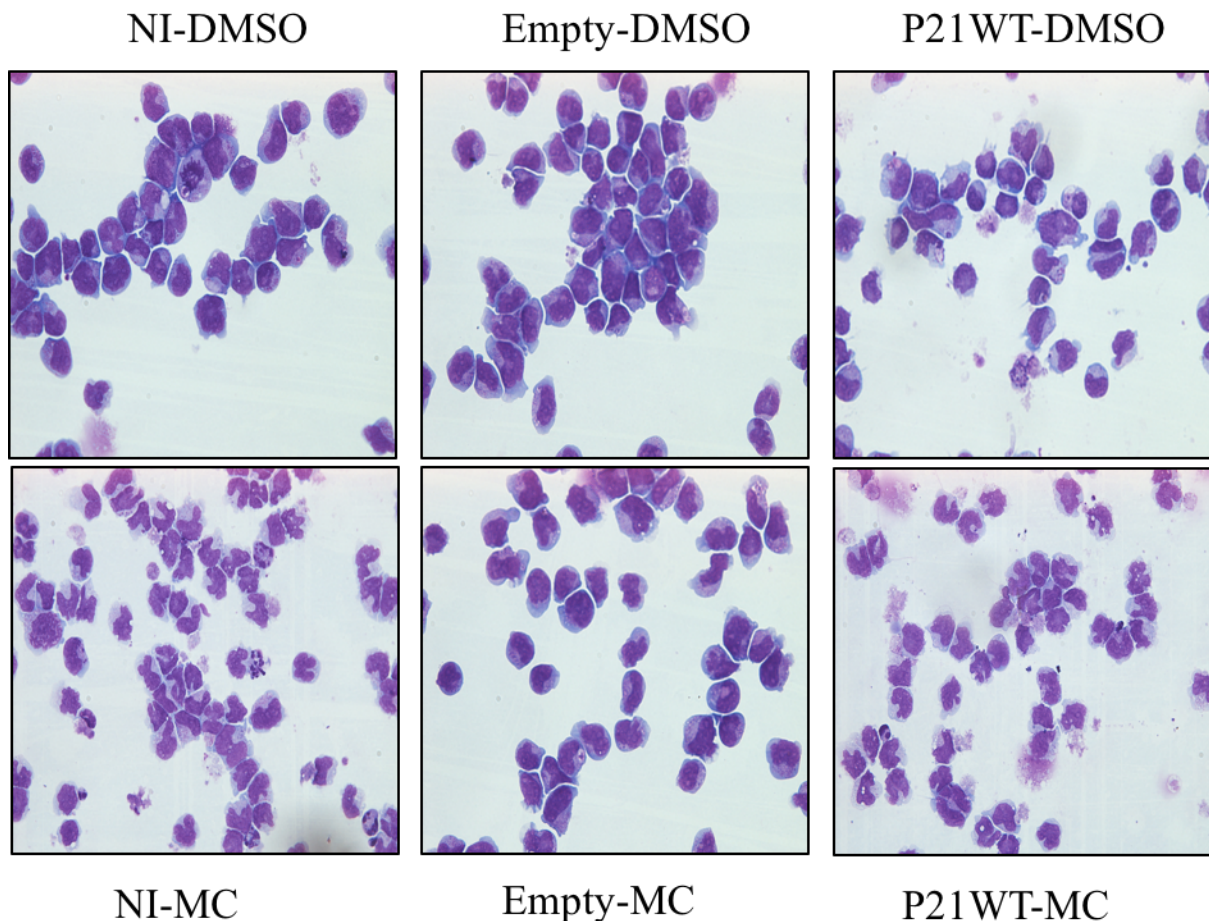
Figure 36. **Suppression of p21 rescued UF1 cells from induction of differentiation induced by inhibition of LSD1.** Representive light micrograph show Wright-Giemsa staining of UF1 cells stably transduced with shRNA targeting p21 following transfection with empty or p21 expression vector following treatment with MC or DMSO. (NI: Not Infected).

Given the identified role for p21, we sought that we can sensitize NB4 cells to MC by overexpression of p21. To this end, we generated a NB4 cells that stably overexpressed p21 and the corresponding control cell line (infected with an empty vector). Then cells were treated with MC for a six-day time course. Consistent with observed phenotype in UF1 cells, p21 overexpression increased MC-induced differentiation, cell growth arrest and G1 cell cycle arrest **(Figure 37)**.
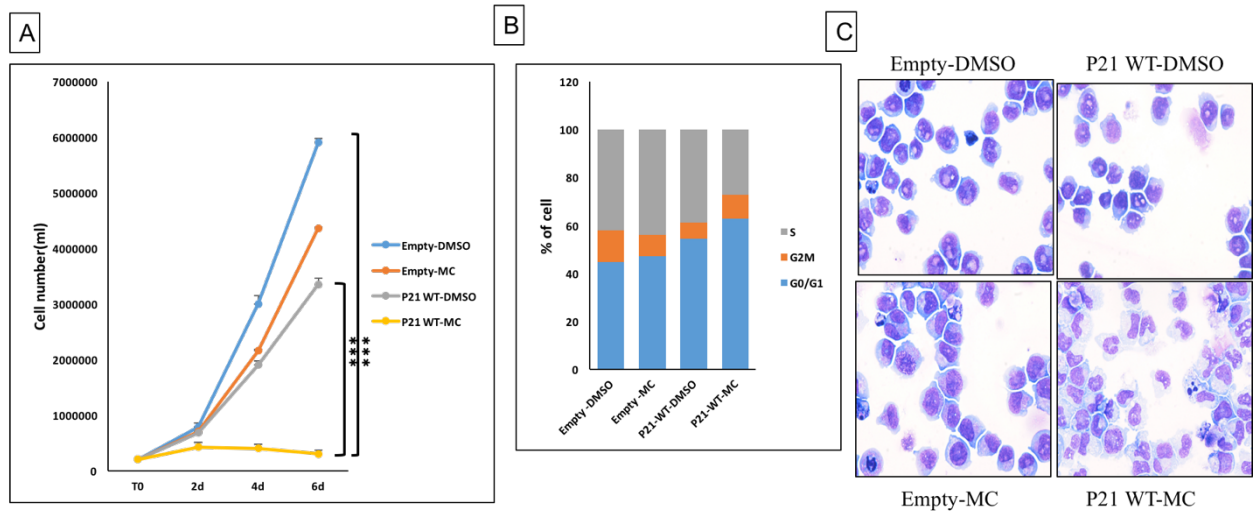
Figure 37. **Overexpression of p21 sensitize NB4 cells to LSD1 inhibition.** (A) Relative proliferation of NB4 cells stably transduced with empty or p21 expression vector following treatment with MC or DMSO. Data are presented as mean of triplicates ± SD. (B) Summary of cell-cycle status of NB4 cells stably transduced with empty or p21 expression vector following treatment with MC or DMSO. (C) Representative light micrograph show Wright-Giemsa staining of UF1 cells stably transduced with empty or p21 expression vector following treatment with MC or DMSO. P value < 0.05 (*), P < 0.01 (**) and P <0.001 (***).

Overall, these genetic rescue experiments demonstrate that WT p21 mediates increased MC-induced cell cycle arrest, cell growth inhibition and cell differentiation.

Pharmacological induction of p21 sensitizes resistant cells to LSD1 inhibition

The efficacy of LSD1 inhibitor as a single agent is limited to a few cell lines. Given the identified role for p21, we reasoned that we can sensitize a resistant cell line (such as NB4 cells) to LSD1 inhibitor by p21 induction through drugs. We used HDAC inhibitors, well known to lead to an upregulation of p21. NB4 cells were treated with two HDAC inhibitors, Vorinostat (SAHA) and Trichostatin A (TSA) for a short time to induce p21 expression. Finally, cells were treated with MC **(Figure 38A)**. P21 upregulation by HDAC inhibitors was comparable with the basal level of p21 in UF1 cells **(Figure 38C)**.

119
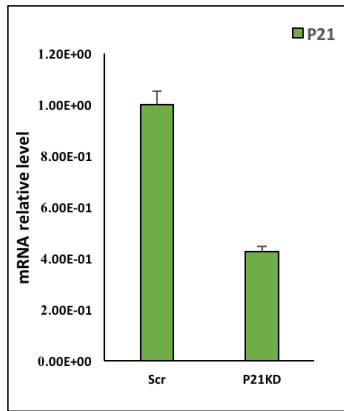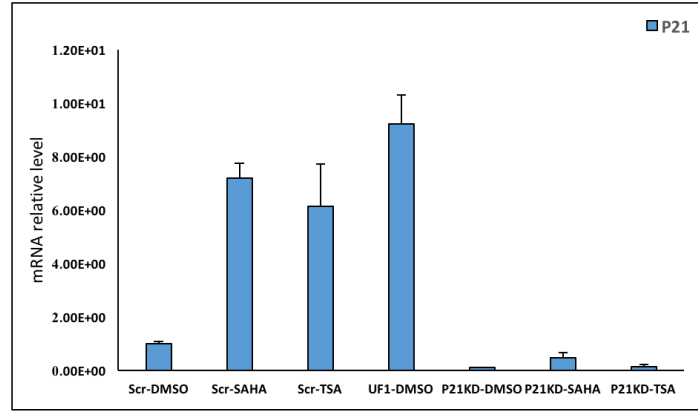
Figure 38. **Pharmacological induction of P21 sensitizes NB4 cells to LSD1 inhibition.** (A) Schematic representation of co-treatment of HDACis with LSD1 inhibitor in NB4 cells. (B) Analysis of p21 mRNA relative levels in UF1 cells, transduced with the indicated lentiviral vectors. Values were normalized against GAPDH and referred to SCR. (C) Analysis of p21 mRNA relative levels in UF1 cells, transduced with either control shRNA (SCR) or shRNA targeting p21 following treatment with SAHA, TSA or DMSO.

While SAHA and TSA treatment with relatively lower concentrations and short time were well tolerated, p21 induction by HDAC inhibitors sensitized NB4 cells to LSD1 inhibitor **(Figure 39)**.
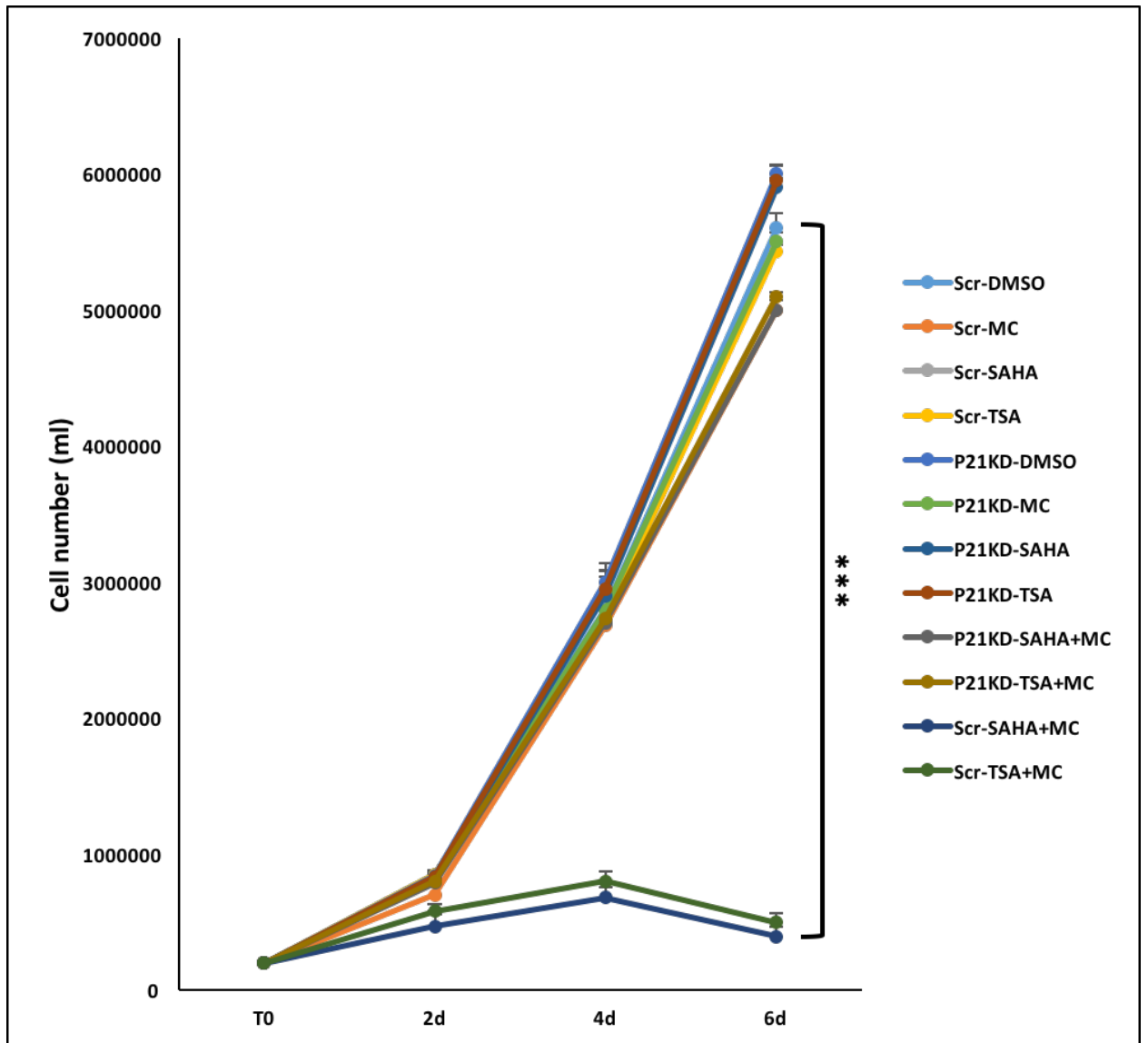
Figure 39. **P21 induction by HDACis sensitizes NB4 cells to LSD1 inhibitors.** Relative proliferation of NB4 cells stably transduced with either control shRNA (SCR) or shRNA targeting p21 following treatment with SAHA or TSA for 24 h following treatment with MC or DMSO. Data are presented as mean of triplicates ± SD. P value < 0.05 (*), P < 0.01 (**) and P <0.001 (***).

This combination therapy inhibited cell proliferation, induced G1 phase arrest and promoted cell differentiation and knockdown of p21 significantly decreased the effects of this combination therapy **(Figure 39, 40)**.
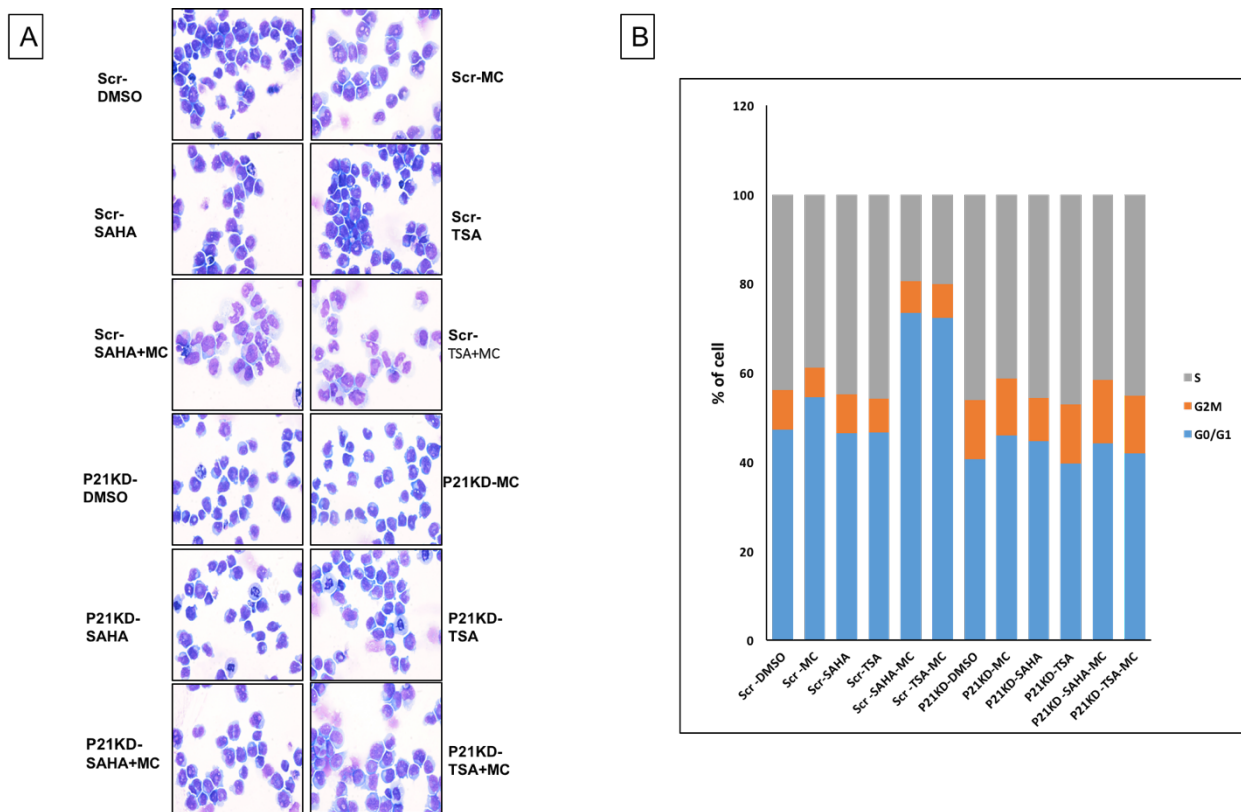
Figure 40. **P21 induction by HDACis sensitizes NB4 cells to LSD1 inhibitors.** (A) Representative light micrograph show Wright-Giemsa staining of NB4 cells stably transduced with either control shRNA (SCR) or shRNA targeting p21 following treatment with SAHA or TSA for 24 h following treatment with MC or DMSO. (B) Summary of cell-cycle status of NB4 cells stably transduced with either control shRNA (SCR) or shRNA targeting p21 following treatment with SAHA or TSA for 24 h following treatment with MC or DMSO.

Collectively, these finding strongly support that induction of p21 sensitize resistant cells to LSD1 inhibitor.

Effects mediated by LSD1 inhibition in non-APL AML and SCLC cell lines is p21-dependent

To broaden our observation to other cancers, we performed additional experiment on two sensitive cell lines to LSD1 inhibitors, Kasumi cells which is an AML cell line with AML-ETO chromosomal translocation and NCI-H69 which is small cell lung carcinoma (SCLC)

cell line [McGrath, 2016; Mohammad, 2015].

Multiple days of treatment required to elicit the maximal effects of antiproliferative activity of MC in Kasumi cells **(Figure 41)**.
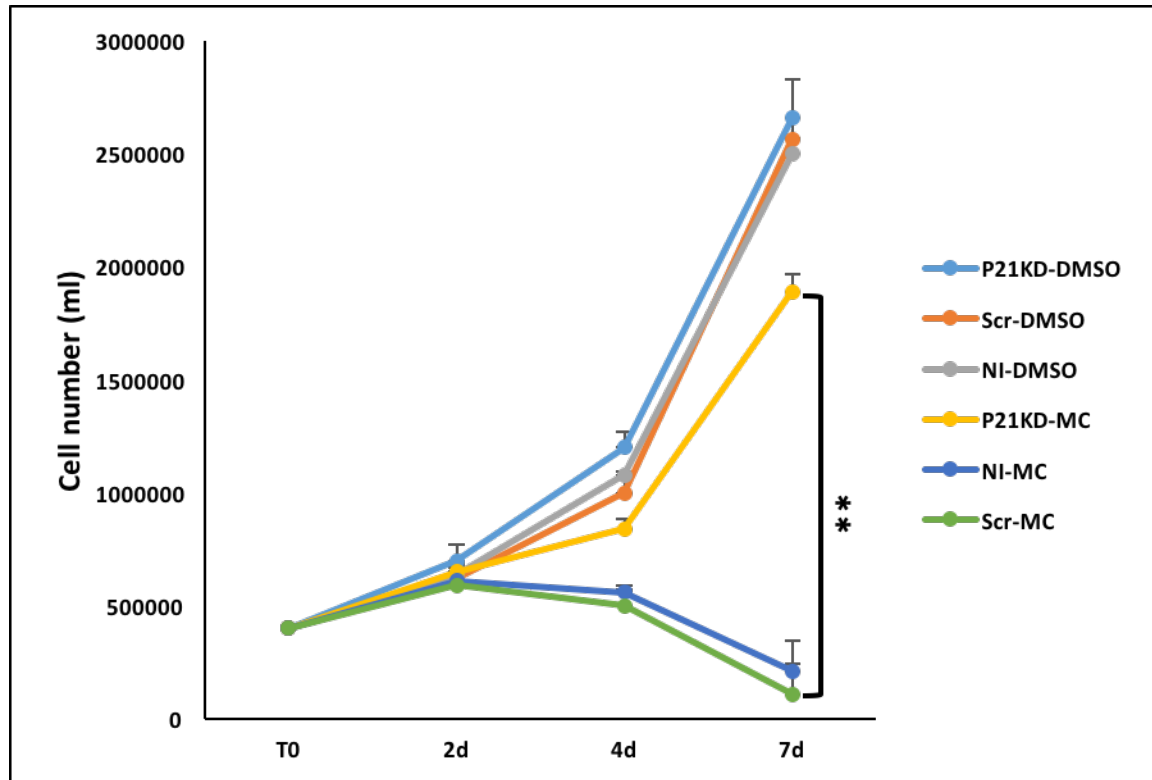
Figure 41. **Suppression of p21 rescued Kasumi cells from cell growth inhibition induced by inhibition of LSD1.** Relative proliferation of Kasumi cells stably transduced with either control shRNA or shRNA targeting p21 following treatment with MC or DMSO. Data are presented as mean of triplicates ± SD. P value < 0.05 (*****), P < 0.01 (*** ***) and P <0.001 (*** * ***). (NI: Not Infected).

LSD1 inhibition increased the G1 cell population, promoted myeloid differentiation and induced p21 expression **(Figure 42)**.

To evaluate the direct role exerted by the activation of p21 in the MC-induced cell growth inhibition and cell cycle arrest, we performed knockdown of p21**(Figure 43)**. To this end, Kasumi cells were infected with shRNA#1 because of its greater effectiveness **(Figure 30)**.
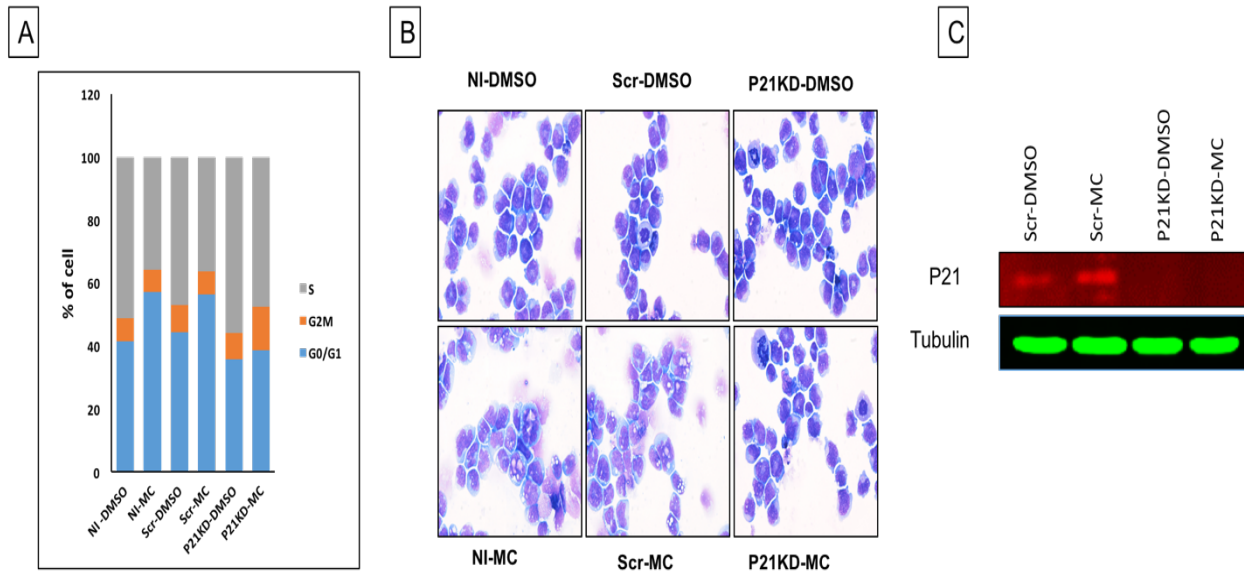
Figure 42. **Suppression of p21 rescued Kasumi cells from induction of differentiation, cell cycle arrest and p21 induction induced by inhibition of LSD1. (A)** Summary of cell-cycle status of Kasumi cells stably transduced with either control shRNA or shRNA targeting p21 following treatment with MC or DMSO. (B) Representive light micrograph show Wright-Giemsa staining of Kasumi cell stably transduced with either control shRNA (SCR) or shRNA targeting p21following treatment with MC or DMSO. (C) Immunoblot analysis of p21 expression in Kasumi cells stably transduced with either control shRNA (SCR) or shRNA targeting p21 following treatment with MC or DMSO. Tubulin was used as a loading control. (NI: Not Infected).
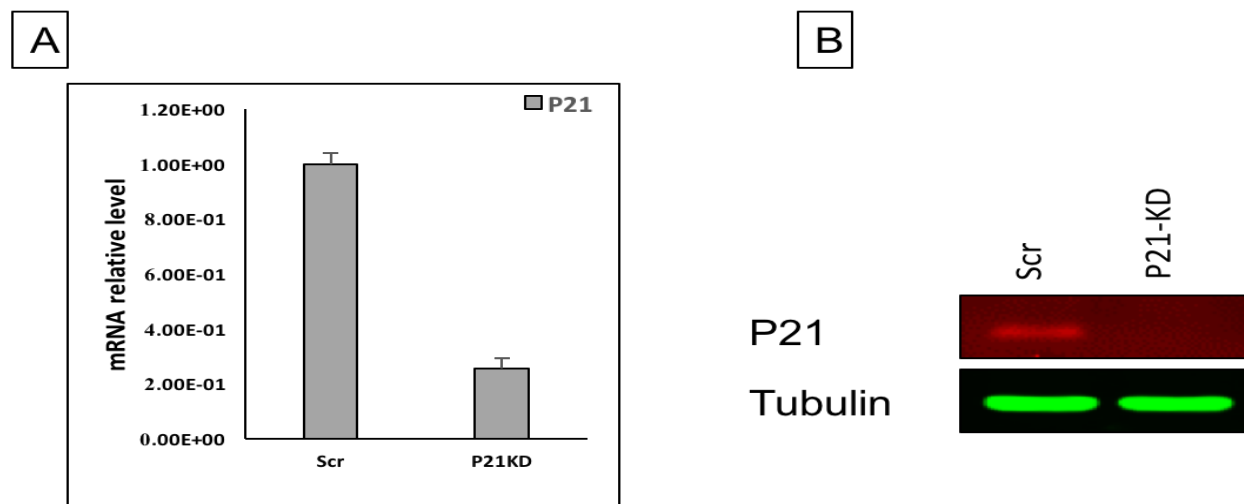
Figure 43. **P21 depletion in Kasumi cells.** (A) Analysis of p21 mRNA relative levels in Kasumi cells, transduced with either control shRNA (SCR) or shRNA targeting p21. Values were normalized against GAPDH and referred to SCR. (B) Immunoblot analysis of p21 expression in Kasumi cells. Tubulin was used as a loading control.

Like UF1 cells, knockdown of p21 rescued Kasumi cells from the cell growth inhibition, G1 cell cycle arrest and differentiation mediated by MC **(Figure 41, 42)**.

SCLC is a highly prevalent, rarely cured tumor type representing approximately 15% of all lung cancers. It has been shown that some SCLC cell lines are sensitive to LSD1 inhibition which prompted us to evaluate the role of p21 in effect of LSD1 inhibitor in this type of cancer. NCI-H69 cells were treated for up to 10 days with MC, growth inhibition was not detected until 4 days of treatment, after which antiproliferative activity was apparent (**Figure 44A**). Like Kasumi cells multiple days of dosing led to G1 phase arrest **(Figure 44 B)**.
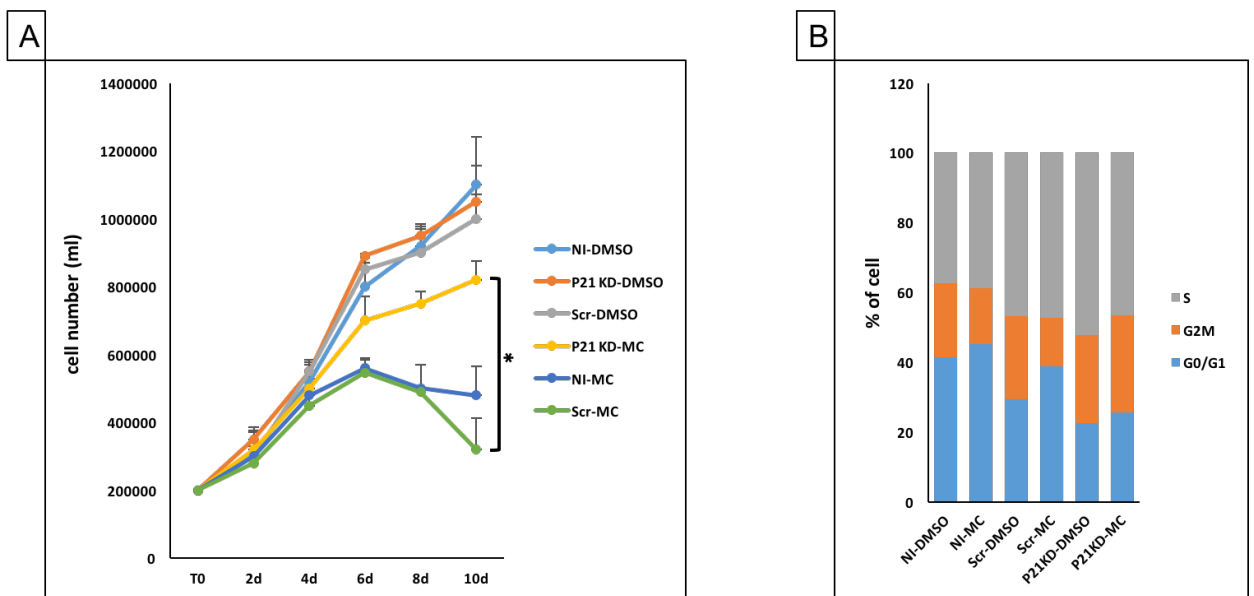
Figure 44. **Suppression of p21 rescued NCI-H69 cells from cell growth inhibition and cell cycle arrest induced by inhibition of LSD1.** (A) Relative proliferation of NCI-H69 cells stably transduced with either control shRNA or shRNA targeting p21 following treatment with MC or DMSO. Data are presented as mean of triplicates ± SD. (B) Summary of cell-cycle status of NCI-H69 cells stably transduced with either control shRNA or shRNA targeting p21 following treatment with MC or DMSO. P value < 0.05 (*****), P < 0.01 (*** ***) and P <0.001 (*** * ***). (NI: Not Infected).

To check the impact of LSD1 inhibitor in SCLC differentiation, the expression of neuroendocrine marker gene was interrogated in NCI-H69 cells. LSD1 inhibitor downregulated GRP expression in a time dependent manner. This loss of expression of GRP, a

125

marker that reflects the neuroendocrine origin of SCLC, is reminiscent of the differentiation state **(Figure 45)**.
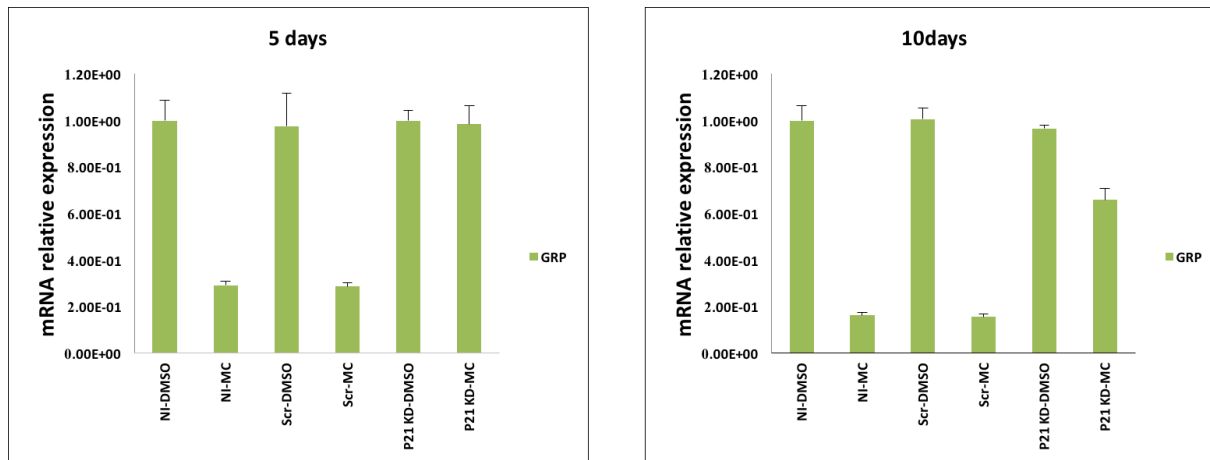
Figure 45. **Suppression of p21 rescued NCI-H69 cells from induction of differentiation induced by inhibition of LSD1.** Analysis of GRP mRNA relative levels in NCI-H69 cells stably transduced with either control shRNA or shRNA targeting p21 following treatment with MC or DMSO. Values are normalized against GAPDH and referred to SCR. (NI: Not Infected).

Like Kasumi cells, knockdown of p21in NCI-H69 **(Figure 46)**, rescued cells from cell growth inhibition, induction of differentiation and cell cycle arrest mediated by MC **(Figure 44,45)**.
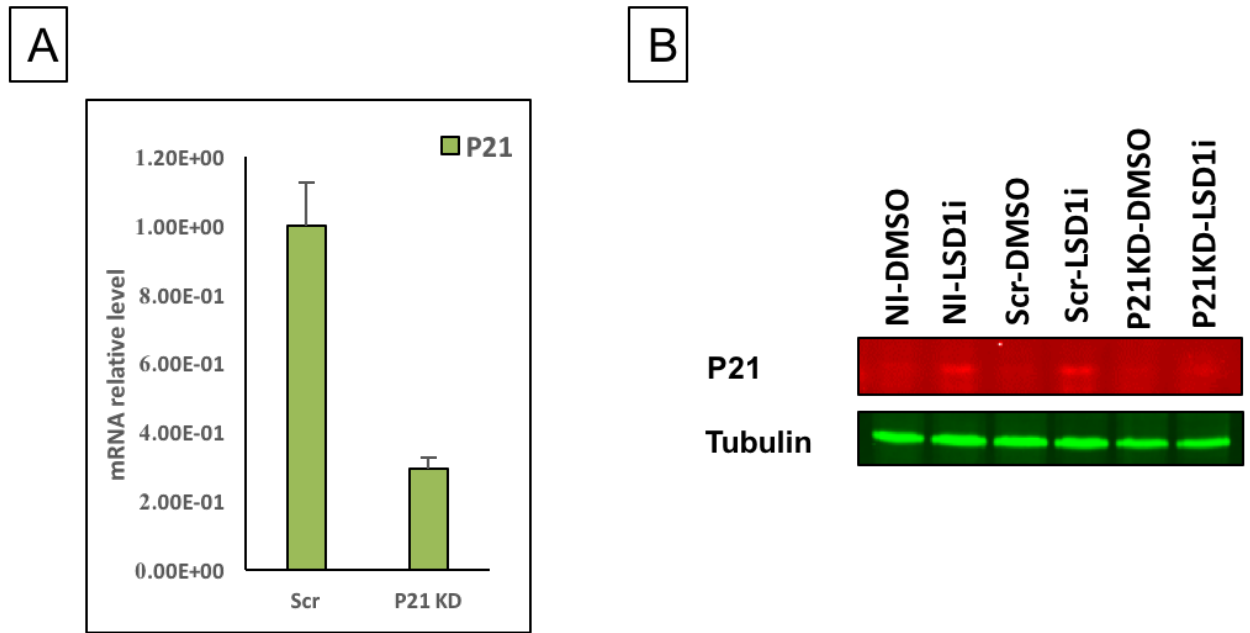
Figure 46. **Suppression of p21 inhibits the p21 induction induced by inhibition of LSD1.** (A) Analysis of p21 mRNA relative levels in NCI-H69 cells, transduced with either control shRNA (SCR) or shRNA targeting p21. Values are normalized against GAPDH and referred to SCR. (B) Immunoblot analysis of p21 expression in NCI-H69 cells stably transduced with either control shRNA (SCR) or shRNA targeting p21 following treatment with MC or DMSO. Tubulin was used as a loading control. (NI: Not Infected).

LSD1 regulates p21 expression

The finding reported above strongly suggest that LSD1 suppress the expression of p21. To further understand the regulation of p21 by LSD1, we took advantage of chromatin immunoprecipitation (ChIP) coupled to high-throughput DNA sequencing (ChIP-seq) using specific antibodies against LSD1, H3K4me2 and H3K27ac, in NB4 and UF1 cells treated with DMSO or MC.

We could identify three regulatory elements defined as LSD1, H3K4me2 and H3K27ac peaks in the p21 locus. Element A is the promoter of p21 while element B and element C were thought to be putative enhancers because of location far from the gene body and elevated H3K27ac peaks, which are a marker of active enhancers **(Figure 47)**. The analyses of LSD1-

ChIP sequencing data showed the differential deposition patterns, as shown by the genomic

snapshots retrieved by UCSC genome browser in UF1 and NB4 cells.
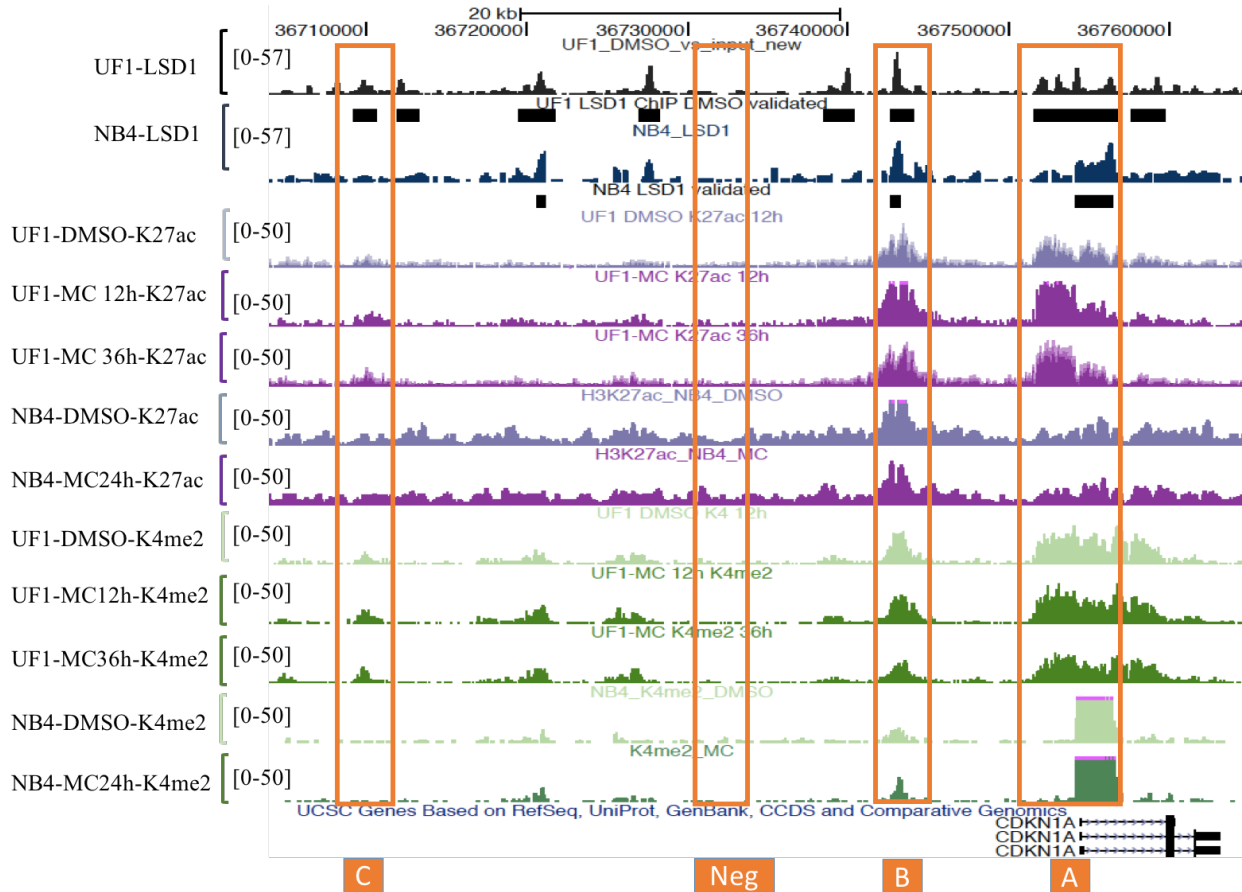
Figure 47. **LSD1 regulates p21 expression.** ChIP-seq profiles of LSD1, H3K4me2 and H3K27ac in the CDKN1A (p21) locus in UF1 and NB4 cells treated with DMSO or MC.SE is indicated by horizontal bars.

LSD1 was enriched at the promoter (element A) and element B in both cells While on element

C, LSD1 was only enriched in UF1 cells. Consistent with the high basal level of p21 in UF1

cells the level of H3K27ac at promoter (element A) was higher compared with NB4 cells and

MC treatment significantly increased the H3K27ac level (more than 2 fold) specially after 12

hours' treatment in UF1 cells but not in NB4. Similarly, MC treatment increased the level of

H3K27ac on element B and element C in UF1 cells but not in NB4 cells. To validate the ChIP-seq results, ChIP-qPCR was performed checking the level of LSD1, H3K27ac and H3K4me2 before and after MC treatment on all the elements and neg region as a negative control. These ChIP-qPCR confirmed that LSD1 only occupied the element C in UF1 cells **(Figure 48)**.
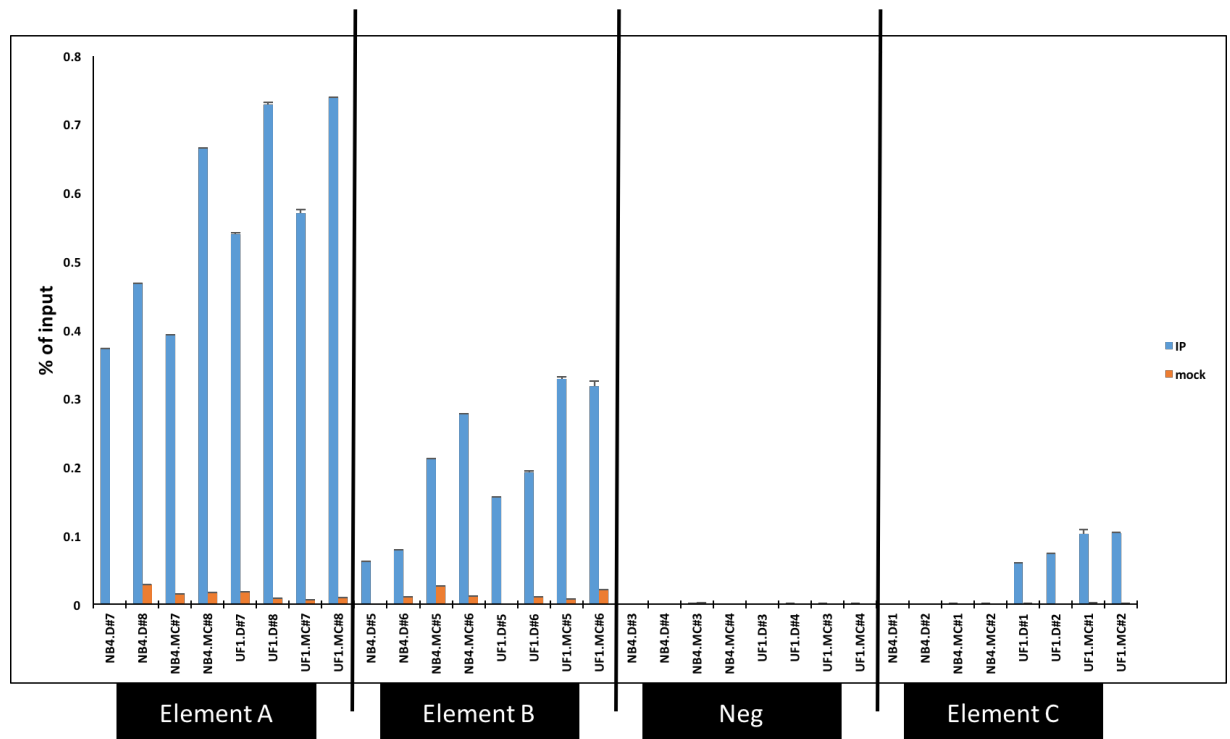
Figure 48. **ChIP-qPCR occupancy analysis of LSD1 on p21 genomic loci in UF1 and NB4 cells treated with DMSO or MC for 24 hours.** (For each element we used two different primers).

Consistent with the ChIP-seq results, MC treatment increased the level of H3K27ac at element A, B and C in UF1 cells but not in NB4 cells **(Figure 49)**. One mechanism proposed to explain the interplay between histone acetylation and methylation is the physical association of HDAC1 and LSD1 by which each enzyme influences the activity of the other. As both demethylation and deacetylation are essential epigenetic mechanisms in controlling gene transcription, interplay between deacetylation and demethylation is a logical scenario. Indeed,

past studies have indicated that optimal deacetylation of nucleosomes requires the demethylase activity of LSD1.
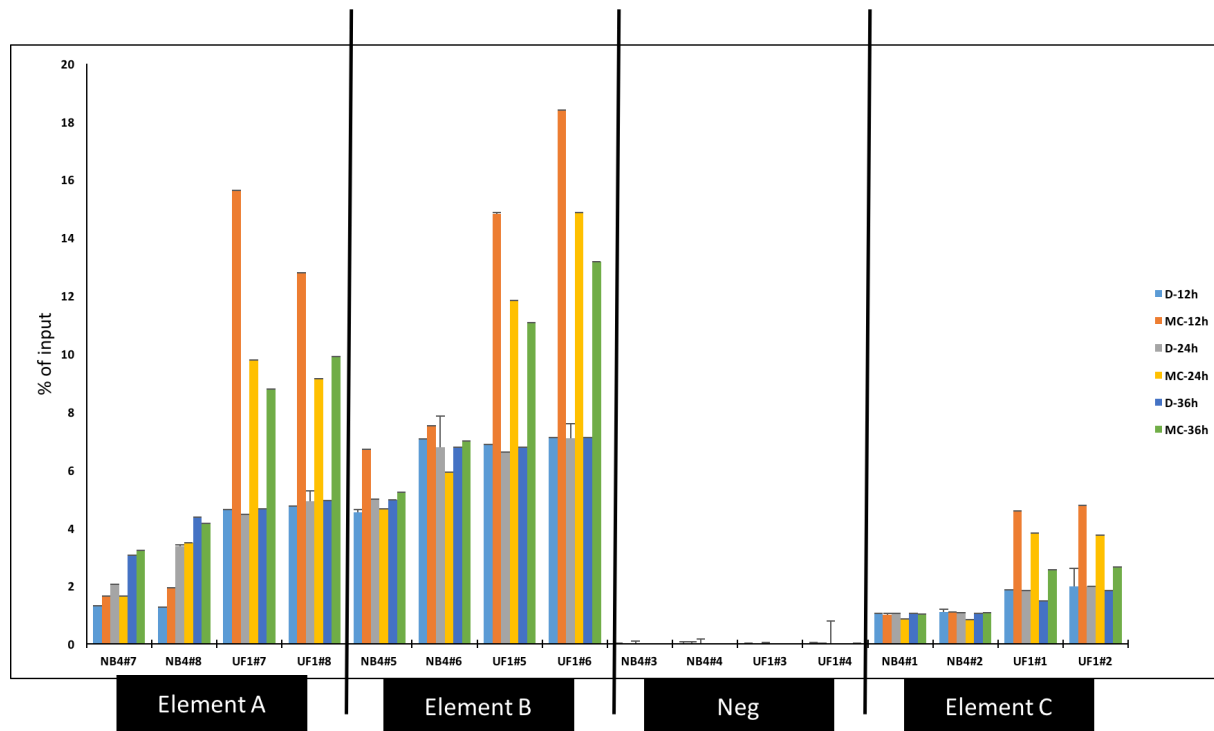
Figure 49. **ChIP-qPCR occupancy analysis of H3K27ac on p21 genomic loci in UF1 and NB4 cells treated with DMSO or MC for 12h, 24h and 36h.** (For each element we used two different primers).

Finally, we analyzed the dimethylation of histone H3 on lysine 4 (H3K4me2), on element A, B and C in the presence of DMSO or MC **(Figure 50)**. In contrast to H3K27ac, no significant difference in the level of the active mark, H3K4me2, was detected after MC treatment on element A and B but on element C, MC treatment increased the level of H3K4me2 only in UF1 cells.
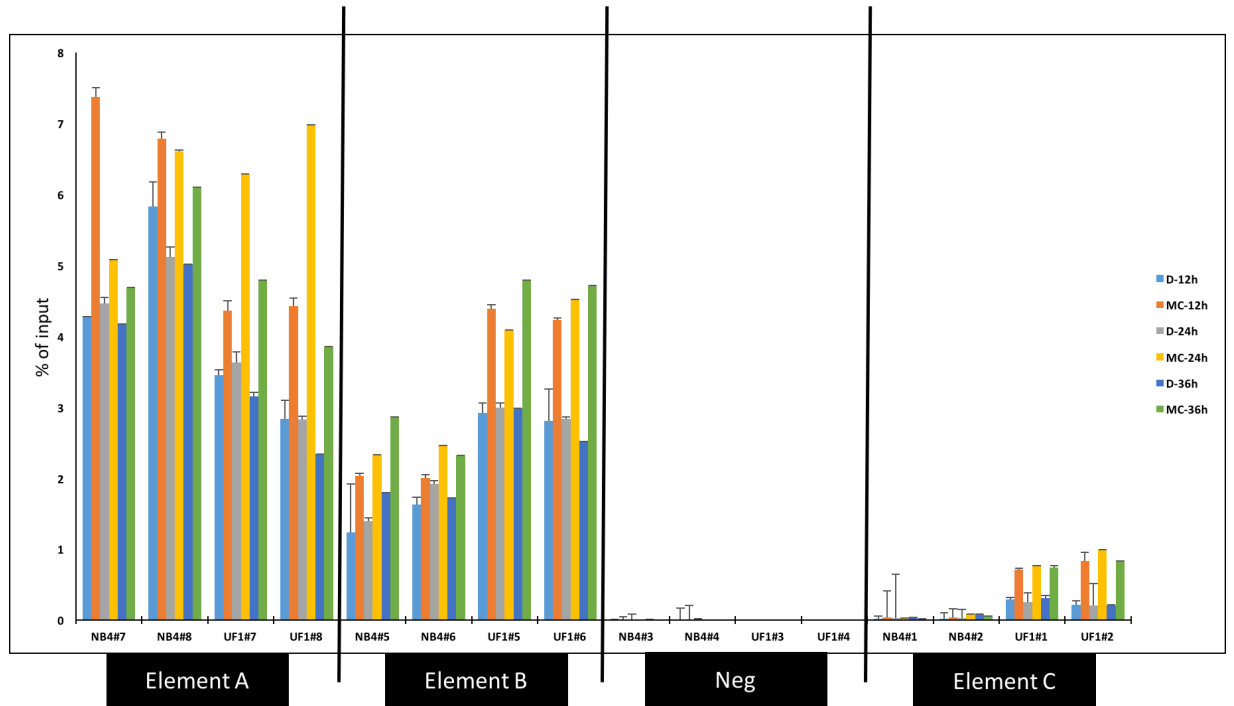
Figure 50. **ChIP-qPCR occupancy analysis of H3K4me2 on P21 genomic loci in UF1 and NB4 cells treated with DMSO or MC for 12h, 24h and 36h.** (For each element we used two different primers).

Overall these results demonstrate that LSD1 associated with the p21 promoter and putative enhancers and can regulate p21 expression. Furthermore, the element C was only enriched for LSD1 occupancy in UF1 cells compared with NB4 cells and MC treatment increased the level of H3K4me2 and H3K27ac on this element. NB4 cells were resistant to MC-mediated growth inhibition, in which expression of p21 was not induced after exposure to MC. Induction of H3K27ac at promoter and putative enhancers as well as H3K4me2 on element C were not prominent in NB4 cells after exposure to MC. This may be a reason why MC failed to induce expression of p21 in NB4 cells.

P21 by binding to CDK sensitize cells to LSD1 inhibitor

P21-mediated growth inhibition depends on two non-overlapping structural domains: PCNA binding domain and CDK binding domain [Abbas, 2009] **(Figure 51A)**. We performed a detailed analysis of growth inhibition mediated by LSD1 inhibition. On the basis of previous studies that have identified p21 residues critical for interaction with CDKs and PCNA in the amino- and carboxy-terminal halves of the protein respectively, we used p21 mutants impaired in either one or the other interaction.

To this end, p21 was knockdown in UF1 cells, since the NB4 cells express very low levels of endogenous p21, can thus be considered functionally equivalent to p21$^{-/-}$ cells. Then both NB4 and UF1 cells were infected with the three expression vectors for full length of p21 (P21 WT), p21 CDK mutant (CDKm) and p21 PCNA mutant (PCNAm) following treatment with MC or DMSO **(Figure 51B)**.

In a mutant called p21CDKm, referring to the loss of interaction with CDKs, residues tryptophane 49, phenylalanine 51 and aspartic acid 52 were replaced by arginine, serine, and alanine respectively. In the mutant called p21PCNAm, residues methionine 147, aspartic acid 149 and phenylalanine 150 were mutated to alanine in order to abolish the interaction with PCNA. A triple hemagglutinin (HA) tag was also introduced in frame with the p21 sequence at the carboxy-terminus to allow the detection of the protein products and to determine their intracellular localization **(Figure 51C)**.
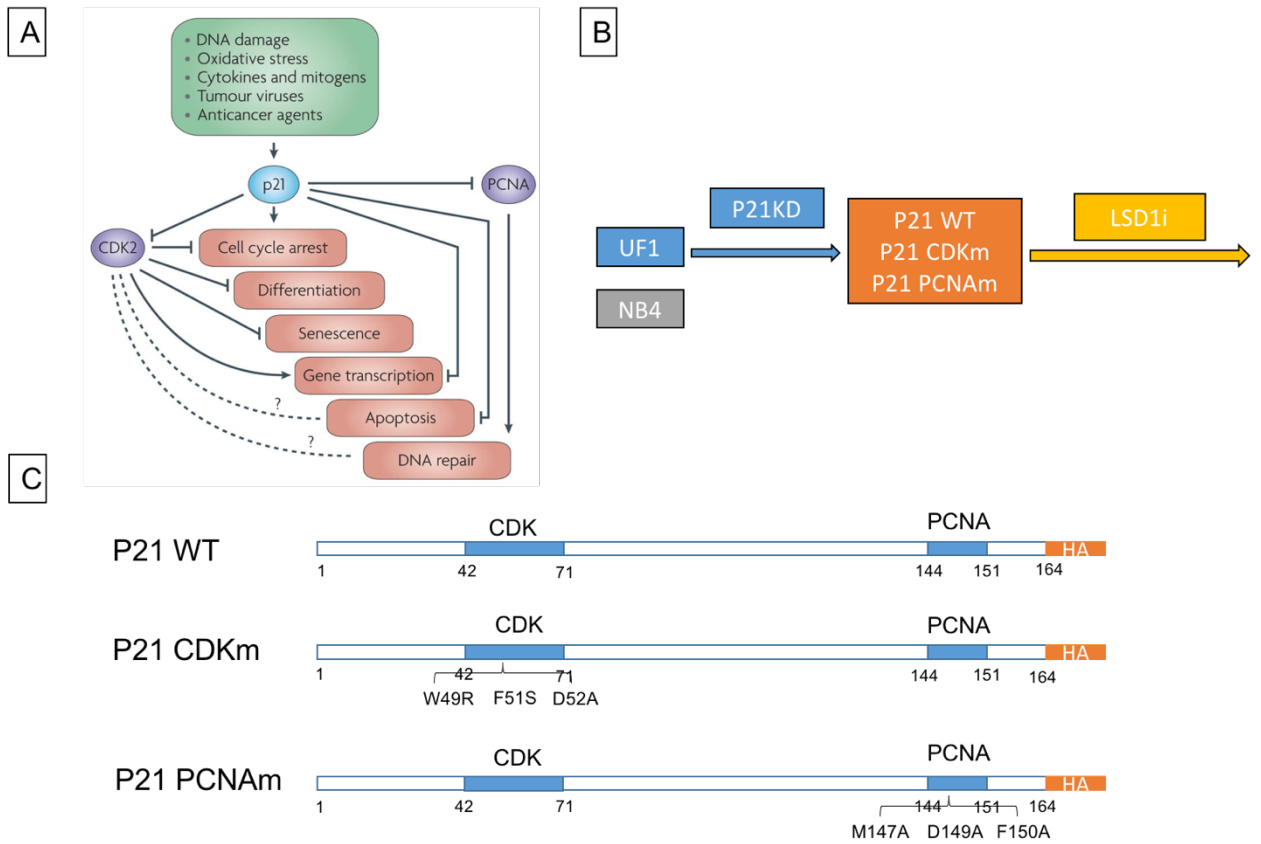
Figure 51. **P21 has two non-overlapping structural domains: PCNA binding domain and CDK binding domain.** (A, B) Schematic representation of experiment. (C) Expression constructs of p21-WT, p21-CDK mutant and p21-PCNA mutant.

LSD1 inhibitor in NB4 and UF1cells which were infected with p21WT and PCNAm expression vectors significantly led to cell cycle arrest, cell growth inhibition and induction of differentiation but had less effect in cells were infected by CDKm expression construct **(Figure 52, 53)**.
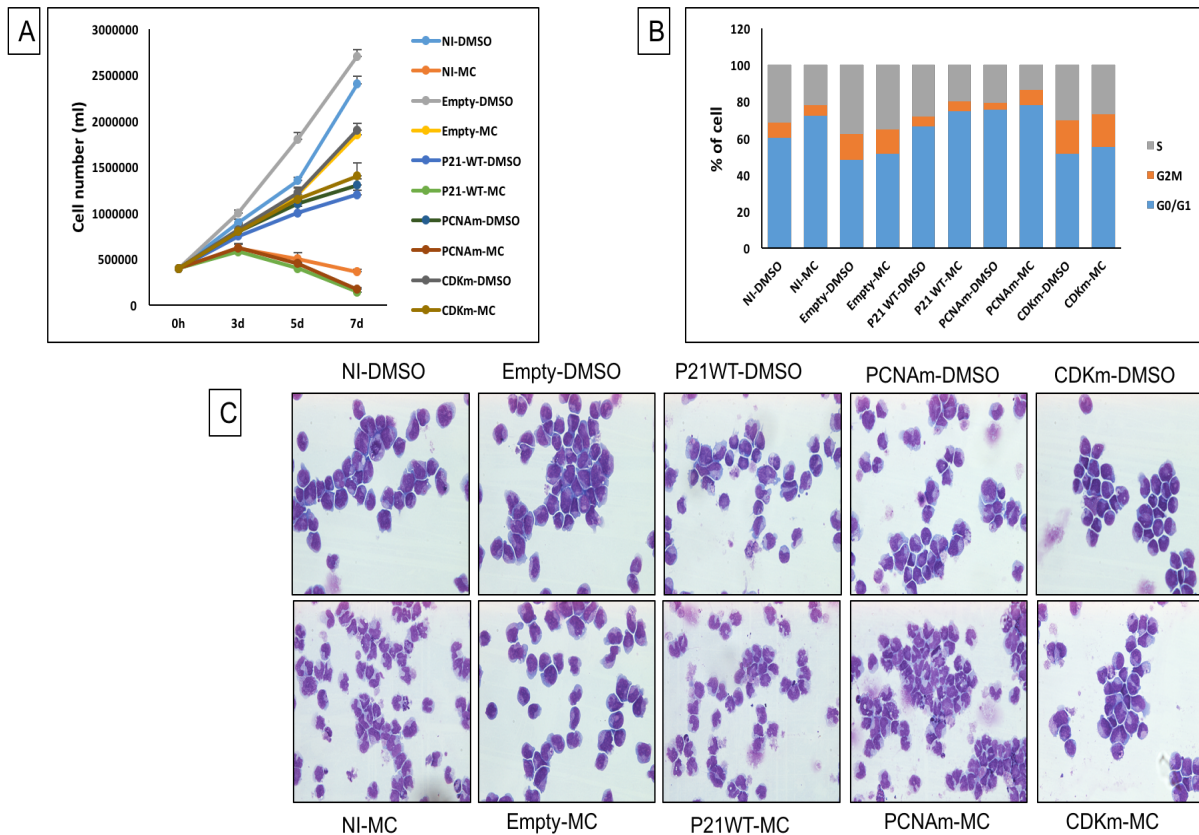
Figure 52. **P21 by binding to CDK leads to cell cycle arrest and sensitize cells to LSD1 inhibitor.** (A)Relative proliferation of UF1cells stably transduced with shRNA targeting p21 following transfection with empty or p21-WT, p21-PCNAm, p21- CDKm expression vector following treatment with MC or DMSO. Data are presented as mean of triplicates ± SD. (B) Summary of cell-cycle status of UF1 cells stably transduced with shRNA targeting p21 following transfection with empty or p21-WT, p21-PCNAm, p21- CDKm expression vector following treatment with MC or DMSO. (C) Representative light micrograph show Wright-Giemsa staining of UF1 cell stably transduced with shRNA targeting p21 following transfection with empty or p21-WT, p21-PCNAm, p21- CDKm expression vector following treatment with MC or DMSO. P value < 0.05 (*), P < 0.01 (**) and P <0.001 (***). (NI: Not Infected).

Figure 53. **P21 by binding to CDK leads to cell cycle arrest and sensitize cells to LSD1 inhibitor.** (A) Relative proliferation of NB4 cells stably transduced with empty or p21-WT, p21-PCNAm, p21-CDKm expression vector following treatment with MC or DMSO. Data are presented as mean of triplicates ± SD. (B) Summary of cell-cycle status of NB4 cells stably transduced with empty or p21-WT, p21-PCNAm, p21-CDKm expression vector following treatment with MC or DMSO. (C) Representative light micrograph show Wright-Giemsa staining of UF1 cell stably transduced with empty or p21-WT, p21-PCNAm, p21- CDKm expression vector following treatment with MC or DMSO. P value < 0.05 (*), P < 0.01 (**) and P <0.001 (***).

These results suggest that p21 by binding to CDK leads to cell growth inhibition and G1 cell cycle and sensitize resistant cells to LSD1 inhibitor.

Forced cell cycle inhibition sensitizes resistant cells to LSD1 inhibitor

We observed that p21 by binding to CDK leads to G1 cell cycle arrest and sensitizes resistant cells to LSD1 inhibitor which prompted us to evaluate a new combination therapy of CDK inhibitor with LSD1 inhibitor. To address this hypothesis, we used Palbociclib, a CDK4/6 inhibitor in AML cell lines. To this end, we incubated NB4 cells with increasing concentrations of Palbociclib for 24 hours. Increase in G1 cell cycle arrest were observed after

135

24 hours' exposure to Palbociclib in a dose dependent manner. While 50nM Palbociclib did not induce cell growth arrest but mediate cell-cycle arrest at G1-S checkpoint comparable to UF1 cells. Thus we decided to use 50 nM Palbociclib for further experiments **(Figure 54)**.
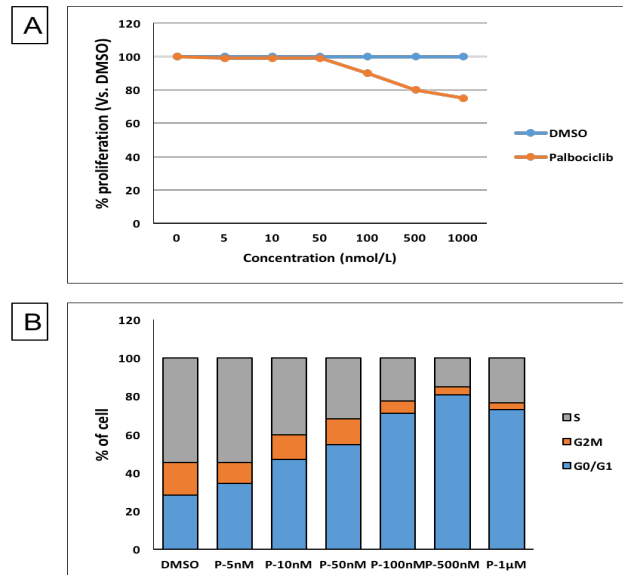
Figure 54. **Palbociclib increased G1 phase in a dose dependent manner.** NB4 cells were treated with Palbociclib at increasing concentration for 24 hours and then analyzed for viability (A) and cell cycle (B).

NB4 cells were infected by p21 shRNA and 48 hours after sorting, GFP^{+} cells were treated with 50nM palbociclib for 24 hours to induce cell cycle arrest following treatment with MC for a six-days time course **(Figure 55)**.

Pretreatment with Palbociclib, increased percentage of cells population in G1 phase and sensitize NB4 cells to MC and this co-treatment significantly inhibited cell growth **(Figure 56)**.

This results suggest that forced cell cycle inhibition sensitize resistant cells to LSD1inhibitor to inhibit cell growth, induce cell cycle arrest and differentiation.
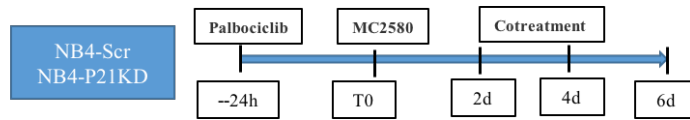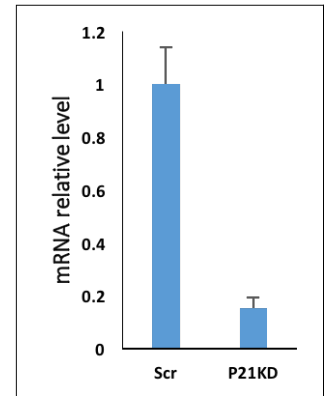
Figure 55. **Co-treatment of NB4 cells with LSD1 inhibitor and palbociclib.** (A) Schematic representation of co-treatment of Palbociclib with LSD1 inhibitor in NB4 cells. (B) Analysis of p21 mRNA relative levels in NB4 cells, transduced with the indicated lentiviral vectors. Values are normalized against GAPDH and referred to SCR.
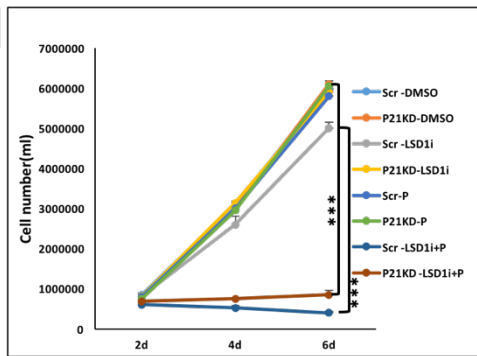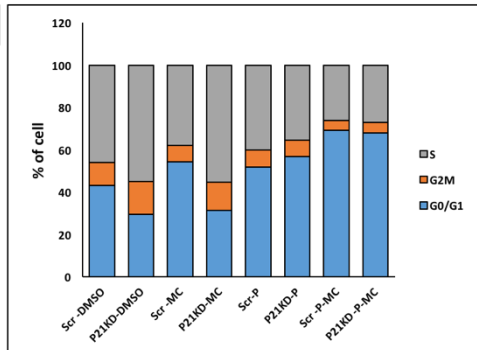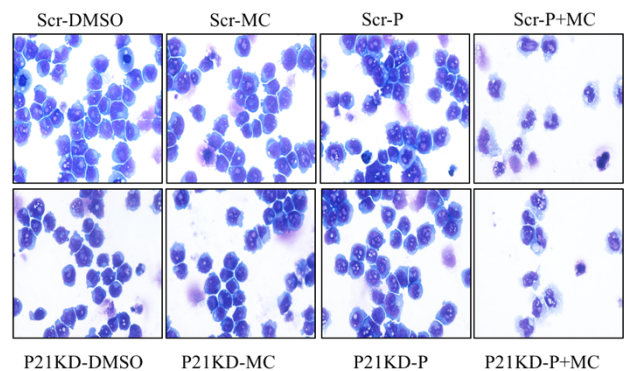
Figure 56. **Force cell cycle inhibition sensitizes NB4 cells to LSD1 inhibitor.** (A) Relative proliferation of NB4 cells stably transduced with either control shRNA (SCR) or shRNA targeting p21 following treatment with Palbociclib for 24 h following co-treatment with MC or DMSO. Data are presented as mean of triplicates ± SD. (B) Summary of cell-cycle status of NB4 cells stably transduced with either control shRNA (SCR) or shRNA targeting p21 following treatment with Palbociclib for 24 h following co-treatment with MC or DMSO. (C) Representative light micrograph show Wright-Giemsa staining of NB4 cells stably transduced with either control shRNA (SCR) or shRNA targeting p21 following treatment with Palbociclib for 24 h following co-treatment with MC or DMSO. P value < 0.05 (*****), P < 0.01 (*** ***) and P <0.001 (*** * ***).

LSD1 inhibition in primary melanoma cells

In order to validate our findings obtained in cell lines by using more sophisticated models, we performed additional experiments in human primary melanoma cells. We used six different primary melanoma cells according to their cell growth rate (doubling time) and the level of p21**(Figure 57)**.
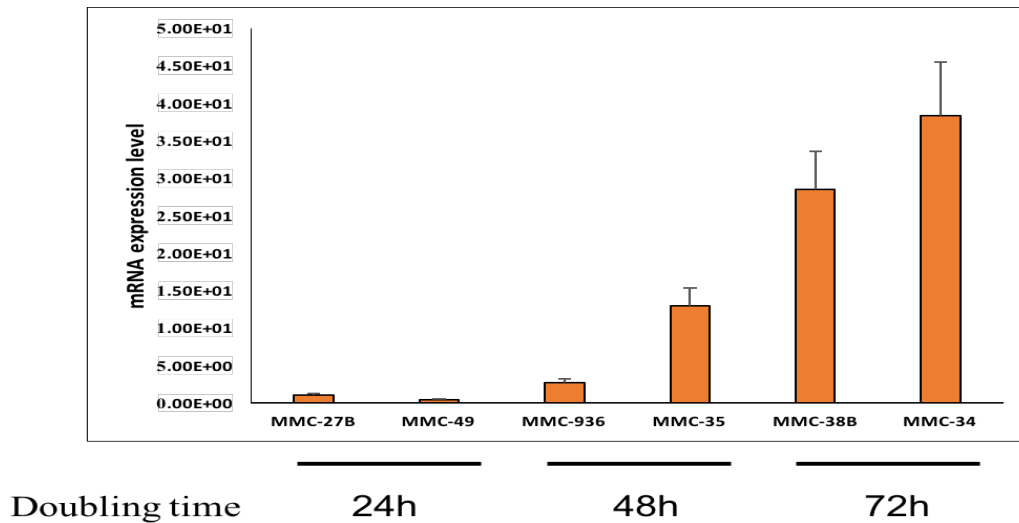
Figure 57. **Slow-cycling melanoma cells have high level of p21.** Analysis of p21 mRNA relative levels in primary human melanoma cells. Values are normalized against GAPDH.

Mirroring the results in cell lines, primary cells that have high level of p21 and slower cell growth were more sensitive to MC compared with fast growing cells with low level of p21**(Figure 58)**.
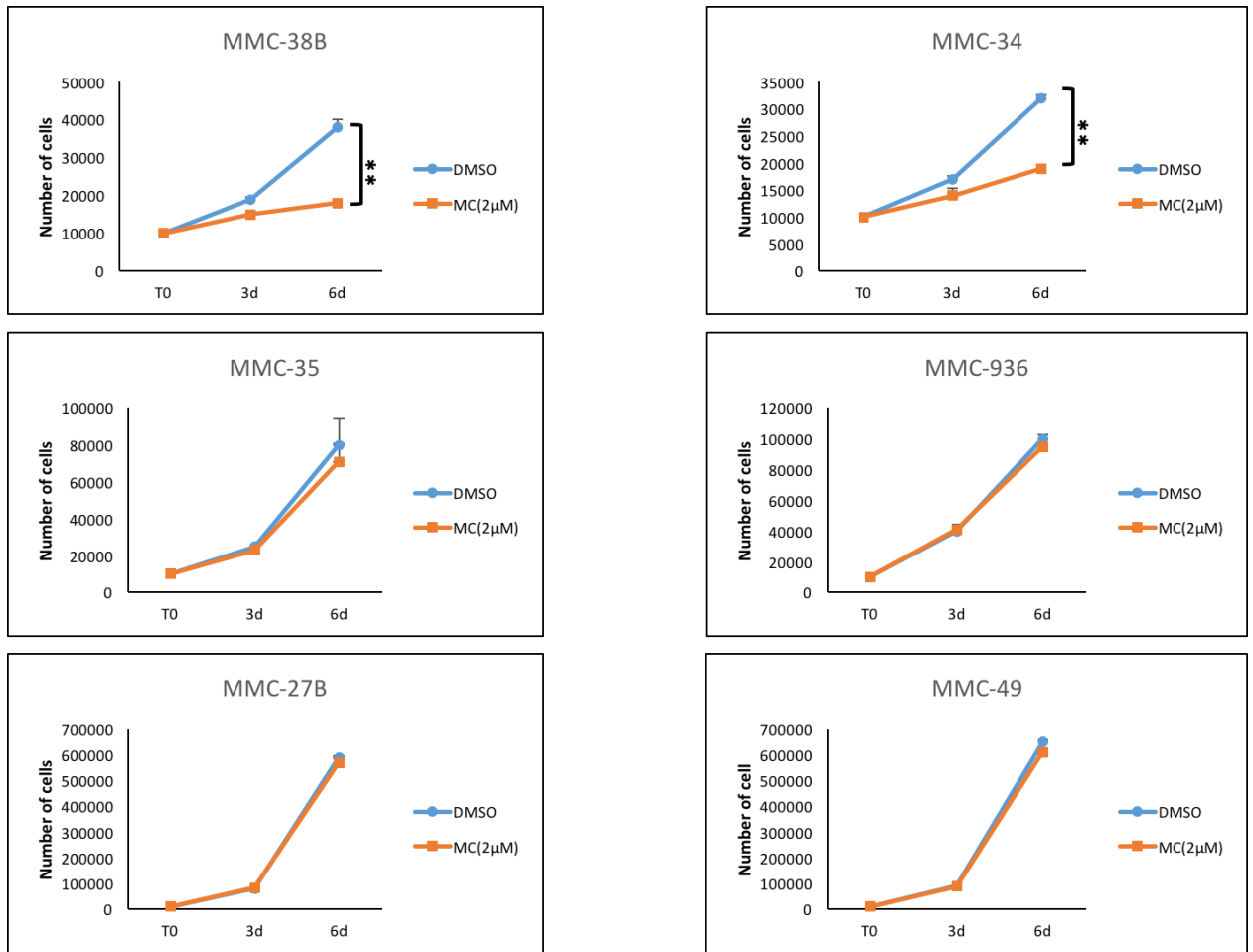
Figure 58. **Slow-cycling melanoma cells are more sensitive to LSD1 inhibitor.** Relative proliferation of primary human melanoma cells treated with MC or DMSO. Data are presented as mean of triplicates ± SD. P value < 0.05 (*****), P < 0.01 (******) and P <0.001 (*******).

Effects mediated by LSD1 inhibition in human primary melanoma cells is p21-dependent

To determine whether the upregulation of p21 induced by MC contributes to growth and cell cycle arrest, we utilized RNA interference to suppress p21 induction. P21 was depleted efficiently with a lentivirally derived shRNA. In p21 KD melanoma cells, there was a slight but consistent decrease in the G1 phase population when compared with control cells, with an

increase of S phase cells, indicating that the presence of p21 at its constitutive levels exerts a modest inhibitory effect regulating the G1/S transition. This effect was corroborated by a trend toward increased cell proliferation in p21-depleted cells **(Figure 59, 60)**.
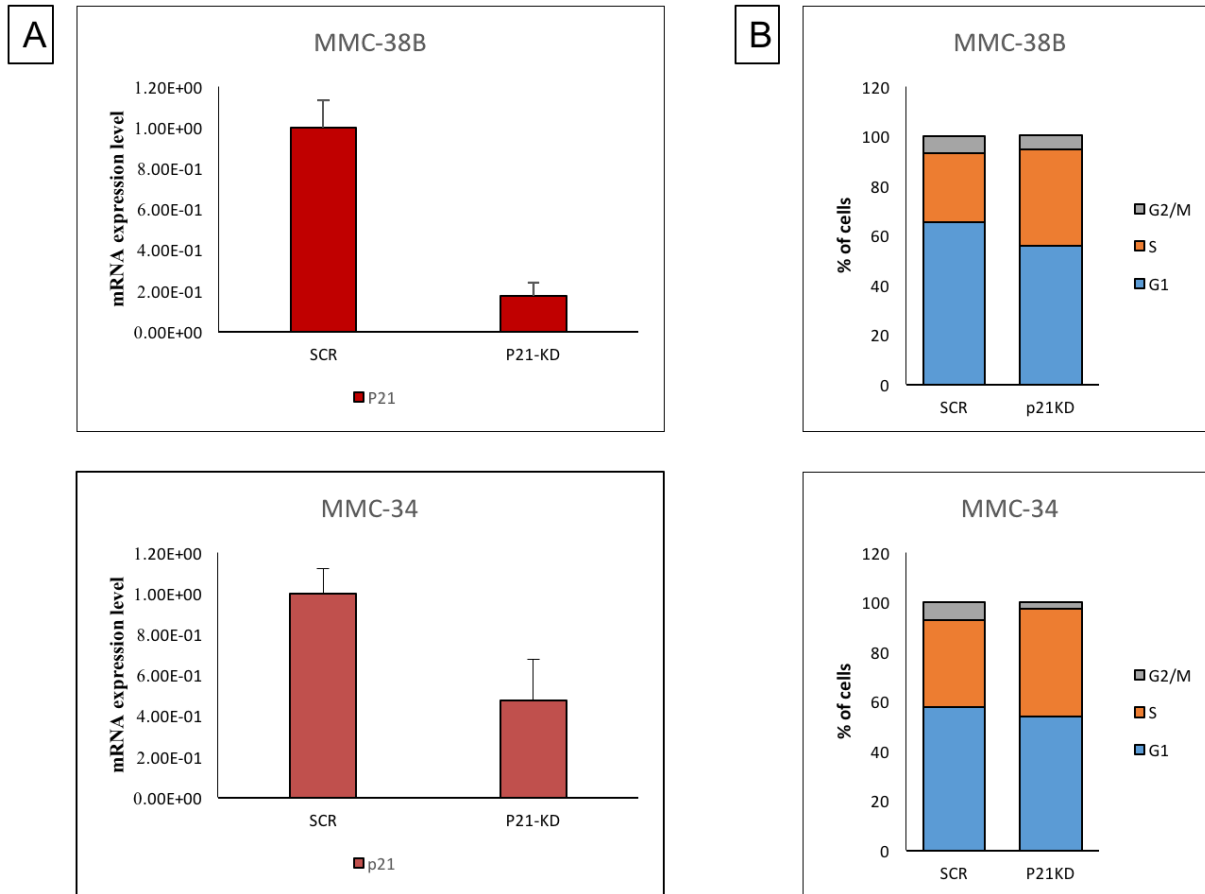
Figure 59. **P21 depletion in Melanoma cells.** (A) Analysis of p21 mRNA relative levels in melanoma cells, transduced with either control shRNA (SCR) or shRNA targeting p21. Values are normalized against GAPDH and referred to SCR. (B) Summary of cell-cycle status of melanoma cells infected with either control shRNA (SCR) or shRNA targeting p21.

We then inhibited LSD1 in these stable cells and showed that p21 shRNA could suppress p21 induction under these conditions. While in control cells MC treatment resulted in an increase of G1 phase population, in p21-Kd cells the G1 population slightly increased. The difference between the percentage of MC treated cells with and without p21 was significant **(Figure 60)**.
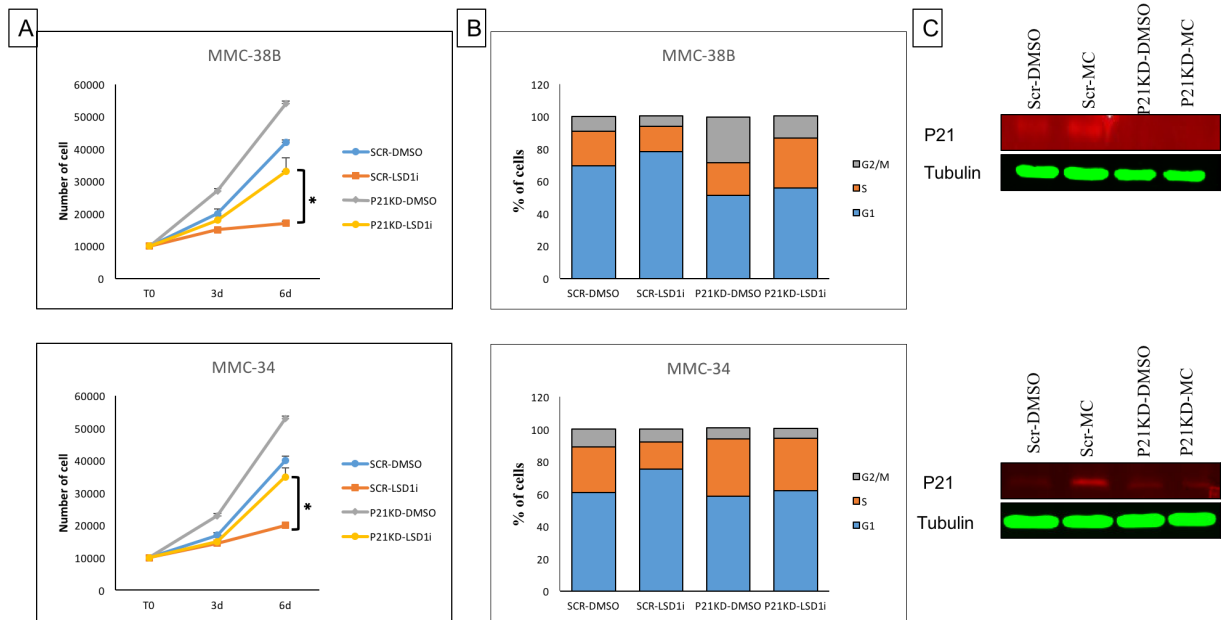
Figure 60. **Suppression of p21 rescued human primary melanoma cells from cell growth inhibition, cell cycle arrest and p21 induction induced by inhibition of LSD1.** (A) Relative proliferation of melanoma cells stably transduced with either control shRNA or shRNA targeting p21 following treatment with MC or DMSO. Data are presented as mean of triplicates ± SD. (B) Summary of cell-cycle status of melanoma cells stably transduced with either control shRNA or shRNA targeting p21 following treatment with MC or DMSO. (C) Immunoblot analysis of p21 expression in melanoma cells stably transduced with either control shRNA (SCR) or shRNA targeting p21 following treatment with MC or DMSO. Tubulin was used as a loading control. P value < 0.05 (*), P < 0.01 (* *) and P <0.001 (* * *).

Together, these data indicate that suppression of p21 inhibits the G1 cell cycle arrest caused by LSD1 inhibition. Hence, repression of p21 by LSD1 promotes cell cycle progression.

Forced cell cycle inhibition sensitize resistant primary melanoma cells to LSD1 inhibitor

To determine if cell cycle inhibition sensitize resistant melanoma cells to MC, the resistant cells were pre-treated with Palbociclib. MC was administrated at 24 hours after adding Palbociclib, when G1 phase enrichment was achieved **(Figure 61)**.
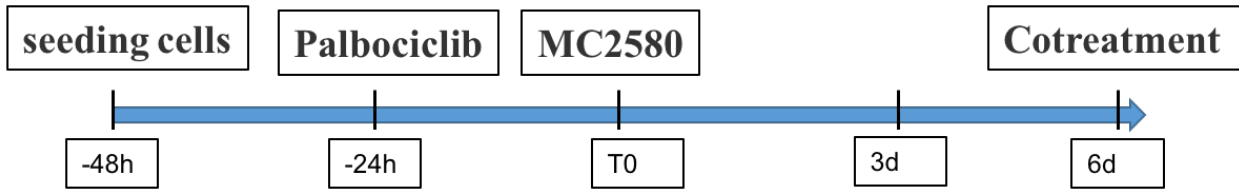
Figure 61. **Co-treatment of melanoma cells with LSD1 inhibitor and palbociclib.** Schematic representation of co-treatment of Palbociclib with LSD1 inhibitor in melanoma cells.

The sensitization effect was observed when cells pre-treated with Palbociclib at dose that had minor effects in the single-agent treatment **(Figure 62)**.
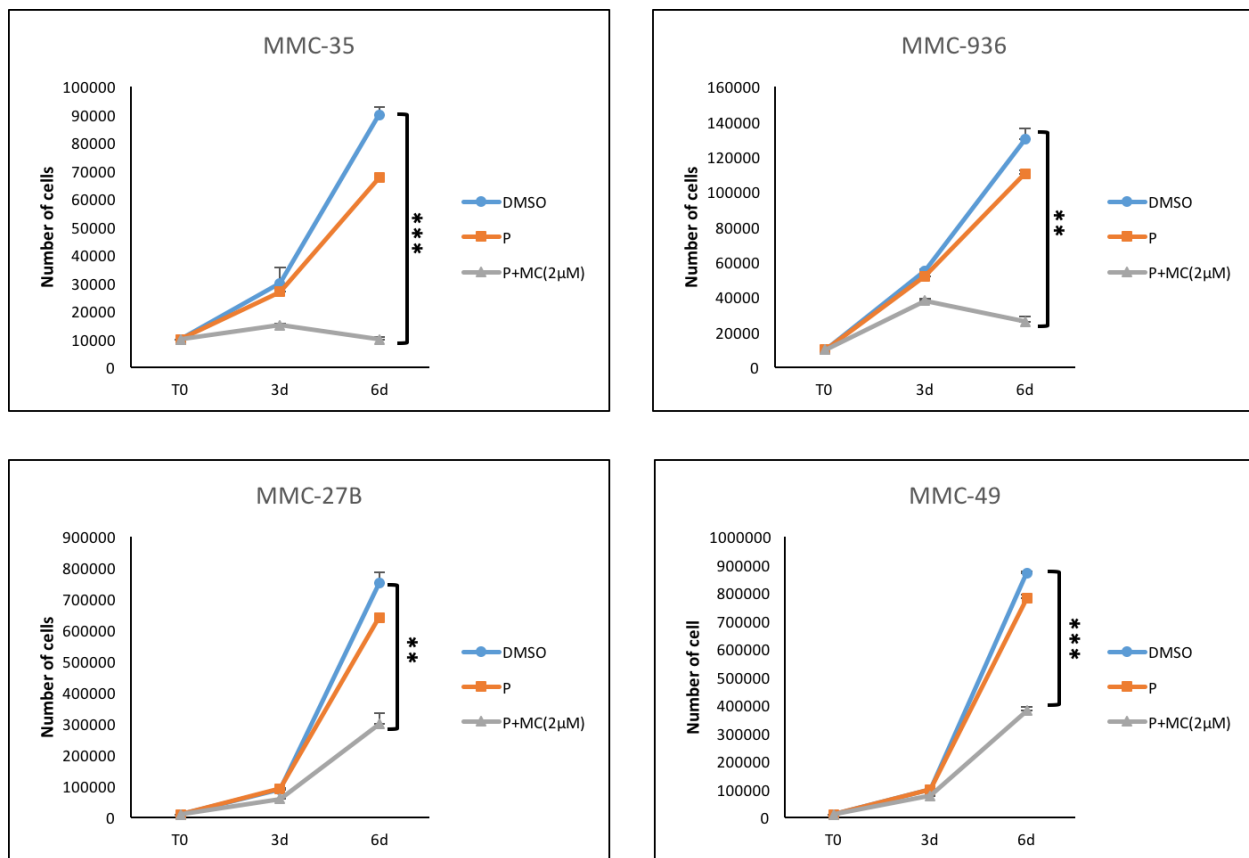
Figure 62. **Force cell cycle inhibition sensitizes resistant melanoma cells to LSD1 inhibitor.** Relative proliferation of treated-melanoma cells with Palbociclib for 24 h following co-treatment with MC or DMSO. Data are presented as mean of triplicates ± SD. P value < 0.05 (*****), P < 0.01 (*** ***) and P <0.001 (*** * ***).

Taken together, our results indicate that forced cell cycle inhibition sensitizes resistant primary melanoma cells to LSD1 inhibitor.

Discussion

Acute Myeloid Leukemia (AML) is a form of cancer that affects the myeloid blood cells produced in the bone marrow. AML is characterized by a rapid increase of immature blood cells that do not perform the normal function. In AML, myeloid progenitor cells in the bone marrow undergo a malignant transformation resulting in accelerated production of poorly differentiated myeloblasts that are not able to mature into more differentiated cell types but remain as immature cells [Estey& Dohner, 2006]. According to French-American-British (FAB) classification, AML has been classified into 8 subtypes (M0 to M7) defined by morphological, immune-phenotypic and cytochemical criteria [Bennett, 1976]. The different subclasses represent different states of maturation of the leukemic blast cells and what lineage that is engaged. Acute promyelocytic leukemias (APLs) represents 10-15% of AMLs in adults, characterized by a block of granulocytic differentiation and accumulation of promyelocytes in the bone marrow, blood and other extramedullary tissues. Although five different chromosome translocations have been associated with APL, about 99% of APL cases are PML-RARα positive [Saeed, 2011; Minucci, 2002; Mehdipour, 2017; Matthews, 2015]. The fusion product, PML-RARα, encodes a functionally altered transcription factor that recruits CoREST and other corepressor complexes at retinoic acid (RA) target genes, which in turn silence genes crucial for hematopoietic differentiation [Lokken& Zeleznik-Le, 2012]. The standard treatment regimen for non-promyelocytic AML includes chemotherapy with combination of different anti-cancer drugs depending on the leukemia subtype. Given the unsatisfactory clinical outcome associated with standard chemotherapy in acute myeloid leukemia (AML), there is an essential need for new targets. All-trans retinoic acid (ATRA) elicits complete remission by binding to RARα portion of PML-RARα-driven APLs at pharmacological doses, and has been successfully used in treatment of APLs. Pharmacological

dose of RA triggers the dissociation of co-repressor complexes by PML-RARα conformational change and degradation, promoting cell differentiation. However, a major obstacle to successfully treating APL patients is retinoic acid resistance, which often associated with mutations in the RARα moiety of PML-RARα [Gallagher, 2002]. Thus other clinical approaches, that could enhance ATRA clinical effect, like treatment with epi-drugs such as LSD1 inhibitors may be beneficial.

LSD1 is a flavin-containing amine oxidase that act as a transcriptional co-repressor, as a part of CoREST complex [Shi Y, 2004; Forneris, 2005; Edmondson, 2007]. Deregulation of LSD1 is a common feature of a number of cancers, including lung, breast, melanoma and hematological malignancies. Thus LSD1 has gained great interest for its use as anticancer therapeutic [Hosseini, 2017]. LSD1 shares a sequence similarity with MAO-A and MAO-B, therefore soon after its discovery, well-known MAOs inhibitors were tested on LSD1 to evaluate their activity. Among them was tranylcypromine (TCP), which previously used in treatment of depression. TCP inhibits LSD1 by covalently binding to FAD, forming a covalent adduct with the flavin ring as found in MAOs. Given the lack of potency and specificity of TCP versus LSD1, a number of TCP analogues have been developed. Despite the similarity in sequence and catalytic activity of LSD1 with other FAD-dependent amine oxidases, the substrate-binding subdomain is much larger than in other MAO-A and MAO-B. In this view many groups have made peripheral modification to the surrounding scaffold to improve affinity for LSD1 and increase selectivity to LSD1 over other MAOs. Our lab, in collaboration with prof. Antonello Mai and prof. Andrea Mattevi, previously developed a new compound working as an LSD1 specific inhibitor, MC [Binda, 2010]. This compound is an analog of tranylcypromine/Parnate (TCP) with increasing larger substituents that contained a mix of hydrophobic and hydrophilic group. By taking advantage of this inhibitor, we have previously shown that LSD1 inhibition sensitizes NB4 cells to RA treatment and induces cell growth

arrest and differentiation when combined with a physiological concentration of RA (RA low) [Binda, 2010]. Moreover, LSD1 inhibitors unlocked the ATRA-driven therapeutic response in non-APL AML by increasing H3K4me2 level and reactivating the retinoic acid signaling pathway [Schenk, 2012].

Starting from these observations, we hypothesized that LSD1 inhibition sensitize UF1 cells, that were established from a patient who was clinically resistant to RA treatment and harbor a point mutation in ligand binding domain (LBD) of RARα moiety. Surprisingly LSD1 inhibition in UF1 cells led to cell growth inhibition, induced cell differentiation and promoted G1 phase arrest, being active as a single agent. Additionally, we found that MC treatment inhibits colony forming activity of UF1 cells.

As mentioned above, pharmacological doses of RA (RA high) induces differentiation of APL cells by PML-RARα fusion protein degradation, which has been proposed as a crucial goal in order to eradicate APL. We observed that LSD1 inhibition induces cell differentiation without inducing PML-RARα degradation. Thus LSD1 inhibition can overcome PML-RARα expression to reach differentiation and growth arrest of APL-UF1 cells.

Moreover, depletion of LSD1 in UF1 cells by functional knock-down approach inhibited cell proliferation, induced cell cycle arrest and differentiation suggesting on-target effects of MC as LSD1 depletion effectively mimics the effect of LSD1 inhibitor.

Considering that cancer is so diverse and clinical outcome predictions often vary from patient to patient, a considerable amount of effort is being invested to discover molecular biomarkers that can categorize cancer patients with distinct clinical outcomes to expand prognostic capabilities. These molecular biomarkers can play roles before cancer diagnosis, at diagnosis and after diagnosis for selecting additional therapy. These molecular biomarkers could also

potentially improve clinical prognosis and allow for the development of better therapeutic agents.

Given the unsatisfactory clinical outcome associated with standard chemotherapy in some cancers such as acute myeloid leukemia (AML) and melanoma treatment, there is an essential need for new targets. Recently LSD1 have gained great interest for their use as anticancer therapeutics. However, the efficacy of LSD1 inhibitors is limited to a substantial subset of cancer cells. Thus, identification of good predictive biomarkers for sensitivity to treatment with LSD1 inhibitors will be of great value in determining the most suitable therapeutic setting.

To this end, we performed a genome-wide expression analysis comparing gene expression profiling of the two cell lines which differently response to LSD1 inhibition, before and after MC treatment. Our RNA-seq results, comparing gene expression of UF1 cells with NB4 cells, showed high correlation in basal gene expression profiling. Though, there are 86 and 101 genes which up regulated and down regulated respectively in UF1 cells in comparison with NB4 cells. One of those upregulated genes was p21 (CDKN1). High level of p21 in UF1 cells, is consistent with the fact that UF1 cells are in higher percentage in G1 phase and lower growth rate. Furthermore, we observed that LSD1 inhibition led to further p21 expression in UF1 cells, suggesting that the induction of p21 was associated with the induction of G1 phase arrest and inhibition of cell growth. To further explore this association, p21 has been knocked down to check the cell viability after LSD1 inhibition. Our results showed that Knockdown of p21, rescued UF1 cells from cell growth inhibition, cell differentiation and G1 phase arrest mediated by LSD1 inhibitor. Furthermore, rescue experiments demonstrated that p21 mediates increased MC-induced cell cycle arrest, cell growth inhibition and cell differentiation.

we extended our study to non-APL AML and SCLC cell lines by using two sensitive cell lines

to LSD1 inhibitors, Kasumi and NCI-H69 cells. Similar to APL cells, Knock-down of p21 in non-APL AML and SCLC cell lines, rescued cells from the effects of LSD1 inhibitor. As compared with other cyclin-dependent kinase inhibitor genes, p21 is a more general inhibitor that targets multiple CDKs, which may explain why it is that repression of this particular target so potently rescues the LSD1 inhibitor phenotype [Lim & Kaldis, 2013].

Activation of p21 occurring upon LSD1 inhibition appears p53-independent as these cell line contains mutated p53 [Krejci, 2008; Ito, 2004]. Overall, increased expression of P21 mediated by LSD1 inhibitor, is associated with differentiation and cell growth inhibition in cancer cells and p21 provoked by LSD1 inhibitors could serves as a biomarker to verify pharmacological activity and a prognostic tool reflecting responsiveness to LSD1i in the clinic.

Given that the efficacy of LSD1 inhibitor as a single-agent are limited in some AML cell lines and also exhibit toxicity and intolerable *in vivo* activity in the mouse models of AML, we reasoned that we can sensitize resistant cells to LSD1 inhibitor by p21 induction through drugs. We used two HDAC inhibitors, Vorinostat (SAHA) and Trichostatin A (TSA) for a short time to induce p21 expression. While SAHA and TSA treatment with relatively lower concentrations and short time were well tolerated, p21 induction by HDAC inhibitors sensitize NB4 cells to LSD1 inhibitor. The sensitization effect was observed when cells pre-treated with HDACis at dose that had minor effects in the single-agent treatments.

The transcriptional regulation of p21 has been extensively studied. P21 is a transcriptional target of p53 and plays a crucial role in mediating growth arrest when cells are exposed to DNA-damaging agents [el-Deiry, 1993; el-Deiry, 1994]. P53 activates p21 transcription via two consensus binding sites located at -2285 and -1394 base pairs upstream from the transcription initiation site.

However, it has been shown that p21 is up-regulated in cells where p53 is mutated or silenced, indicating that other transcription factors and other stimuli such as growth factors, hormones, intracellular signaling molecules are involved. Many transcription factors have been shown to regulate p21 expression, such as Sp1/3, Egr1, SALL2, KLF4, c-Myc, STAT 1/3 and Smad3/4 [Gartel, 1999; Choi, 2008; Li, 2004; Mori, 2012; Xie, 1997; Gartel, 2000; Moustakas, 1998; Kitaura, 2000]. The regulation of chromatin structure such as DNA modifications and histone modifications has been described as a second level of transcriptional regulation for p21. DNA hypermethylation of the p21 gene has been reported in p21-silenced cells in some cancer types [Chen, 2000; Roman-Gomez, 2002]. Another epigenetic mechanism shown to regulate p21 transcription is histone acetylation and methylation [Nian, 2008; Wang, 2008; Duan, 2005]. For more than a decade now, histone deacetylase inhibitors have been investigated for their ability to increase acetylation and promote expression of p21 gene. Here in this study we demonstrated that LSD1 regulates p21 expression by binding to promoter and putative enhancers of p21 gene. LSD1 inhibition substantially increased histone acetylation (H3k27ac) and H3K4me2 at promoter and enhancers of p21 gene. The increase in histone acetylation could be due to loss of HDAC1 at p21. One mechanism proposed to explain the interplay between histone acetylation and methylation is the physical association of HDAC1 and LSD1 by which each enzyme influences the activity of the other. Indeed, past studies have indicated that optimal deacetylation of nucleosomes requires the demethylase activity of LSD1 [Lee, 2006; Mendenhall, 2013]. Additionally, it has been previously shown that affecting one histone modifying enzyme can have effects on others. For example, Meng et al showed that treating ovarian cancer cells (SKOV3) with trichostatin A (TSA) and decitabine, HDAC and DNMT1 inhibitors respectively, lowered the expression levels of LSD1 and increased H3K4me2 levels [Meng, 2013]. Vasilatos et al also showed that knockdown of LSD1 expression in breast cancer cells decreased mRNA levels of HDAC isozymes [Vasilatos,

2013].

NB4 cells were resistant to MC-mediated growth inhibition, in which expression of p21 was not induced after exposure to MC. Induction of H3K27ac as well as H3K4me2 at promoter and putative enhancers were not prominent in NB4 cells after exposure to MC. This may be a reason why MC failed to induce expression of p21 in NB4 cells. We also found a unique enhancer (element C) was only enriched for LSD1 occupancy in UF1 cells compared with NB4 cells and MC treatment increased the level of H3K4me2 and H3K27ac on this element. The precise mechanism to determine how LSD1 regulates p21 require further investigation using techniques that enable exploration of long-range chromatin interactions. Our observation that LSD1 inhibitor in synergy with HDAC inhibitors activates p21 expression further through enhancing acetylation at p21 suggests a potential approach to cancer therapy.

P21 also known as cyclin-dependent kinase inhibitor 1 or CDK-interacting protein 1 (CIP1) or wild-type p53-activated factor (WAF1) is a protein that is encoded by the CDKN1A gene located on chromosome 6 (6p21.2) in the human genome [Harper, 1993; Shin, 2011]. CDK inhibitors are negative regulators of cell proliferation and are often deregulated in human cancers. The p21 protein binds and inhibits the activity of CDK4/6 complexes, cyclin E-CDK2 and cyclin B-CDK1, and thus functions as a regulator of cell cycle progression at G1 and S phase **(Figure 63)** [Bunz, 1998; Chan, 2000; Charrier-Savournin, 2004]. These kinases responsible for the phosphorylation of the retinoblastoma (Rb) protein. Specifically, phosphorylation of Rb on Ser780 allows dissociation of the transcription factor E2F from the Rb/E2F complexes and the subsequent transcription of E2F target genes, which are responsible for the progression through the G1 and S phase transition [Kitagawa, 1996; Lundberg, 1998; Chen, 2009; Classon, 2002]. A unique feature of p21 that sets it apart from the other CdkIs is that it can also bind to PCNA, that is essential for replication mismatch

repair and DNA replication thus blocking both DNA replication and repair **(Figure 61)**
[Abbas, 2009]. We showed that expression of the N-terminal region of p21 inhibits G1 cell
cycle as efficiently as full length of p21 in both NB4 and UF1 cells and sensitize both NB4
and p21-KD UF1 cells to MC treatment.
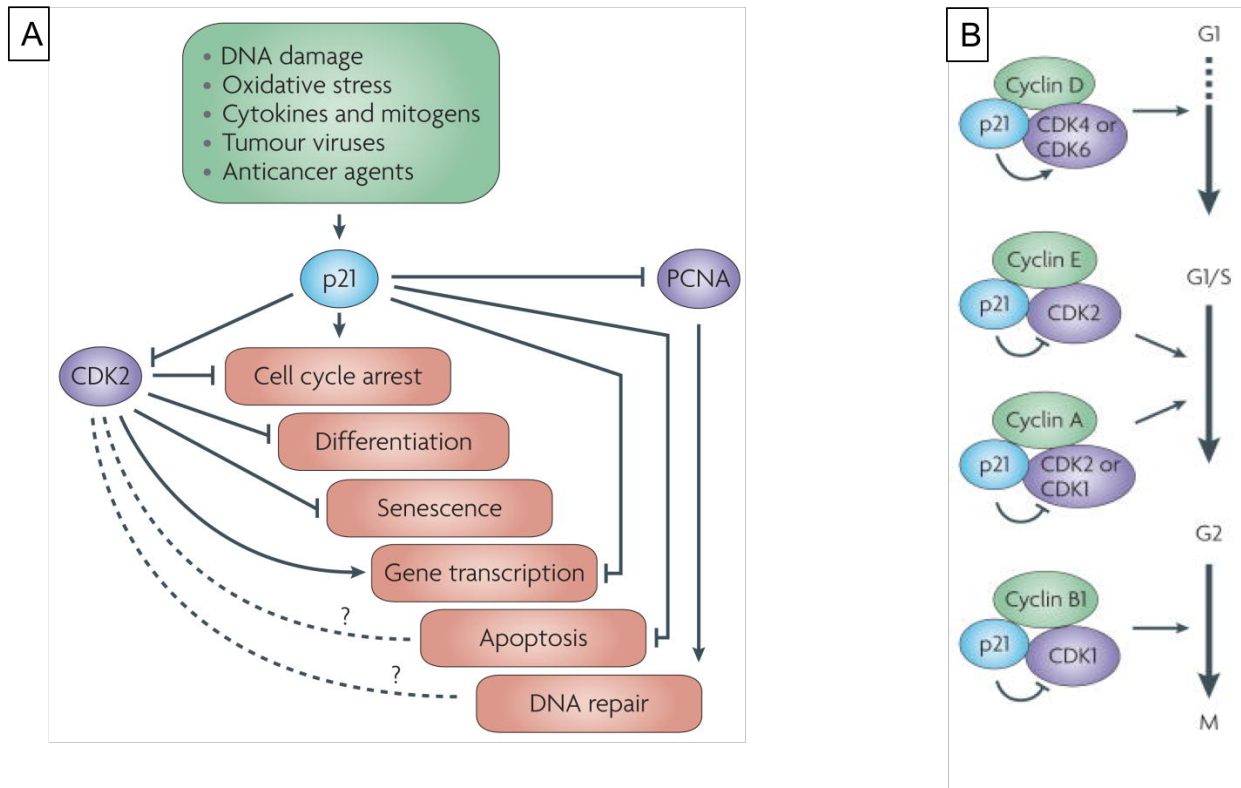
Figure 63 **P21 function**. (A)P21-mediated growth inhibition depends on two non-overlapping structural domains: PCNA binding domain and CDK binding domain. (B) P21 protein binds and inhibits the activity of cyclinD-CDK4/6 complexes, cyclin E-CDK2 and cyclin B-CDK1. Adapted from Abbas et al. Nat Rev Cancer 2009.

This observation that p21 by binding to CDK leads to G1 cell cycle arrest and sensitizes
resistant cells to LSD1 inhibitor prompted us to evaluate a new combination therapy of
CDK4/6 inhibitor with LSD1 inhibitor. Further understanding of mechanism of CDK4 and
CDK6 dysregulation in cancer led to the understanding that targeting these CDKs should
specifically lead to cytostatic arrest in G1 phase, and directly suppress Rb initiated gene

expression and cell proliferation. Palbociclib (PD-0332991) is an orally available, highly selective inhibitor of CDK4/6 kinase activity, with a high level of specificity for these over other CDKs and other protein kinases that inhibits Rb phosphorylation and therefore prevents cellular DNA synthesis by inhibiting progression of the cell cycle from G1 to S phase **(Figure 64)**. Palbociclib binds to the ATP binding pocket of CDK4 and CDK6, with specific interaction with residues within the ATP binding cleft. This inhibition causes downstream loss of expression of S phase cycles, nucleotide biosynthesis, DNA replication machinery and cell cycle regulatory genes. Currently, palbociclib is approved by the US FDA (Food and Drug Administration), for the treatment of estrogen positive metastatic breast cancer [Asghar, 2015]. Our results have shown that treatment of NB4 cells at nanomolar concentrations results in effective G1-phase arrest and sensitize cells to LSD1 inhibition.
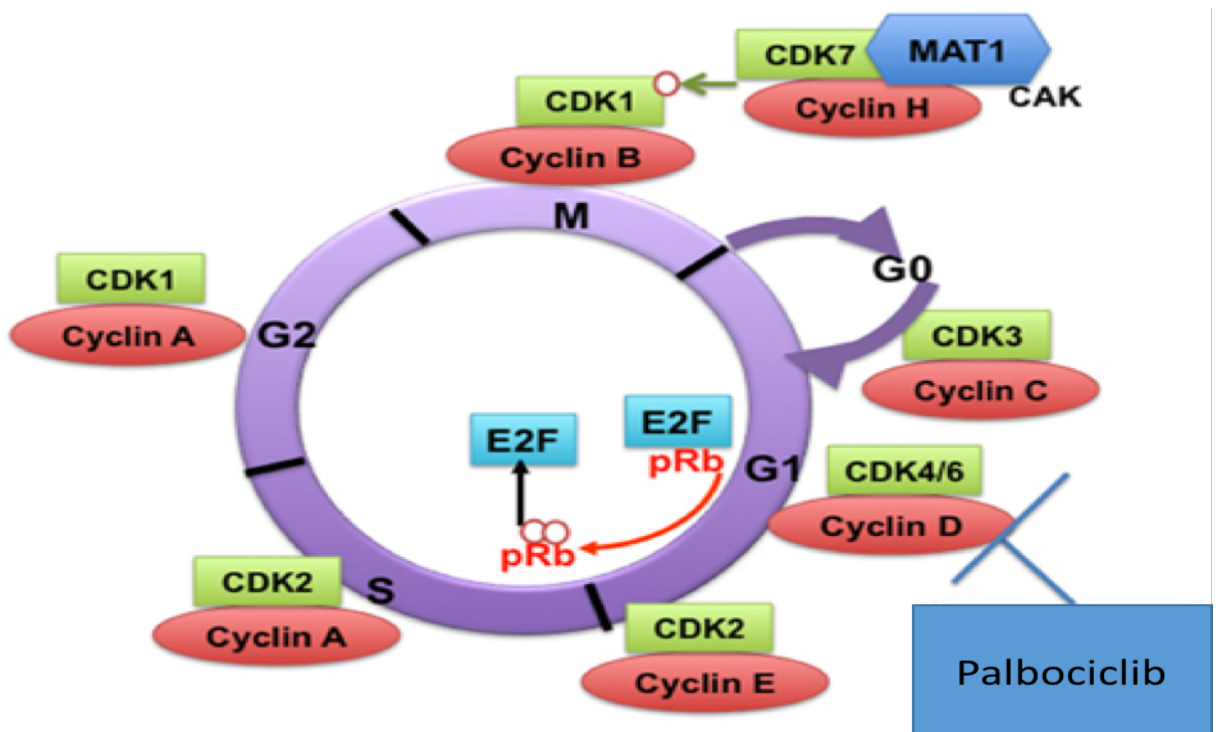
Figure 64. **Palbociclib.** Palbociclib is a small molecule inhibitor of CDK4/6, blocking the phosphorylation of Rb inducing cell cycle arrest and preventing cell proliferation. Adapted from Aleem& Arceci. Front Cell Dev Biol 2015.

In order to validate our findings obtained in cell lines by using more sophisticated models, we performed additional experiments in human primary melanoma cells. Melanoma is an aggressive form of skin cancer originating from melanocytes, a cell type found in the basal layer of epidermis, hair bulbs, eyes, ears and meninges [Bandarchi, 2010]. A large number of genes have been found to be mutated or altered in melanoma, these are often subtype-specific and some occur more frequently than others. The majority of the commonly found mutations affect two signaling pathways MAPK/ERK and PI3K/Akt pathway that regulate proliferation and survival. More than 80 % of melanomas arising in the skin have activating mutations in either B-RAF (V600E) or N-RAS (Q61K), highlighting the importance of MAPK/ERK and PI3K/Akt pathways in melanoma. However, mutations in B-RAF and N-RAS are almost always mutually exclusive [Davies, 2002; Goel, 2006]. In addition to NRAS and BRAF mutations, a number of other genes have been found to be mutated in melanoma such as, CDKN2A (p16), PTEN, c-KIT, p53, MITF, MC1R, GRIN2A and EGFR [Woodman, 2012; Hocker, 2008, Garraway, 2005]. Melanoma is considered to be the deadliest form of skin cancer and is known for its resistance to conventional therapy. However, development of novel personalized targeted therapy strategies may bring new hope [Palathinkal, 2014].

Vemurafenib and Dabrafenib are inhibitors of V600E mutant BRAF that limit the activity of the MAPK/ERK signaling pathway. Treatment with Vemurafenib has resulted in complete or partial tumor regression in the majority of melanoma patients carrying B-RAF V600E mutations. Unfortunately, melanoma is a heterogeneous disease and the modifications within the tumors and metastases make it difficult to treat by targeted therapy [Flaherty, 2010; Sosman, 2012].

Conventional chemotherapies and radiotherapies target proliferating cells and require active cycling for induction of apoptosis. The slow-cycling nature of many cancer stem cell pools is

therefore an inherent mechanism for resistance and cell survival in response to conventional therapies. In melanoma, the slow-cycling cells identified by Roesch et al., repress notch signaling directly though JARID1B interaction with the Notch Ligand Jagged 1 promoter, consequently reducing intracellular Notch and controlling proliferation. This group found that primary melanoma cell lines contained a PKH26 label retaining population that was almost specifically identified by the H3K4 demethylase JARID1B. This population of cells was found to incorporate BrdU more slowly, retain it for a longer period of time, lack staining for the proliferation marker Ki67, and have a doubling time of up to 4 weeks in vitro. When GFP was placed under the control of the JARID1B promoter, GFP$^+$ cells demonstrated increased sphere forming ability in vitro, suggesting increased CSC properties within these cells [Roesch, 2010].

Quiescence regulation of a stem cell population is most comprehensively understood in the hematopoietic system. In the hematopoietic system, p21 has been found to control entry into quiescence and maintenance of the quiescent state, allowing cells to activate a DNA damage-like response. Mice that are p21 null demonstrate an increase in the number of stem cells present and lose the ability to repopulate the bone marrow in serial transplant experiments, suggesting uncontrolled expansion and eventual exhaustion of the stem cell pool [Cheng, 2000; Viale, 2009].

Here we found a strong connection between high level of p21 and slow-cycling cells and their doubling time. Consistent with our obtained finding in cell lines, melanoma cells with high level of p21 and slow-cycling were more sensitive to LSD1 inhibition. Furthermore, in p21 KD melanoma cells, there was a slight but consistent decrease in the G1 phase population when compared with control cells, with an increase of S phase cells, indicating that the presence of p21 at its constitutive levels exerts a modest inhibitory effect by itself. This effect

was corroborated by a trend toward increased cell proliferation in p21-depleted cells. Moreover, Suppression of p21 rescued human primary melanoma cells from cell growth inhibition, cell cycle arrest and p21 induction induced by LSD1 inhibitor. The existence of slow growing drug-resistant side populations, which have also been reported to have expression of JARID1B, might be effectively targeted by LSD1 inhibitors, which also kill non-proliferating cells.

Interestingly, forced cell cycle inhibition with palbociclib sensitized resistant primary melanoma cells to LSD1 inhibitor. The sensitization effect was observed when cells pre-treated with Palbociclib at dose that had minor effects in the single-agent treatments. These data provide tempting target for *in vivo* validation that we are currently investigating.

Our data delineate a model whereby LSD1 drives unrestricted cycling of cancer cells by directing repressing CDKN1A (p21) gene, which allows unrestricted G1-S transition. Proliferation and cell cycle arrest is the dominant and most obvious effect of LSD1 inhibitor or LSD1 shRNA in our study. These effect was strongly and specifically linked to p21 derepression. In line with the H3K9me1/2 demethylase activity of LSD1 in prostate cancer, He et al have recently shown that LSD1 promotes S-phase entry and tumorigenesis by increasing the expression of the cell cycle-promoting genes such as SKP2 and CDC25A [He, 2017]. They showed that LSD1 significantly bind at S-phase genes in G1 phase and facilitate S-phase gene expression and G1-S phase transition and LSD1 inhibition either with inhibitor or shRNA significantly increased G1 phase arrest and inhibited cell proliferation, though mechanisms have not been clearly proposed. Here we demonstrated that LSD1 inhibition resulted in higher p21 expression and knock-down of p21 in sensitive cells rescued cells from LSD1 inhibitor phenotypes. Furthermore, p21 genetic rescue experiments or induction of p21 by HDAC inhibitors sensitized resistant cells to LSD1 inhibitor which further confirmed our

observation **(Figure 65A)**. LSD1 has been supposed to have a dual role in regulating transcription, both as a co-repressor and a co-activator. Transcriptional profiling in APL cells model provided strong support for a role of the LSD1 in transcriptional repression, by acting on H3K4me2 rather than H3K9me2. LSD1 inhibition increased level of H3K4me2 and H3K27ac modifications at promoter of myeloid-differentiation associated genes lead to expression of these genes such as CD11b, CD86 and LY96. These results were in accordance with a general repressive role of LSD1. These finding indicate that the selective demethylation of H3K4me or H3K9me by LSD1 occur in a manner dependent on cell type, the stage of development or the phases of the cell cycle. It's important to note that LSD1 associated factors such as AR, ER and PELP1, play a pivotal role in tipping the activity of LSD1 away from H3K4 methylation toward H3K9 methylation in different cellular setting. As our results showed that LSD1 by inhibiting the expression of p21 leads to S-phase entry, in prostate cancer cell lines by increasing the expression of the cell cycle-promoting genes leads to S-phase entry.

Given modest efficacy of LSD1 inhibitors against a subset of cancer cells, combination therapy with LSD1 inhibitors will be in our opinion a critical approach for future therapeutic intervention. In this study we showed that forced cell cycle inhibition either with p21 induction by HDAC inhibitors or directly by CDK inhibitors presents a promising therapeutic strategy in solid and hematologic cancers **(Figure 65B)**.
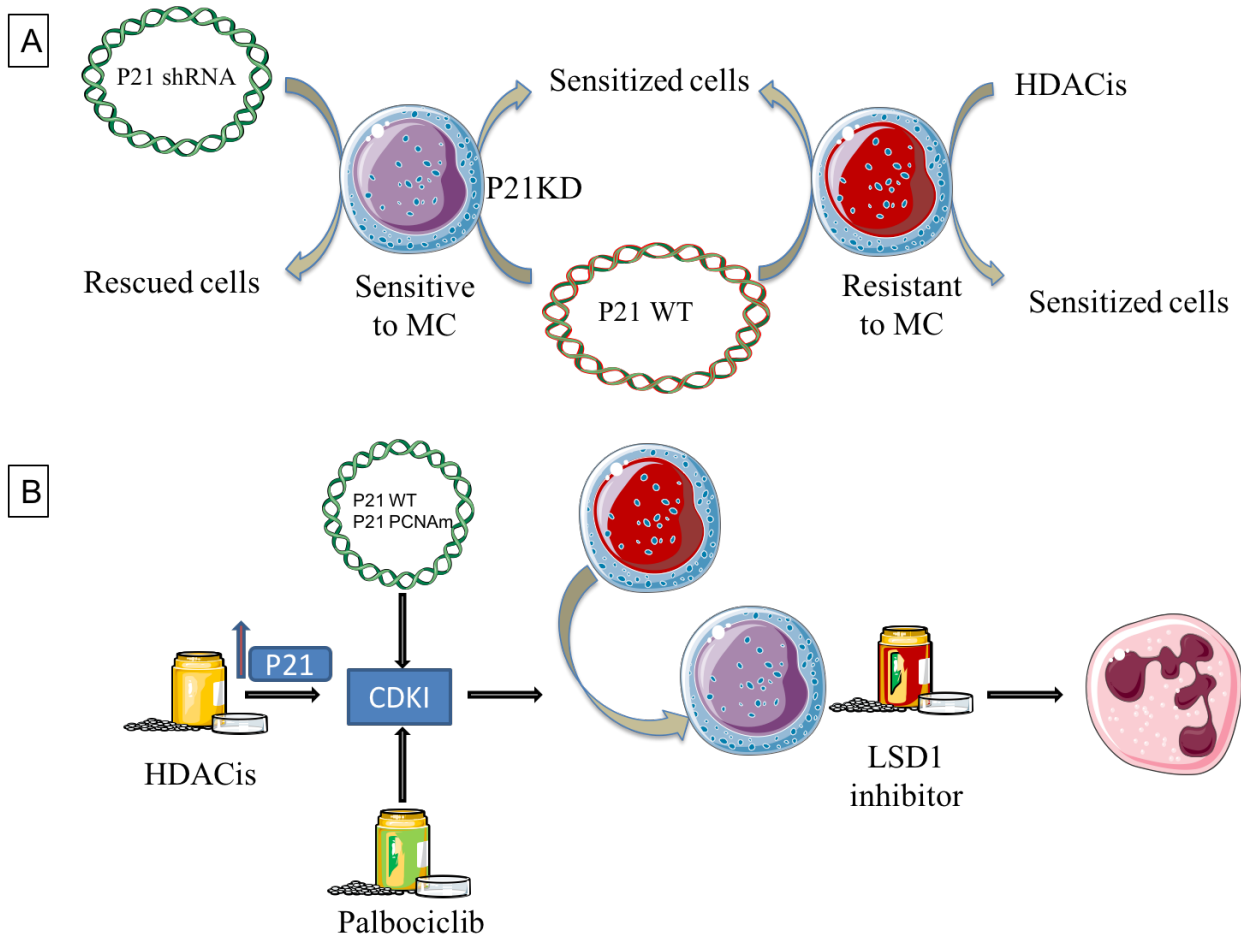
Figure 65. **Working model.** (A) LSD1 inhibition resulted in higher p21 expression and knock-down of p21 in sensitive cells rescued cells from LSD1 inhibitor phenotypes. Furthermore, p21 genetic rescue experiments or induction of p21 by HDAC inhibitors sensitized resistant cells to LSD1 inhibitor. (B) Forced cell cycle inhibition either with p21 induction by HDAC inhibitors or directly by CDK4/6 inhibitor(Palbociclib) sensitize cells to LSD1 inhibitor.

This observation can be explained by the association of LSD1 to the chromatin of G1 phase cells to suppress the expression of its target genes and dissociation from the chromatin of S-phase cells **(Figure 66)** [Zhang, 2013].
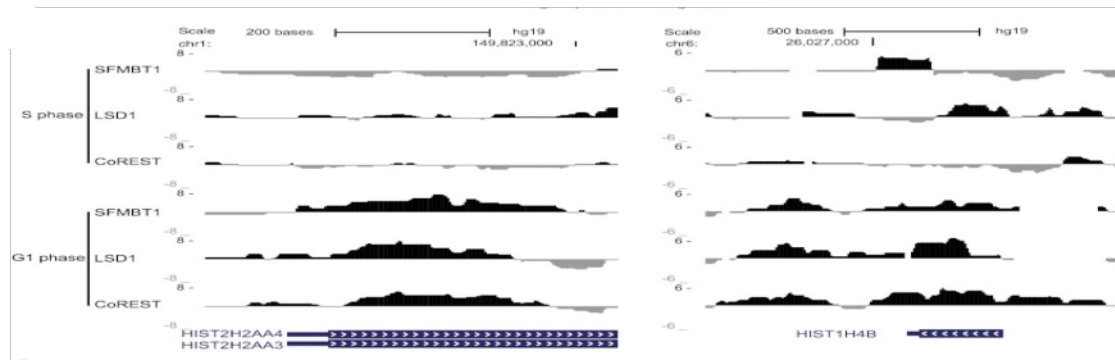
Figure 66. **LSD1 recruits and colocalize with other factors in a cell cycle-dependent manner.** LSD1 bind to the chromatin of G1 phase cells and dissociate from the chromatin of S-phase cells. Adapted from Zhang et al. Genes Dev 2013.

It has been shown that LSD1 recruits and colocalize with other factors in a cell cycle-dependent manner [Nair, 2012; Zhang, 2013; Peng, 2017; Cho, 2011; Hayami, 2011]. Nair et al have shown that LSD1 recruits to the chromatin of G1/S/G2 cells, and displaces from the chromatin of M-phase cells. Interestingly, they observed a decrease in the level of CoREST protein in cells synchronized to G2/M phase without change in the stability of CoREST, suggesting that the reduction of CoREST is correlated with a decrease in the association between LSD1 and CoREST proteins. These associations of LSD1 to the chromatin of G1 phase and dissociation from the chromatin of M-phase cell result in transcriptional repression and activation of LSD1 target genes respectively [Nair, 2012]. Occupancy of LSD1 with SFMBT1, is regulated during the cell cycle and correlates with the loss of RNA polymerase II at the promoter of their target genes. Zhang et al have shown that LSD1 and CoREST colocalize with SFMBT1 in chromatin of G1 phase but not S phase [Zhang, 2013]. Our knowledge of cell cycle-dependent manner functions of LSD1 will increase with further study. Furthermore, our data suggest that p21 loss of function or perhaps deregulation of CDK4/6 could result in acquired resistance to LSD1 inhibitors and should be considered in patients who break through LSD1 inhibitor therapy.

Abbas T, Dutta A. P21 in cancer: intricate networks and multiple activities. Nat Rev Cancer. 2009;9(6):400-14

Abu-Farha M, Lambert JP, Al-Madhoun AS, Elisma F, Skerjanc IS, Figeys D. The tale of two domains: proteomics and genomics analysis of SMYD2, a new histone methyltransferase. Mol Cell Proteomics. 2008; 7(3):560–572.

Adamo A, Sesé B, Boue S et al. LSD1 regulates the balance between self-renewal and differentiation in human embryonic stem cells. Nat. Cell Biol. 2011;13(6), 652–659.

Aleem E1, Arceci RJ. Targeting cell cycle regulators in hematologic malignancies. Front Cell Dev Biol. 2015; 3:16.

Allis CD, Berger SL, Cote J, Dent S, Jenuwien T, Kouzarides T, et al. New nomenclature for chromatin-modifying enzymes. Cell. 2007; 131:633–636.

Anand R, Marmorstein R. Structure and Mechanism of Lysine-specific Demethylase Enzymes. J. Biol. Chem. 2007; 282, 35425–35429.

Allis CD, Jenuwein T. The molecular hallmarks of epigenetic control. Nat Rev Genet. 2016;17(8):487-500.

Angrand PO, Apiou F, Stewart AF, Dutrillaux B, Losson R, Chambon P. NSD3, a new SET domain-containing gene, maps to 8p12 and is amplifyed in human breast cancer cell lines. Genomics. 2001; 74(1):79–88.

Asghar U, Witkiewicz A, Turner N, Knudsen E. The history and future of targeting cyclin-dependent kinases in cancer therapy. Nature Reviews Drug Discovery. 2015;14(2):130-46.

Asou H, Tashiro S, Hamamoto K, Otsuji A, Kita K, Kamada N. Establishment of a human acute myeloid leukemia cell line (Kasumi-1) with 8;21 chromosome translocation. Blood. 1991;77(9):2031-6.

Atsumi A, Tomita A, Kiyoi H, Naoe T. Histone deacetylase 3 (HDAC3) is recruited to target promoters by PML-RARalpha as a component of the N-CoR co-repressor complex to repress transcription in vivo. Biochem Biophys Res Commun. 2006; 345(4):1471-80.

Ballas N, Grunseich C, Lu DD, Speh JC, Mandel G. REST and its corepressors mediate plasticity of neuronal gene chromatin throughout neurogenesis. Cell. 2005; 121(4), 645–657.

Bandarchi B, Ma L, Navab R, Seth A, Rasty G: From melanocyte to metastatic malignant melanoma. Dermatol Res Pract. 2010;2010. pii: 583748.

Bannister AJ, Kouzarides T. Regulation of chromatin by histone modifications. Cell Res. 2011 ;21(3):381-95

Bannister AJ, Zegerman P, Partridge JF, Miska EA, Thomas JO, Allshire RC, et al. Selective recognition of methylated lysine 9 on histone H3 by the HP1 chromo domain. Nature. 2001; 410:120–124.

Barski A1, Cuddapah S, Cui K, Roh TY, Schones DE, Wang Z, et al. High-resolution profiling of histone methylations in the human genome. Cell. 2007; 129,823–837.

Bartke T, Vermeulen M, Xhemalce B, Robson SC, Mann M, Kouzarides T. Nucleosome-interacting proteins regulated by DNA and histone methylation. Cell. 2010; 43:470–484.

Beaumont KA, Newton RA, Smit DJ, Leonard JH, Stow JL, Sturm RA. Altered cell surface expression of human MC1R variant receptor alleles associated with red hair and skin cancer risk. Human molecular genetics. 2005; 14, 2145-2154.

Bedford MT and Richard S. Arginine methylation: an emerging regulator of protein function. Mol Cell. 2005; 18,263-272

Bennani-Baiti IM, Machado I, Llombart-Bosch A, Kovar H. Lysine-specific demethylase 1 (LSD1/KDM1A/AOF2/BHC110) is expressed and is an epigenetic drug target in chondrosarcoma, Ewing's sarcoma, osteosarcoma, and rhabdomyosarcoma. Hum. Pathol. 2012; 43, 1300–1307.

Bennett J, Catovsky D, Daniel M, et al. Proposals for the classification of the acute leukaemias. French-American-British (FAB) co-operative group. Br J Haematol. 1976

;33(4):451-8.

Berger SL, Kouzarides T, Shiekhattar R, Shilatifard A. An operational definition of epigenetics. Genes Dev. 2009; 23(7):781-3.

Bernstein BE, Mikkelsen TS, Xie X, Kamal M, Huebert DJ, Cuff J, et al. A bivalent chromatin structure marks key developmental genes in embryonic stem cells. Cell. 2006; 125:315-326.

Binda C, Valente S, Romanenghi M, et al. Biochemical, structural, and biological evaluation of tranylcypromine derivatives as inhibitors of histone demethylases LSD1 and LSDJ. Am. Chem. Soc. 2010; 132, 6827–6833.

Bird A. DNA methylation patterns and epigenetic memory. Genes Dev. 2002 ;16(1):6-21.

Biswas D, Milne TA, Basrur V, Kim J, Elenitoba-Johnson KSJ, Allis CD, Roeder RG. Function of leukemogenic mixed lineage leukemia 1 (MLL) fusion proteins through distinct partner protein complexes. Proc. Natl. Acad. Sci. U. S. A. 2011;108, 15751–15756.

Bitter MA, Le Beau MM, Rowley JD, Larson RA, Golomb HM, Vardiman JW. Associations between morphology, karyotype, and clinical features in myeloid leukemias. Hum Pathol. 1987;18, 211-225.

Booth MJ, Branco MR, Ficz G, Oxley D, Krueger F, Reik W, Balasubramanian S. Quantitative sequencing of 5-methylcytosine and 5-hydroxymethylcytosine at single-base resolution. Science. 2012; 336(6083):934–937.

Bunz, F., et al., Requirement for p53 and p21 to sustain G2 arrest after DNA damage. Science, 1998; 282(5393): p. 1497-501.

Buschbeck M, Hake SB. Variants of core histones and their roles in cell fate decisions, development and cancer. Nat Rev Mol Cell Biol. 2017;18(5):299-314

Butler JS, Dent SY. The role of chromatin modifiers in normal and malignant hematopoiesis. Blood. 2013;121(16):3076-84.

Camacho L, Soignet S, Chanel S, et al. Leukocytosis and the retinoic acid syndrome in patients with acute promyelocytic leukemia treated with arsenic trioxide. J Clin Oncol.

2000 ;18(13):2620-5.

Carbone R, Botrugno OA, Ronzoni S, et al. Recruitment of the Histone Methyltransferase SUV39H1 and Its Role in the Oncogenic Properties of the Leukemia- Associated PML-Retinoic Acid Receptor Fusion Protein. Molecular and Cellular Biology. 2006; 26:1288–1296.

Castaigne S, Chomienne C, Daniel MT, et al. All-trans retinoic acid as a differentiation therapy for acute promyelocytic leukemia. I. Clinical results. Blood. 1990; 76:1704–1709.

Cayrol C, Knibiehler M, Ducommun B. p21 binding to PCNA causes G1 and G2 cell cycle
arrest in p53-deficient cells. Oncogene. 1998;16(3):311-20.

Cerutti H, Casas-Mollano JA. Histone H3 phosphorylation: universal code or lineage specifi c dialects? Epigenetics. 2009; 4(2):71–75

Cesaroni M, Cittaro D, Brozzi A, Pelicci PG, Luzi L. CARPET: a web-based package for the analysis of ChIP-chip and expression tiling data. Bioinformatics. 2008;24(24):2918-20.

Champagne KS, Kutateladze TG. Structural insight into histone recognition by the ING PHD fingers. Curr Drug Targets 2009; 10:432–441.

Chan TA, Hwang PM, Hermeking H, Kinzler KW, Vogelstein B. Cooperative effects of genes controlling the G (2)/M checkpoint. Genes Dev, 2000. 14(13): p. 1584-8.

Charrier-Savournin FB, Château MT, Gire V, Sedivy J, Piette J, Dulic V. p21-Mediated nuclear retention of cyclin B1-Cdk1 in response to genotoxic stress. Mol Biol Cell. 2004; 15(9): p. 3965-76.

Chen B, He L, Savell VH, Jenkins JJ, Parham DM. Inhibition of the interferon-g/signal transducers and activators of transcription (STAT) pathway by hypermethylation at a STAT-binding site in the p21WAF1 promoter region. Cancer Res. 2000; 60:3290–8.

Chen G, Shen Z, Wu F, et al. Pharmacokinetics and efficacy of low-dose all-trans retinoic acid in the treatment of acute promyelocytic leukemia. Leukemia. 1996;10(5):825-8.

Chen G, Shi X, Tang W, et al. Use of arsenic trioxide (As2O3) in the treatment of acute promyelocytic leukemia (APL): I. As2O3 exerts dose-dependent dual effects on APL cells. Blood. 1997 ;89(9):3345-53.

Chen Y, Yang Y, Wang F, Wan K, Yamane K, Zhang Y, Lei M. Crystal structure of human histone lysine-specific demethylase 1 (LSD1). Proc. Natl Acad. Sci. USA. 2006; 103, 13956–13961

Chen HZ, Tsai SY, Leone G. Emerging roles of E2Fs in cancer: an exit from cell cycle control. Nat. Rev. Cancer. 2009; 9, 785–797.

Cheng T, Rodrigues N, Shen H, Yang Y, Dombkowski D, Sykes M, Scadden DT. Hematopoietic stem cell quiescence maintained by p21cip1/waf1. Science. 2000; 287:1804-1808.

Cho HS, Suzuki T, Dohmae N, Hayami S, Unoki M, Yoshimatsu M et al. Demethylation of RB regulator MYPT1 by histone demethylase LSD1 promotes cell cycle progression in cancer cells. Cancer Res. 2011;71(3):655-60.

Choi BH, Kim CG, Bae YS, Lim Y, Lee YH, Shin SY. p21 Waf1/Cip1 expression by curcumin in U-87MG human glioma cells: role of early growth response-1 expression. Cancer Res. 2008; 68:1369–77.

Choi J, Jang H, Kim H, Kim ST, Cho EJ, Youn HD. Histone demethylase LSD1 is required to induce skeletal muscle differentiation by regulating myogenic factors. Biochem. Biophys. Res. Commun. 2010; 401(3), 327–332.

Clapier CR, Iwasa J, Cairns BR, Peterson CL. Mechanisms of action and regulation of ATP-dependent chromatin-remodelling complexes. Nat Rev Mol Cell Biol. 2017;18(7):407-422

Classon, M. & Harlow, E. The retinoblastoma tumour suppressor in development and cancer. Nat. Rev. Cancer. 2002; 2, 910–917.

Clayton AL, Rose S, Barratt MJ, Mahadevan LC. Phosphoacetylation of histone H3 on c-fos- and c-jun-associated nucleosomes upon gene activation. EMBO J. 2000; 19(14):3714–3726.

Cloos PA, Christensen J, Agger K, Helin K. Erasing the methyl mark: histone demethylases at the center of cellular differentiation and disease. Genes Dev. 2008;22(9):1115-40.

Cole AJ, Clifton-Bligh RJ, Marsh DJ. Ubiquitination and cancer: histone H2B monoubiquitination – roles to play in human malignancy. Endocr Relat Cancer. 2015 ;22(1): T19-33.

Copeland RA, Solomon ME and Richon VM. Protein methyltransferases as a target class for drug discovery. Nat Rev Drug Discov. 2009; 8(9):724-732.

Curtin JA, Fridlyand J, Kageshita T, Patel HN, Busam KJ, Kutzner H, et al. Distinct sets of genetic alterations in melanoma. The New England journal of medicine. 2005; 353, 2135-2147.

Cuthbert GL, Daujat S, Snowden AW, Erdjument-Bromage H, Hagiwara T, Yamada M, et al. Histone deimination antagonizes arginine methylation. Cell. 2004; 118:545–553.

Davie JR, Murphy LC. Level of ubiquitinated histone H2B in chromatin is coupled to ongoing transcription. Biochemistry. 1990; 29(20):4752–4757

Davies H, Bignell GR, Cox C, Stephens P, Edkins S, Clegg S et al.: Mutations of the BRAF gene in human cancer. Nature. 2002, 417: 949-954.

Dawson MA. The cancer epigenome: Concepts, challenges, and therapeutic opportunities. Science. 2017;355(6330):1147-1152.

de Thé H, Lavau C, Marchio A, Chomienne C, Degos L, Dejean A. The PML-RAR alpha fusion mRNA generated by the t (15;17) translocation in acute promyelocytic leukemia encodes a functionally altered RAR. Cell. 1991;66(4):675-84.

de Thé H, Le Bras M, Lallemand-Breitenbach V. The cell biology of disease: Acute promyelocytic leukemia, arsenic, and PML bodies. J Cell Biol. 2012;198(1):11-21

Dhall A, Wei S, Fierz B, Woodcock CL, Lee TH, Chatterjee C. Sumoylated human histone H4 prevents chromatin compaction by inhibiting long-range internucleosomal interactions. J Biol Chem. 2014;289(49):33827-37.

Di Lorenzo A and Bedford MT. Histone arginine methylation. FEBS Lett. 2011

585(13),2024-2031

Ding W, Li Y, Nobile L, et al. Leukemic cellular retinoic acid resistance and missense mutations in the PML-RARalpha fusion gene after relapse of acute promyelocytic leukemia from treatment with all-trans retinoic acid and intensive chemotherapy. Blood. 1998;92(4):1172-83.

Duan Z, Zarebski A, Montoya-Durango D, Grimes HL, Horwitz M. Gfi1 coordinates epigenetic repression of p21Cip/WAF1 by recruitment of histone lysine methyltransferase G9a and histone deacetylase 1. Mol Cell Biol 2005; 25:10338–51.

DuBridge RB, Tang P, Hsia HC, Leong PM, Miller JH, Calos MP. Analysis of mutation in human cells by using an Epstein-Barr virus shuttle system. Mol Cell Biol. 1987;7(1):379-87.

Duteil D, Metzger E, Willmann D, Karagianni P, Friedrichs N, Greschik H, et al. LSD1 promotes oxidative metabolism of white adipose tissue. Nat. Commun. 2014; 5, 4093.

Edmondson DE, Binda C and Mattevi A. Structural insights into the mechanism of amine oxidation by monoamine oxidases A and B. Arch Biochem Biophys. 2007; 464,269–276.

El-Deiry WS, Harper JW, O'Connor PM, et al. WAF1/ CIP1 is induced in p53-mediated G1 arrest and apoptosis. Cancer Res. 1994; 54:1169–74.

El-Deiry WS, Tokino T, Velculescu VE, et al. WAF1, a potential mediator of p53 tumor suppression. Cell. 1993; 75:817–25.

Estey, E. and H. Dohner. Acute myeloid leukaemia. Lancet. 2006; 368(9550): 1894-1907.

Fedorenko IV, Gibney GT, Sondak VK, Smalley KS: Beyond BRAF: where next for melanoma therapy? Br J Cancer. 2015, 112: 217-226.

Fenaux P, Wang ZZ, Degos L. Treatment of Acute Promyelocytic Leukemia by Retinoids. Current Topics in Microbiology and Immunology. 2007; 313:101–128.

Feng Q, Wang H, Ng HH, Erdjument-Bromage H, Tempst P, Struhl K, et al. Methylation of H3-lysine 79 is mediated by a new family of HMTases without a SET domain. Curr Biol 2002; 12:1052–1058.

Ferrari-Amorotti G, Fragliasso V, Esteki R, et al. Inhibiting interactions of lysine demethylase LSD1 with snail/slug blocks cancer cell invasion. Cancer Res. 2013; 73(1), 235–245.

Figueroa ME, Lugthart S, Li Y, et al. DNA methylation signatures identify biologically distinct subtypes in acute myeloid leukemia. Cancer cell. 2010;17(1):13-27.

Finn, L., S.N. Markovic, and R.W. Joseph, Therapy for metastatic melanoma: the past, present, and future. BMC Med. 2012. 10: p. 23.

Fiskus W, Sharma S, Shah B, Portier BP, Devaraj SGT, Liu K, et al. Highly effective combination of LSD1 (KDM1A) antagonist and pan-histone deacetylase inhibitor against human AML cells. Leukemia. 2014;28(11):2155-64.

Flaherty KT, Puzanov I, Kim KB, Ribas A, McArthur GA, Sosman JA et al.: Inhibition of mutated, activated BRAF in metastatic melanoma. N Engl J Med. 2010, 363: 809-819.

Flavahan WA, Gaskell E, Bernstein BE. Epigenetic plasticity and the hallmarks of cancer. Science. 2017;357(6348).

Forneris F, Binda C, Vanoni MA, Battaglioli E, Mattevi A. Human histone demethylase LSD1 reads the histone code. J Biol Chem. 2005; 280(50),41360–41365.

Foster CT, Dovey OM, Lezina L, et al. Lysine-specific demethylase 1 regulates the embryonic transcriptome and CoREST stability. Mol. Cell Biol. 2010; 30(20), 4851–4863.

Fraga MF, Ballestar E, Villar-Garea A, Boix-Chornet M, Espada J, Schotta G, et al. Loss of acetylation at Lys16 and trimethylation at Lys20 of histone H4 is a common hallmark of human cancer. Nat Genet. 2005; 37:391–400.

Gallagher RE. Retinoic acid resistance in acute promyelocytic leukemia. Leukemia. 2002 ;16(10):1940-58.

Gao WL, Liu HL. DOT1: a distinct class of histone lysine methyltransferase. Yi Chuan. 2007; 29(12):1449–1454.

Garcia-Bassets I, Kwon YS, Telese F, et al. Histone methylation-dependent mechanisms impose ligand dependency for gene activation by nuclear receptors. Cell. 2007; 128, 505–518.

Garraway LA, Widlund HR, Rubin MA, Getz G, Berger AJ, Ramaswamy S, et al. Integrative genomic analyses identify MITF as a lineage survival oncogene amplified in malignant melanoma. Nature. 2005. 436(7047): p. 117-22.

Gartel AL, Tyner AL. Transcriptional regulation of the p21((WAF1/CIP1)) gene. Exp Cell Res. 1999;246: 280–9.

Gartel, A.L., et al., Sp1 and Sp3 activate p21 (WAF1/CIP1) gene transcription in the Caco-2 colon adenocarcinoma cell line. Oncogene. 2000. 19(45): p. 5182-8.

Goel VK, Lazar AJ, Warneke CL, Redston MS, Haluska FG: Examination of mutations in BRAF, NRAS, and PTEN in primary cutaneous melanoma. J Invest Dermatol. 2006; 126: 154-160.

Goldberg AD, Allis CD, Bernstein E. Epigenetics: a landscape takes shape. Cell. 2007 ;128(4):635-8.

Graham, F. L., J. Smiley, W. C. Russell and R. Nairn. Characteristics of a human cell line transformed by DNA from human adenovirus type 5. J Gen Virol. 1977; 36(1): 59-74.

Gray-Schopfer, V.C., da Rocha Dias, S., and Marais, R. The role of B-RAF in melanoma. Cancer metastasis reviews. 2005; 24, 165-183.

Grignani F, De Metteis S, Nervi C, et al. Fusion proteins of the retinoic acid receptora recruit histone deacteylase in promyelocytic leukemia. Nature. 1998; 391:815-818.

Grignani F, Gelmetti V, Fanelli M, et al. Formation of PML/RARa high molecular weight complexes through the PML coiled-coil region is essential for the PML/RARamediated retinoic acid response. Oncogene. 1999; 18:6313-6321.

Grimwade D. The pathogenesis of acute promyelocytic leukaemia: evaluation of the role of molecular diagnosis and monitoring in the management of the disease. Br J Haematol. 1999;106(3):591-613.

Guidez F, Ivins S, Zhu J, et al. Reduced retinoic acid-sensitivities of nuclear receptor co-repressor binding to PML- and PLZF-RARa underlie molecular pathogenesis and treatment of acute promyelocytic leukemia. Blood. 1998; 91:2634-2642.

Hakimi MA, Bochar DA, Chenoweth J, Lane WS, Mandel G, Shiekhattar R. A core-

BRAF35 complex containing histone deacetylase mediates repression of neuronal-specific genes. Proc. Natl Acad. Sci. USA. 2002; 99(11), 7420–7425.

Hakimi, M.A., Dong, Y., Lane, W. S., Speicher, D. W., and Shiekhattar, R. A candidate X-linked mental retardation gene is a component of a new family of histone deacetylase-containing complexes. J. Biol. Chem. 2003; 278, 7234–7239.

Halkidou K, Gaughan L, Cook S, Leung HY, Neal DE, Robson CN. Upregulation and nuclear recruitment of HDAC1 in hormone refractory prostate cancer. Prostate. 2004 ;59(2):177-89.

Hamamoto R, Furukawa Y, Morita M, Iimura Y, Silva FP, Li M, et al. SMYD3 encodes a histone methyltransferase involved in the proliferation of cancer cells. Nat Cell Biol. 2004; 6(8):731–740.

Hamid O, Robert C, Daud A, Hodi FS, Hwu WJ, Kefford R, et al. Safety and tumor responses with lambrolizumab (anti-PD-1) in melanoma. N Engl J Med. 2013, 369: 134-144.

Hammond CM, Strømme CB, Huang H, Patel DJ, Groth A. Histone chaperone networks shaping chromatin function. Nat Rev Mol Cell Biol. 2017;18(3):141-158.

Harper, J.W., et al., The P21 Cdk-Interacting Protein Cip1 Is a Potent Inhibitor of G1 Cyclin-Dependent Kinases. Cell. 1993; 75(4): p. 805-816.

Harris WJ, Huang X, Lynch JT et al. The histone demethylase KDM1A sustains the oncogenic potential of MLL-AF9 leukemia stem cells. Cancer Cell. 2012; 21, 473–487.

Harris NL, Jaffe ES, Diebold J, Flandrin G, Muller-Hermelink HK, Vardiman J, et al. The World Health Organization classification of hematological malignancies report of the Clinical Advisory Committee Meeting, Airlie House, Virginia, November 1997. Mod Pathol. 2000; 13, 193-207.

Hausinger RP. FeII/alpha-ketoglutarate-dependent hydroxylases and related enzymes. Crit Rev Biochem Mol Biol. 2004; 39, 21–68.

Hayami S, Kelly JD, Cho HS, Yoshimatsu M, Unoki M, Tsunoda T, et al. Overexpression of LSD1 contributes to human carcinogenesis through chromatin regulation in various

cancers. Int J Cancer. 2011;128(3):574-86.

He LZ, Guidez F, Triboli C, et al. Distinct interactions of PML-RARa and PLZFRARa with co-repressors determine differential responses to RA in APL. Nature Genetics. 1998; 18:126-135.

He Y, Zhao Y, et al. LSD1 promotes S-phase entry and tumorigenesis via chromatin co-occupation with E2F1 and selective H3K9 demethylation. Oncogene. 2017.

Healy S, Khan P, He S, Davie JR. Histone H3 phosphorylation, immediate-early gene expression, and the nucleosomal response: a historical perspective. Biochem Cell Biol 2012; 90(1):39–54.

Henderson E, J M. Diagnosis, Classification and Assessment of Response to Treatment. In: Henderson E, Lister T, Greaves M, editors. Leukemia. 7 ed. Philadelphia London New York St. Louis Sydney Toronoto: Saunders; 2002. p. 739.

Hocker, T.L., M.K. Singh, and H. Tsao, Melanoma genetics and therapeutic approaches in the 21st century: moving from the benchside to the bedside. J Invest Dermatol, 2008. 128(11): p. 2575-95.

Højfeldt JW, Agger K, Helin K. Histone lysine demethylases as targets for anticancer therapy. Nat Rev Drug Discov. 2013; 12(12):917-30.

Hosseini A, Minucci S. A comprehensive review of lysine-specific demethylase 1 and its roles in cancer. Epigenomics. 2017;9(8):1123-1142.

Hou H and Yu H. Structural insights into histone lysine demethylation. Curr Opin Struct Biol. 2010; 20(6):739–748.

Howell PM Jr, Liu S, Ren S, Behlen C, Fodstad O, Riker AI. Epigenetics in human melanoma. Cancer Control. 2009;16(3):200-18.

Hu X, Li X, Valverde K et al. LSD1-mediated epigenetic modification is required for TAL1 function and hematopoiesis. Proc. Natl Acad. Sci. USA. 2009; 106(25), 10141–10146.

Huang J, Sengupta R, Espejo AB et al. p53 is regulated by the lysine demethylase LSD1. Nature. 2007; 449(7158), 105–108.

Huang ME, Ye YC, Chen SR, et al. Use of all-trans retinoic acid in the treatment of acute promyelocytic leukemia. Blood. 1988; 72:567–572.

Huang Y, Greene E, Murray Stewart T, Goodwin AC, Baylin SB, et al. Inhibition of lysine-specific demethylase 1 by polyamine analogues results in reexpression of aberrantly silenced genes. Proc. Natl. Acad. Sci. U. S. A. 2007; 104, 8023–8028.

Huang Z, Li S, Song W, Li X, Li Q, Zhang Z, et al. Lysine-Specific Demethylase 1 (LSD1/KDM1A) Contributes to Colorectal Tumorigenesis via Activation of the Wnt/B-Catenin Pathway by Down-Regulating Dickkopf-1 (DKK1). PLoS ONE. 2013; 8, e70077.

Hussussian CJ, Struewing JP, Goldstein AM, Higgins PA, Ally DS, Sheahan MD, et al. Germline p16 mutations in familial melanoma. Nature genetics. 1994; 8, 15-21.

Ishikawa Y, Gamo K1, Yabuki M et al. A novel LSD1 inhibitor T-3775440 disrupts GFI1B-containing complex leading to transdifferentiation and impaired growth of AML cells. Mol. Cancer Ther. 2017; 16(2), 273–284.

Ito K, Nakazato T, Yamato K, Miyakawa Y, Yamada T, Hozumi N, et al. Induction of apoptosis in leukemic cells by homovanillic acid derivative, capsaicin, through oxidative stress: implication of phosphorylation of p53 at Ser-15 residue by reactive oxygen species. Cancer Res. 2004;64(3):1071-8.

Jablonka, E., and Lamb, M. J. The changing concept of epigenetics. Ann N Y Acad Sci. 2002;981, 82-96.

Jaffe ES, Harris NL, Stein H, Vardiman, JW, eds. World Health Organization Classification of Tumours. Pathology and Genetics of Tumours of Haematopoietic and Lymphoid Tissues (Lyon, IARC Press). 2001

Jin L, Hanigan CL, Wu Y, Wang W, Park BH, Woster PM, Casero RA. Loss of LSD1 (lysine-specific demethylase 1) suppresses growth and alters gene expression of human colon cancer cells in a p53 and DNMT1(DNA methyltransferase 1)-independent manner. Biochem. J. 2013; 449, 459–468.

Jones PA, Takai D. The role of DNA methylation in mammalian epigenetics. Science 2001; 293(5532):1068–70.

Jones PA. et al. A blueprint for a Human Epigenome Project: the AACR Human Epigenome Workshop. Cancer Res. 2005; 65, 11241-11246.

Kakizuka A, Miller WJ, Umesono K, et al. Chromosomal translocation t (15;17) in human acute promyelocytic leukemia fuses RAR alpha with a novel putative transcription factor, PML. Cell. 1991;66(4):663-74.

Kamashev D, Vitoux D, De Thé H. PML-RARA-RXR oligomers mediate retinoid and rexinoid/cAMP cross-talk in acute promyelocytic leukemia cell differentiation. J Exp Med. 2004 ;199(8):1163-74.

Kashyap V1, Ahmad S, Nilsson EM, Helczynski L, Kenna S, Persson JL, et al. The lysine specific demethylase-1 (LSD1/KDM1A) regulates VEGF-A expression in prostate cancer. Mol. Oncol. 2013; 7, 555– 566.

Khan P, Drobic B, Perez-Cadahia B, Healy S, He S, Davie JR. Mitogen- and stress-activated protein kinases 1 and 2 are required for maximal trefoil factor 1 induction. PLoS One. 2013; 8(5): e63189.

Kim J, Singh AK, Takata Y et al. LSD1 is essential for oocyte meiotic progression by regulating CDC25B expression in mice. Nat. Commun. 2015; 6, 10116.

Kitagawa, M. et al. The consensus motif for phosphorylation by cyclin D1-Cdk4 is different from that for phosphorylation by cyclin A/E-Cdk2. EMBO J. 2015; 15, 7060– 7069.

Kitaura, H., et al., Reciprocal regulation via protein-protein interaction between c-Myc and p21(cip1/waf1/sdi1) in DNA replication and transcription. J Biol Chem, 2000. 275(14): p. 10477-83.

Kizaki M, Matsushita H, Takayama N, Muto A, Ueno H, Awaya N, et al. Establishment and characterization of a novel acute promyelocytic leukemia cell line (UF1) with retinoic acid-resistant features. Blood 1996; 88:1824-1833.

Klose RJ, Bird AP. Genomic DNA methylation: the mark and its mediators. Trends Biochem Sci. 2006;31(2):89-97.

Klose RJ, Zhang Y. Regulation of histone methylation by demethylimination and

demethylation. Nat Rev Mol Cell Biol 2007; 8:307–318.

Kontaki H, Talianidis I. Lysine methylation regulates E2F1- induced cell death. Mol. Cell. 2010; 39(1), 152–160.

Kooistra SM, Helin K. Molecular mechanisms and potential functions of histone demethylases. Nature Rev Mol Cell Biol. 2012; 13, 297–311.

Kornberg RD, Lorch Y. Twenty-five years of the nucleosome, fundamental particle of the eukaryote chromosome. Cell 1999; 98:285–294.

Kornerber RD. Chromatin structure: A repeating unit of histones and DNA. Science 1974; 184:868–871.

Kouzarides, T. Chromatin modifications and their function. Cell. 2007; 128(4): 693-705.

Krejci O, Wunderlich M, Geiger H, Chou FS, Schleimer D, Jansen M, et al. p53 signaling in response to increased DNA damage sensitizes AML1-ETO cells to stress-induced death. Blood. 2008;111(4):2190-9.

Krishnan S, Horowitz S, Trievel RC. Structure and function of histone H3 lysine 9 methyltransferases and demethylases. Chembiochem. 2011; 12(2):254–263.

Krivtsov AV, Armstrong SA. MLL translocations, histone modifi cations and leukaemia stem-cell development. Nat Rev Cancer. 2007; 7(11):823–833.

Krug AW1, Tille E, Sun B, Pojoga L, Williams J, Chamarthi B, et al. Lysine-specific demethylase-1 modifies the age effect on blood pressure sensitivity to dietary salt intake. Age Dordr. Neth. 2013; 35, 1809–1820.

Lai WKM, Pugh BF. Understanding nucleosome dynamics and their links to gene expression and DNA replication. Nat Rev Mol Cell Biol. 2017; 24

Lamouille S, Xu J, Derynck R. Molecular mechanisms of epithelial–mesenchymal transition. Nat. Rev. Mol. Cell Biol. 2014; 15, 178–196.

Lan W, Zhang D, Jiang J. The roles of LSD1-mediated epigenetic modifications in maintaining the pluripotency of bladder cancer stem cells. Med. Hypotheses. 2013; 81, 823–825.

Langmead B, Trapnell C, Pop M, Salzberg SL. Ultrafast and memory-efficient alignment of short DNA sequences to the human genome. Genome Biol. 2009;10(3): R25

Lanotte M, Martin-Thouvenin V, Najman S, Balerini P, Valensi F, Berger R. NB4, a maturation inducible cell line with t(15;17) marker isolated from a human acute promyelocytic leukemia (M3). Blood. 1991;77(5):1080-6.

Lee MG, Wynder C, Bochar DA, Hakimi MA, Cooch N, Shiekhattar R. Functional interplay between histone demethylase and deacetylase enzymes. Mol Cell Biol. 2006;26(17):6395-402.

Lee MG, Wynder C, Schmidt DM, McCafferty DG, Shiekhattar R. Histone H3 lysine 4 demethylation is a target of nonselective antidepressive medications. Chem Biol. 2006 ;13(6):563-7.

Lee MG, Wynder C, Cooch N, Shiekhattar R. An essential role for CoREST in nucleosomal histone 3 lysine 4 demethylation. Nature. 2005; 437, 432–435.

Li Y et al. The target of the NSD family of histone lysine methyltransferases depends on the nature of the substrate. J Biol Chem. 2009; 284(49):34283–34295.

Li, D.W., et al., P150(Sal2) is a p53-independent regulator of p21WAF1/CIP. Molecular and Cellular Biology, 2004. 24(9): p. 3885-3893.

Lim S, Janzer A, Becker A, et al. Lysine-specific demethylase 1 (LSD1) is highly expressed in ER-negative breast cancers and a biomarker predicting aggressive biology. Carcinogenesis. 2010; 31(3), 512–520.

Lim S, Kaldis P. Cdks, cyclins and CKIs: roles beyond cell cycle regulation. Development. 2013;140(15):3079-93.

Lin RJ, Nagy L, Inoue S, et al. Role of the histone deacetylase complex in acute promyelocytic leukemia. Nature. 1998; 391:811-814.

Lin Y, Wu Y, Li J et al. The SNAG domain of Snail1 functions as a molecular hook for recruiting lysine-specific demethylase. EMBO J. 2010; 29(11), 1803–1816.

Liyanage VR, Rastegar M. Rett syndrome and MeCP2. Neuromolecular Med. 2014 ;16(2):231-64

Lo Coco F, Diverio D, Falini B, Biondi A, Nervi C, Pelicci P. Genetic diagnosis and molecular monitoring in the management of acute promyelocytic leukemia. Blood. 1999 ;94(1):12-22.

Lo-Coco F, Ammatuna E. The biology of acute promyelocytic leukemia and its impact on diagnosis and treatment. Hematology Am Soc Hematol Educ Program. 2006:156-61, 514.

Lokken AA, Zeleznik-Le NJ. Breaking the LSD1/KDM1A addiction: therapeutic targeting of the epigenetic modifier in AML. Cancer Cell. 2012;21(4):451-3.

Luger K, Mader AW, Richmond RK, Sargent DF, Richmond TJ. Crystal structure of the nucleosome core particle at 2.8 A resolution. Nature 1997; 389:251–260.

Lundberg, A. S. & Weinberg, R. A. Functional inactivation of the retinoblastoma protein requires sequential modification by at least two distinct cyclin-cdk complexes. Mol. Cell Biol. 1998; 18, 753–761.

Maresca TJ, Freedman BS, Heald R. Histone H1 is essential for mitotic chromosome architecture and segregation in Xenopus laevis egg extracts. J Cell Biol 2005; 169:859–869

Maresca TJ, Heald R. The long and the short of it: linker histone H1 is required for metaphase chromosome compaction. Cell Cycle 2006; 5:589–591

Margueron R et al. Ezh1 and Ezh2 maintain repressive chromatin through different mechanisms. Mol Cell. 2008; 32(4):503–518.

Martens JH, Brinkman AB, Simmer F, et al. PML-RARalpha/RXR Alters the Epigenetic Landscape in Acute Promyelocytic Leukemia. Cancer cell. 2010;17(2):173- 85.

Martin C and Zhang Y. The diverse functions of histone lysine methylation. Nat   Rev Mol Cell Biol. 2005; 6,838–849.

Matthews GM, Mehdipour P, Cluse LA, Falkenberg KJ, Wang E, Roth M, et al. Functional-genetic dissection of HDAC dependencies in mouse lymphoid and myeloid malignancies. Blood. 2015;126(21):2392-403.

Maurer-Stroh S, Dickens NJ, Hughes-Davies L, Kouzarides T, Eisenhaber F, Ponting CP. The Tudor domain 'Royal Family': Tudor, plant Agenet, Chromo, PWWP and MBT

domains. Trends Biochem Sci 2003; 28:69–74.

McDonough MA. Structural studies on human 2-oxoglutarate dependent oxygenases. Curr Opin Struct Biol. 2010; 20,659–672.

McGrath JP, Williamson KE, Balasubramanian S et al. Pharmacological inhibition of the histone lysine demethylase KDM1A suppresses the growth of multiple acute myeloid leukemia subtypes. Cancer Res. 2016; 76(7), 1975–1988.

Mehdipour P, Santoro F, Botrugno OA, Romanenghi M, Pagliuca C, Matthews GM, et al. HDAC3 activity is required for initiation of leukemogenesis in acute promyelocytic leukemia. Leukemia. 2017; 31(4):995-997.

Mellen M, Ayata P, Dewell S, Kriaucionis S, Heintz N. MeCP2 binds to 5hmC enriched within active genes and accessible chromatin in the nervous system. Cell. 2012; 151(7):1417–1430.

Mendenhall EM, Williamson KE, Reyon D, Zou JY, Ram O, Joung JK, Bernstein BE. Locus-specific editing of histone modifications at endogenous enhancers. Nat Biotechnol. 2013;31(12):1133-6.

Meng F, Sun G, Zhong M, Yu Y, Brewer MA. Inhibition of DNA methyltransferases, histone deacetylases and lysine-specific demethylase-1 suppresses the tumorigenicity of the ovarian cancer ascites cell line SKOV3. Int J Oncol. 2013;43(2):495-502.

Messner S, Hottiger MO. Histone ADP-ribosylation in DNA repair, replication and transcription. Trends Cell Biol. 2011; 21(9):534–542.

Metzger E, Wissmann M, Yin N, Müller JM, Schneider R, Peters AH, et al. LSD1 demethylates repressive histone marks to promote androgen-receptor-dependent transcription. Nature 2005; 437:436–439.

Miller AJ, Mihm MC Jr. Melanoma. N Engl J Med. 2006;355(1):51-65.

Minucci S, Monestiroli S, Giavara S, Ronzoni S, Marchesi F, Insinga A, et al. PMLRAR induces promyelocytic leukemias with high efficiency following retroviral gene transfer into purified murine hematopoietic progenitors. Blood. 2002;100(8):2989-2995.

Miura S, Maesawa C, Shibazaki M, Yasuhira S, Kasai S, Tsunoda K, et al.

Immunohistochemistry for histone h3 lysine 9 methyltransferase and demethylase proteins in human melanomas. Am J Dermatopathol. 2014;36(3):211-6.

Mohammad HP, Smitheman KN, Kamat CD et al. A DNA hypomethylation signature predicts antitumor activity of LSD1 inhibitors in SCLC. Cancer Cell. 2015; 28(1), 57–69.

Mori, K., et al., A HIC-5- and KLF4-dependent mechanism transactivates p21(Cip1) in response to anchorage loss. J Biol Chem, 2012. 287(46): p. 38854-65.

Mosammaparast N, Shi Y. Reversal of histone methylation: biochemical and molecular mechanisms of histone demethylases. Annu Rev Biochem. 2010; 79:155–179

Moustakas, A. and D. Kardassis, Regulation of the human p21/WAF1/Cip1 promoter in hepatic cells by functional interactions between Sp1 and Smad family members. Proceedings of the National Academy of Sciences of the United States of America, 1998. 95(12): p. 6733-6738.

Mrozek, K., Heinonen, K., de la Chapelle, A., and Bloomfield, C. D. Clinical significance of cytogenetics in acute myeloid leukemia. Semin Oncol. 1997; 24, 17-31.

Mujtaba S, Zeng L, Zhou MM. Structure and acetyl-lysine recognition of the bromodomain. Oncogene 2007; 26:5521–5527.

Murr R. Interplay between different epigenetic modifications and mechanisms. Adv Genet 2010; 70:101–141.

Murray-Stewart T, Woster PM, Casero RA Jr. The re-expression of the epigenetically silenced e-cadherin gene by a polyamine analogue lysine-specific demethylase-1 (LSD1) inhibitor in human acute myeloid leukemia cell lines. Amino Acids. 2014 ;46(3):585-94.

Musri MM, Carmona MC, Hanzu FA, Kaliman P, Gomis R, Párrizas M. Histone demethylase LSD1 regulates adipogenesis. J. Biol. Chem. 2010; 285(39), 30034–30041.

Musselman CA, Lalonde ME, Cote J, Kutateladze TG Perceiving the epigenetic landscape through histone readers. Nat Struct Mol Biol. 2012; 19:1218–1227

Nair SS, Nair BC, Cortez V et al. PELP1 is a reader of histone H3 methylation that facilitates oestrogen receptoralpha target gene activation by regulating lysine demethylase 1 specificity. EMBO Rep. 2010; 11, 438–444.

Nair VD, Ge Y, Balasubramaniyan N, Kim J, Okawa Y, Chikina M, Troyanskaya O, Sealfon SC. Involvement of histone demethylase LSD1 in short-time-scale gene expression changes during cell cycle progression in embryonic stem cells. Mol Cell Biol. 2012;32(23):4861-76

Nakamura, T., Mori, T., Tada, S., Krajewski, W., Rozovskaia, T., Wassell, R., Dubois, G., Mazo, A., Croce, C. M., and Canaani, E. ALL-1 is a histone methyltransferase that assembles a supercomplex of proteins involved in transcriptional regulation. Mol. Cell. 2002; 10, 1119–1128.

Nervi C, Ferrara F, Fanelli M, et al. Caspases mediate retinoic acid-induced degradation of the acute promyelocytic leukemia PML/RARalpha fusion protein. Blood. 1998 ;92(7):2244-51.

Nian H, Delage B, Pinto JT, Dashwood RH. Allyl mercaptan, a garlic-derived organosulfur compound, inhibits histone deacetylase and enhances Sp3 binding on the P21WAF1 promoter. Carcinogenesis. 2008;29: 1816–24.

Niu C, Yan H, Yu T, et al. Studies on treatment of acute promyelocytic leukemia with arsenic trioxide: remission induction, follow-up, and molecular monitoring in 11 newly diagnosed and 47 relapsed acute promyelocytic leukemia patients. Blood. 1999 Nov;94(10):3315-24.

Okano M, Xie S, Li E Cloning and characterization of a family of novel mammalian DNA (cytosine-5) methyltransferases. Nat Genet. 1998; 19(3):219–20.

Oudet P, Gross-Bellard M, Chambon P. Electron microscopic and biochemical evidence that chromatin structure is a repeating unit. Cell. 1975; 4:281–300.

Ouyang, H., Qin, Y., Liu, Y., Xie, Y., and Liu, J. Prox1 directly interacts with LSD1 and recruits the LSD1/NuRD complex to epigenetically co-repress CYP7A1 transcription. PloS One. 2013; 8, e62192.

Palathinkal DM, Sharma TR, Koon HB, Bordeaux JS: Current systemic therapies for melanoma. Dermatol Surg. 2014, 40: 948-963.

Pan, D., Mao, C., and Wang, Y.X. Suppression of Gluconeogenic Gene Expression by LSD1-Mediated Histone Demethylation. PLoS ONE. 2013; 8, e66294.

Pappano WN, et al. The Histone Methyltransferase Inhibitor A-366 Uncovers a Role for G9a/GLP in the Epigenetics of Leukemia. PLoS One. 2015; 10(7): e0131716.

Patel DJ, Wang Z Readout of epigenetic modifications. Annu Rev Biochem 2013; 82:81–118.

Pear WS, Nolan GP, Scott ML, Baltimore D. Production of high-titer helper-free retroviruses by transient transfection. Proc Natl Acad Sci U S A. 1993; 90(18): 8392-8396.

Peng B, Shi R, Jiang W, Ding YH, Dong MQ, Zhu WG, Xu X. Phosphorylation of LSD1 by PLK1 promotes its chromatin release during mitosis. Cell Biosci. 2017; 7:15.

Perez-Cadahia B, Drobic B, Khan P, Shivashankar CC, Davie JR. Current understanding and importance of histone phosphorylation in regulating chromatin biology. Curr Opin Drug Discov Devel. 2010; 13(5):613–622

Perillo B, Ombra MN, Bertoni A, Cuozzo C, Sacchetti S, Sasso A, at al. DNA oxidation as triggered by H3K9me2 demethylation drives estrogen-induced gene expression. Science. 2008; 319, 202–206.

Qin Y, Zhu W, Xu W et al. LSD1 sustains pancreatic cancer growth via maintaining HIF1alpha-dependent glycolytic process. Cancer Lett. 2014; 347, 225–232.

Racanicchi S, Maccherani C, Liberatore C, et al. Targeting fusion protein/corepressor contact restores differentiation response in leukemia cells. EMBO J. 2005;24(6):1232-42.

Ray Chaudhuri A, Nussenzweig A. The multifaceted roles of PARP1 in DNA repair and chromatin remodelling. Nat Rev Mol Cell Biol. 2017; 5

Richon VM et al. chemogenetic analysis of human protein methyltransferases. Chem Biol Drug Des. 2011; 78(2),199-210.

Robinson PJ, Fairall L, Huynh VA, Rhodes D. EM measurements define the dimensions of the ''30-nm'' chromatin fiber: evidence for a compact, interdigitated structure. Proc Natl Acad Sci USA 2006; 103:6506-6511.

Rodriguez-Paredes M, et al. Gene amplification of the histone methyltransferase SETDB1 contributes to human lung tumorigenesis. Oncogene. 2014; 33(21):2807-13.

Roesch A, M Fukunaga-Kalabis, EC Schmidt, SE Zabierowski, PA Brafford, A Vultur, D Basu, P Gimotty, T Vogt and M Herlyn. A temporarily distinct subpopulation of slow-cycling melanoma cells is required for continuous tumor growth. Cell. 2010; 141:583-594.

Roman-Gomez J, Castillejo JA, Jimenez A, et al. 5' CpG island hypermethylation is associated with transcriptional silencing of the p21(CIP1/WAF1/SDI1) gene and confers poor prognosis in acute lymphoblastic leukemia. Blood 2002; 99:2291–6.

Rotili D and Mai A. Targeting histone demethylases: A new avenue for the fight against cancer. GenesCancer. 2011; 2(6):663–679.

Rotili, D., Tomassi, S., Conte, M., Benedetti, R., Tortorici, M., Ciossani, G., et al. Pan-Histone Demethylase Inhibitors Simultaneously Targeting Jumonji C and Lysine-Specific Demethylases Display High Anticancer Activities. J. Med. Chem. 2014; 57, 42–55.

Rouleau M, Patel A, Hendzel MJ, Kaufmann SH, Poirier GG. PARP inhibition: PARP1 and beyond. Nat Rev Cancer. 2010; 10(4):293–301.

Ruthenburg AJ, Allis CD, Wysocka J. Methylation of lysine 4 on histone H3: intricacy of writing and reading a single epigenetic mark. Mol Cell. 2007;25(1):15-30.

S. Saeed, C. Logie, H. G. Stunnenberg, J. H. Martens, Genome-wide functions of PML-RARalpha in acute promyelocytic leukaemia. British journal of cancer. 2011; 104, 554.

Sakabe, K., Wang, Z., and Hart, G. W. Beta-N-acetylglucosamine (O-GlcNAc) is part of the histone code. Proc. Natl. Acad. Sci. U. S. A. 2010; 107, 19915–19920.

Sakamoto A, Hino S, Nagaoka K, et al. Lysine demethylase LSD1 coordinates glycolytic and mitochondrial metabolism in hepatocellular carcinoma cells. Cancer Res. 2015; 75, 1445–1456.

Sanz MA. Treatment of Acute Promyelocytic Leukemia. Hematology. 2006; 1:147- 155.

Sawicka A, Seiser C. Histone H3 phosphorylation – a versatile chromatin modifi cation for different occasions. Biochimie. 2012; 94(11):2193–2201.

Schenk T, Chen WC, Göllner S, et al. Inhibition of the LSD1 (KDM1A) demethylase reactivates the all-trans-retinoic acid differentiation pathway in acute myeloid leukemia. Nat. Med. 2012; 18, 605–611.

Schmidt DM, McCafferty DG. trans-2-Phenylcyclopropylamine is a mechanism-based inactivator of the histone demethylase LSD1. Biochemistry. 2007;46(14):4408-16

Shen Z, Shi Z, Fang J, et al. All-trans retinoic acid/As2O3 combination yields a high quality remission and survival in newly diagnosed acute promyelocytic leukemia. Proc Natl Acad Sci U S A. 2004;101(15):5328-35.

Shi Y, Lan F, Matson C, Mulligan P, Whetstine JR, Cole PA, Casero RA, Shi Y. Histone demethylation mediated by the nuclear amine oxidase homolog LSD1. Cell. 2004 119, 941-953.

Shi YJ, Matson C, Lan F, Iwase S, Baba T, Shi Y. Regulation of LSD1 histone demethylase activity by its associated factors. Mol. Cell. 2005 19, 857–864.

Shiio Y, Eisenman RN. Histone sumoylation is associated with transcriptional repression. Proc Natl Acad Sci U S A. 2003; 100(23):13225–13230.

Shin, S.Y., et al., The ETS family transcription factor ELK-1 regulates induction of the cell cycle-regulatory gene p21(Waf1/Cip1) and the BAX gene in sodium arsenite-exposed human keratinocyte HaCaT cells. J Biol Chem, 2011. 286(30): p. 26860-72.

Shogren-Knaak M, Ishii H, Sun JM, Pazin MJ, Davie JR, Peterson CL. Histone H4-K16 acetylation controls chromatin structure and protein interactions. Science. 2006 ;311(5762):844-7.

Siegel R, Naishadham D, Jemal A: Cancer statistics, 2013. CA Cancer J Clin. 2013, 63: 11-30.

Sims RJ and Reinberg D. Histone H3 Lys 4 methylation: caught in a bind? Genes Dev. 2006; 20(20):2779–2786.

Soignet S, Frankel S, Douer D, et al. United States multicenter study of arsenic trioxide in relapsed acute promyelocytic leukemia. J Clin Oncol. 2001;19(18):3852-60.

Soignet SL. Clinical Experience of Arsenic Trioxide in Relapsed Acute Promyelocytic Leukemia. The Oncologist. 2001;6(suppl2):11-16.

Somervaille TC, Cleary ML. Identification and characterization of leukemia stem cells in murine MLL-AF9 acute myeloid leukemia. Cancer Cell. 2006; 10, 257–268.

Somervaille TC, Matheny CJ, Spencer GJ et al. Hierarchical maintenance of MLL myeloid leukemia stem cells employs a transcriptional program shared with embryonic rather than adult stem cells. Cell Stem Cell. 2009; 4, 129–140.

Sosman JA, Kim KB, Schuchter L, Gonzalez R, Pavlick AC, Weber JS et al.: Survival in BRAF V600- mutant advanced melanoma treated with vemurafenib. N Engl J Med 2012, 366: 707-714.

Stavropoulos P, Blobel G and Hoelz A. Crystal structure and mechanism of human lysine-specific demethylase-1. Nat Struct Mol Biol. 2006; 13:626–632.

Sugino N, Kawahara M, Tatsumi G et al. A novel LSD1 inhibitor NCD38 ameliorates MDS-related leukemia with complex karyotype by attenuating leukemia programs via activating super-enhancers. Leukemia. 2017 ;31(11):2303-2314.

Sun Y, et al. Histone methyltransferase SETDB1 is required for prostate cancer cell proliferation, migration and invasion. Asian J Androl. 2014; 16(2):319-24.

Tachiwana H, Kagawa W, Shiga T, Osakabe A, Miya Y, Saito K, Hayashi-Takanaka Y, Oda T, Sato M, Park S-Y, Kimura H, Kurumizaka H Crystal structure of the human centromeric nucleosome containing CENP-A. Nature. 2011; 476:232–235

Tallman MS, Andersen JW, Schiffer CA, et al. All-trans-retinoic acid in acute promyelocytic leukemia. New England Journal of Medicine. 1997; 337:1021-1028.

Tallman MS. Treatment of relapsed or refractory acute promyelocytic leukemia. Best Practice & Research Clinical Haematology. 2007; 20:57-65.

Tan X et al. SmyD1, a histone methyltransferase, is required for myofi bril organization and muscle contraction in zebrafi sh embryos. Proc Natl Acad Sci USA. 2006; 103(8):2713–2718.

Tao H, et al. Histone methyltransferase G9a and H3K9 dimethylation inhibit the self-renewal of glioma cancer stem cells. Mol Cell Biochem. 2014; 394(1-2):23-30.

Taverna SD, Li H, Ruthenburg AJ, Allis CD, Patel DJ. How chromatin-binding modules interpret histone modifications: lessons from professional pocket pickers. Nat Struct Mol Biol. 2007; 11:1025–1040.

Thiagalingam S, Cheng KH, Lee HJ, Mineva N, Thiagalingam A, Ponte JF. Histone deacetylases: unique players in shaping the epigenetic histone code. Ann N Y Acad Sci. 2003; 983:84–100.

Toffolo E, Rusconi F, Paganini L, Tortorici M, Pilotto S, Heise C, et al. Phosphorylation of neuronal Lysine-Specific Demethylase 1LSD1/KDM1A impairs transcriptional repression by regulating interaction with CoREST and histone deacetylases HDAC1/2. J Neurochem. 2014;128(5):603-16

Tonna, S., El-Osta, A., Cooper, M. E., and Tikellis, C. Metabolic memory and diabetic nephropathy: potential role for epigenetic mechanisms. Nat. Rev. Nephrol. 2010; 6, 332–341.

Trapnell C, Williams BA, Pertea G, Mortazavi A, Kwan G, van Baren MJ et al. Transcript assembly and quantification by RNA-Seq reveals unannotated transcripts and isoform switching during cell differentiation. Nat Biotechnol. 2010;28(5):511-5

Tuck-Muller CM1, Narayan A, Tsien F, Smeets DF, Sawyer J, Fiala ES, et al. DNA hypomethylation and unusual chromosome instability in cell lines from ICF syndrome patients. Cytogenet Cell Genet. 2000;89(1-2):121-8.

Ueda, R., Suzuki, T., Mino, K., Tsumoto, H., Nakagawa, H., Hasegawa, M., Sasaki, R., Mizukami, T., and Miyata, N. Identification of cell-active lysine specific demethylase 1-selective inhibitors. J. Am. Chem. Soc. 2009; 131, 17536–17537.

Unnikrishnan D, Dutcher J, Varshneya N, et al. Torsades de pointes in 3 patients with leukemia treated with arsenic trioxide. Blood. 2001;97(5):1514-6.

Upadhyay, G., Chowdhury, A. H., Vaidyanathan, B., Kim, D., and Saleque, S. Antagonistic actions of Rcor proteins regulate LSD1 activity and cellular differentiation. Proc. Natl. Acad. Sci. U. S. A. 2014; 111, 8071–8076.

Vakoc CR, Mandat SA, Olenchock BA, Blobel GA. Histone H3 lysine 9 methylation and HP1gamma are associated with transcription elongation through mammalian chromatin. Mol Cell. 2005;19(3):381-91.

Valk-Lingbeek ME, Bruggeman SW, van Lohuizen M. Stem cells and cancer; the polycomb connection. Cell. 2004;118(4):409-18.

Vankayalapati H, Sorna V, Warner SL et al. WO2014205213A1 (2014).

Vardiman, J. W., Harris, N. L., and Brunning, R. D. The World Health Organization (WHO) classification of the myeloid neoplasms. Blood. 2002; 100, 2292- 2302.

Vasilatos, S. N., Katz, T. A., Oesterreich, S., Wan, Y., Davidson, N. E., and Huang, Y. Crosstalk between lysine-specific demethylase 1 (LSD1) and histone deacetylases mediates antineoplastic efficacy of HDAC inhibitors in human breast cancer cells. Carcinogenesis. 2013; 34, 1196–1207.

Vermeulen M, Eberl HC, Matarese F, Marks H, Denissov S, Butter F, et al. Quantitative interaction proteomics and genome-wide profiling of epigenetic histone marks and their readers. Cell 2010; 142:967–980.

Viale A, De Franco F, et al. Cell-cycle restriction limits DNA damage and maintains self-renewal of leukemia stem cells. Nature. 2009 ;457(7225):51-6.

Villa R, Morey L, Raker V, et al. The methyl-CpG binding protein MBD1 is required for PML-RARalpha function. Proc Natl Acad Sci U S A. 2006;103(5):1400-5.

Villa R, Pasini D, Gutierrez A, et al. Role of the polycomb repressive complex 2 in acute promyelocytic leukemia. Cancer Cell. 2007; 11:513-525.

Wang GG et al. NUP98-NSD1 links H3K36 methylation to Hox-A gene activation and leukaemogenesis. Nat Cell Biol. 2007; 9(7):804–812.

Wang J, Hevi S, Kurash JK et al. The lysine demethylase LSD1 is required for maintenance of global DNA methylation. Nat. Genet. 2009; 41(1), 125–129.

Wang J, Scully K, Zhu X, et al. Opposing LSD1 complexes function in developmental gene activation and repression programmes. Nature. 2007; 446(7138), 882–887.

Wang J, Telese F, Tan Y et al. LSD1n is an H4K20 demethylase regulating memory formation via transcriptional elongation control. Nat. Neurosci. 2015; 18(9), 1256–1264.

Wang K, Wang P, Shi J, et al. PML/RARalpha targets promoter regions containing PU.1 consensus and RARE half sites in acute promyelocytic leukemia. Cancer cell. 2010;17(2):186-97.

Wang LG, Liu XM, Fang Y, et al. De-repression of the p21 promoter in prostate cancer cells by an isothiocyanate via inhibition of HDACs and c-Myc. Int J Oncol 2008;33:375–80.

Wang Y, et al. Human PAD4 regulates histone arginine methylation levels via demethylimination. Science. 2004; 306, 279–283

Warrell RJ, de Thé H, Wang Z, Degos L. Acute promyelocytic leukemia. N Engl J Med. 1993;329(3):177-89.

Warrell RP, Frankel SR, Miller MH, et al. Differentiation therapy of acute promyelocytic leukemia with tretinoin (all-trans-retinoic acid). New England Journal of Medicine. 1991;324(1385-1393).

Weber M, Hellmann I, Stadler MB, Ramos L, Pääbo S, Rebhan M, Schübeler D. Distribution, silencing potential and evolutionary impact of promoter DNA methylation in the human genome. Nat Genet. 2007;39(4):457-66.

Wissmann M, Yin N, Müller JM, Greschik H, Fodor BD, Jenuwein T, et al. Cooperative demethylation by JMJD2C and LSD1 promotes androgen receptor-dependent gene expression. Nat. Cell Biol. 2007; 9, 347–353.

Woodman, S.E., et al., New strategies in melanoma: molecular testing in advanced disease. Clin Cancer Res, 2012. 18(5): p. 1195-200.

Wright DE, Wang CY, Kao CF. Histone ubiquitylation and chromatin dynamics. Front Biosci (Landmark Ed) 2012; 17:1051–1078

Wysocka J, Swigut T, Xiao H, Milne TA, Kwon SY, Landry J, et al. A PHD finger of NURF couples histone H3 lysine 4 trimethylation with chromatin remodelling. Nature 2006; 442:86–90.

Xie, W., et al., MDA468 growth inhibition by EGF is associated with the induction of the cyclin-dependent kinase inhibitor p21WAF1. Anticancer Res. 1997; 17(4A): p. 2627-33.

Xu, G., Xiao, Y., Hu, J., Xing, L., Zhao, O., and Wu, Y. The combined effect of retinoic acid and LSD1 siRNA inhibition on cell death in the human neuroblastoma cell line SH--SY5Y. Cell. Physiol. Biochem. Int. J. Exp. Cell. Physiol. Biochem. Pharmacol. 2013; 31,

854–862.

Yang J, Huang J, Dasgupta M, et al. Reversible methylation of promoter-bound STAT3 by histone-modifying enzymes. Proc. Natl Acad. Sci. USA. 2010; 107, 21499–21504.

Yang M, Gocke CB, Luo X, et al. Structural basis for CoREST-dependent demethylation of nucleosomes by the human LSD1 histone demethylase. Mol. Cell. 2006; 23, 377–387.

Yokoyama A, Takezawa S, Schüle R, Kitagawa H, Kato S. Transrepressive function of TLX requires the histone demethylase LSD. Mol. Cell Biol. 2008; 28, 3995–4003.

Yokoyama, S., Woods, S.L., Boyle, G.M., Aoude, L.G., MacGregor, S., Zismann, V., Gartside, M., Cust, A.E., Haq, R., Harland, M., et al. A novel recurrent mutation in MITF predisposes to familial and sporadic melanoma. Nature. 2011; 480, 99-103.

Yu, Y., Wang, B., Zhang, K., Lei, Z., Guo, Y., Xiao, H., et al. High expression of lysine-specific demethylase 1 correlates with poor prognosis of patients with esophageal squamous cell carcinoma. Biochem. Biophys. Res. Commun. 2013; 437, 192–198.

Yuan, C., Li, Z., Qi, B., Zhang, W., Cheng, J., and Wang, Y. High expression of the histone demethylase LSD1 associates with cancer cell proliferation and unfavorable prognosis in tongue cancer. J Oral Pathol Med. 2015;44(2):159-65.

Yun M, Wu J, Workman JL, Li B. Readers of histone modifications. Cell Res. 2011; 21:564–578.

Zhang J, Bonasio R, Strino F, Kluger Y, Holloway JK, Modzelewski AJ, Cohen PE, Reinberg D. SFMBT1 functions with LSD1 to regulate expression of canonical histone genes and chromatin-related factors. Genes Dev. 2013;27(7):749-66

Zhang X, Bolt M, Guertin MJ, Chen W, Zhang S, Cherrington BD, et al. Peptidylarginine deiminase 2-catalyzed histone H3 arginine 26 citrullination facilitates estrogen receptor alpha target gene activation. Proc. Natl Acad. Sci. USA. 2012; 109, 13331–13336

Zheng YC, et al. A systematic review of histone lysine-specific demethylase 1 and its inhibitors. Med Res Rev. 2015; 35(5), 1032–1071

Zhou D, Kim S, Ding W, Schultz C, Warrell RJ, Gallagher R. Frequent mutations in the ligand-binding domain of PML-RARalpha after multiple relapses of acute promyelocytic

leukemia: analysis for functional relationship to response to all-trans retinoic acid and histone deacetylase inhibitors in vitro and in vivo. Blood. 2002;99(4):1356-63.

Zibetti C, Adamo A, Binda C, et al. Alternative splicing of the histone demethylase LSD1/KDM1 contributes to the modulation of neurite morphogenesis in the mammalian nervous system. J. Neurosci. 2010; 30(7), 2521–2532.

Acknowledgments

I would like to acknowledge foremost Professor Saverio Minucci, who has supervised me throughout this project. His unceasing support, guidance, and belief have allowed this project to move forward- I cannot express my gratitude enough.

I would also like to express my deep gratitude to my co-supervisors, Dr. Diego Pasini, and Dr. Luciano Di Croce, for their valuable feedbacks and guidance throughout this project. Also, thanks to my thesis examiners, Professor Pier Giuseppe Pelicci and Professor Eric So, for useful discussion and comments.

I send a strong thank you to all the past and present colleagues in Minucci's research group for providing their tutelage, advice and friendship.

Also, I would like to thank Dr. Veronica Viscardi and Dr. Francesca Fiore from SEMM office for all their supports from the beginning of my PhD course till the end.

I would like to give special thanks to my Iranian friends, Sara Rohban, Sara Samdi Shams and Sina Atashpaz, who helped me too much to feel less homesick in Italy.

Finally, I am grateful beyond words to Parinaz and my family for their ever-present support and encouragement.